UNIVERSIDADE DE SÃO PAULO

CENTRO DE ENERGIA NUCLEAR NA AGRICULTURA

ALINE MARIA ZIGIOTTO DE MEDEIROS

Synthesis, characterization and ecotoxicological evaluation of hybrid graphene oxide-silver nanoparticles

Piracicaba
2021

ALINE MARIA ZIGIOTTO DE MEDEIROS

Synthesis, characterization and ecotoxicological evaluation of hybrid graphene oxide-silver nanoparticles

Revised version according to the Resolution CoPGr 6018/2011

Thesis presented to the Center for Nuclear Energy in Agriculture of the University of Sao Paulo as a requisite to the Doctoral Degree in Sciences.

Concentration Area: Chemistry in Agriculture and the Environment

Advisor: Prof. Dr. Diego Stéfani Teodoro Martinez

Piracicaba
2021

Dados Internacionais de Catalogação na Publicação (CIP)

Técnica de Biblioteca - CENA/USP

De Medeiros, Aline Maria Zigiotto

Síntese, caracterização e ecotoxicidade do híbrido de óxido de grafeno decorado com nanopartículas de prata / Synthesis, characterization and ecotoxicological evaluation of hybrid graphene oxide-silver nanoparticles / Aline Maria Zigiotto De Medeiros; orientador Diego Stéfani Teodoro Martinez. - - Versão revisada de acordo com a Resolução CoPGr 6018 de 2011. - - Piracicaba, 2021.
130 p.

Tese (Doutorado – Programa de Pós-Graduação em Ciências. Área de Concentração: Química na Agricultura e no Ambiente) – Centro de Energia Nuclear na Agricultura, Universidade de São Paulo, 2021.

1. Bioindicadores 2. Ecotoxicologia 3. Nanopartículas 4. Nanotecnologia 5. Toxicologia ambiental I. Título.

CDU (574.64 : 620.3)

Elaborada por:
Marilia Ribeiro Garcia Henyei
CRB-8/3631
Resolução CFB Nº 184 de 29 de setembro de 2017

ACKNOWLEDGEMENTS

Throughout the writing of this thesis, I have received a great deal of support and assistance.

I would like to express my sincere gratitude to my advisor Dr. Diego Stéfani Teodoro Martinez, and Dra. Vera Lucia Scherholz de Castro for the continuous support of my PhD study. Your insightful feedback pushed me to sharpen my thinking and brought my work to a higher level.

I would like to acknowledge CENA – USP, Embrapa Ambiente and LNNano – CNPEM to provide all the necessary infrastructure to complete this project.

My special gratitude goes to Profa. Iseult Lynch, my internship advisor at the University of Birmingham, that provided valuable guidance throughout my studies. I would like to also thank the technical staff and my lab colleagues for their wonderful collaboration.

I wish to show my appreciation to Dra. Hozana Castillo (LNBIO – CNPEM) for all support with zebrafish model.

I would extend my special thanks to all my lab mates at LNNano for their scientific and emotional support.

I would acknowledge the support and great love of my family and friends.

I wish to acknowledge the doctoral scholarship supported by the Coordenação de Aperfeiçoamento de Pessoal de Nível Superior – Brasil (CAPES / Brasil) (Finance Code 001 and PrInt SCBA: 88887.379931/2019), and the National Council of Scientific and Technological Development (CNPq / Brasil - Grant 169984/2018-4).

Nothing in life is to be feared, it is only to be understood.
Now is the time to understand more so that we may fear less.

Marie Curie

ABSTRACT

DE MEDEIROS, A. M. Z. **Synthesis, characterization and ecotoxicological evaluation of hybrid graphene oxide-silver nanoparticles**. 2021. 130 p. Tese (Doutorado em Ciências) - Centro de Energia Nuclear na Agricultura, Universidade de São Paulo, Piracicaba, 2021.

The hybrid nanomaterial GO-AgNPs was synthesized using graphene oxide (GO) as substrate and stabilizer for the silver nanoparticles (AgNPs). This nanohybrid has promising technological applications due to its unique physicochemical properties. However, it is necessary to assess proactively the potential risks of these materials for human and environmental health. The aim of this thesis was an integrated ecotoxicological evaluation of the hybrid nanomaterial GO-AgNPs. It was realized in three main steps: i) Preparation and physic-chemical characterisation of the nanomaterial GO-AgNPs (e.g. composition, structure, morphology, size and chemistry of the surface); ii) Dispersion and colloidal stability monitoring (state of aggregation/agglomeration) of nanomaterials in the culture media of organisms-bioindicators and the influence of bio-coronas (environmental-corona and protein-corona); iii) ecotoxicity evaluation of GO-AgNPs, GO and AgNPs dispersions *in vivo* and *in vitro* assays of zebrafish model (*Danio rerio*). In the first chapter, a literature review was realised, and its scope summarises the synthesis, application and toxicological aspects of GO-AgNPs. An integrated study was reported in the second chapter and included the synthesis, characterisation, colloidal stability monitoring, and ecotoxicological assay in zebrafish embryos. GO-AgNPs were synthesised by the chemical reduction method of the silver salt in an aqueous dispersion of GO using sodium borohydride as a reducing agent. The characterisation techniques confirmed the formation of spherical AgNPS with an approximate diameter of 6 nm distributed onto GO sheets. The spontaneous coating formed by the natural organic matter, the eco-corona, positively influenced the stability of the nanomaterials and mitigated the toxicological response. The chorion also shows a protective function. Embryos without chorion exhibited higher rates of deformation and mortality compared to the control group. The median lethal dose (LC_{50}-96h) was 1.5 mg L^{-1}. In the third chapter, the effects of this nanohybrid on zebrafish liver cell line (ZFL) were evaluated. The protein-corona resulting from the interaction with the supplementation of the culture medium with fetal bovine serum (FBS) improved the colloidal stability of the nanomaterials.

Mean inhibitory concentrations (IC_{50}-24h) observed in viability assays (AB, MTT, NRU) ranged from 5.7 to 7.0 µg mL^{-1}. Furthermore, the assays with the embryo and with the liver cells showed the biocompatibility of GO even at high doses (100 mg L^{-1}). Ingestion by embryos and internalisation by cells of this nanomaterial was also observed. The nanohybrid dissolution had a minor influence on the assessment, and most of the toxic response was due to the nanohybrid *per se*. Furthermore, the deleterious effects observed are distinct from the nanomaterials from their counterparts. Thus, the results reinforce the importance of proactive evaluation of this new nanomaterial to minimise the impacts on human and environmental health towards sustainability and responsible innovation

Keywords: Aquatic toxicology. Nanotechnology. Ecotoxicity. Zebrafish.

RESUMO

DE MEDEIROS, A. M. Z. **Síntese, caracterização e ecotoxicidade do híbrido de óxido de grafeno decorado com nanopartículas de prata** 2021. 130 p. Tese (Doutorado em Ciências) - Centro de Energia Nuclear na Agricultura, Universidade de São Paulo, Piracicaba, 2021.

O nanomaterial híbrido GO-AgNPs é sintetizado usando óxido de grafeno (GO) como substrato e agente estabilizante de nanopartículas de prata (AgNPs). O nanohíbrido possui promissoras aplicações tecnológicas devido às suas exclusivas propriedades físico-químicas. Contudo, é necessário avaliar, de maneira proativa, os potenciais riscos destes materiais para saúde humana e ambiental. O objetivo desta tese foi realizar uma avaliação ecotoxicológica integrada do nanomaterial híbrido GO-AgNPs. Este projeto foi realizado 3 etapas sendo: i) preparação e caracterização físico-química do nanomaterial GO-AgNPs (e.g. composição, estrutura, morfologia, tamanho e química da superfície); ii) estudo da dispersão e estabilidade coloidal (estado de agregação/aglomeração) dos nanomateriais nos meios de cultivo dos organismos-bioindicadores e a influência de bio-coronas (“environmental-corona” e “protein-corona”) e, iii) avaliação da ecotoxicidade aguda das dispersões de GO-AgNPs, GO e AgNPs em utilizando ensaios *in vivo* e *in vitro* do modelo “zebrafish” (*Danio rerio*). No primeiro capítulo desta tese, foi realizado um levantamento bibliográfico sobre a síntese, aplicação e aspectos toxicológicos do GO-AgNPs. No segundo capítulo, um estudo integrado foi realizado que abordou a síntese, caracterização, estabilidade coloidal e ensaio ecotoxicológico em embriões de zebrafish. O GO-AgNPs foi sintetizado pelo método de redução química do sal de prata em uma dispersão aquosa de GO utilizando o borohidreto de sódio como agente redutor. As técnicas de caracterização confirmaram a formação de AgNPS esféricas com diâmetro aproximado de 6 nm distribuídas pelas folhas de GO. O revestimento espontâneo formado pela matéria orgânica natural (do inglês: natural organic matter - NOM), a eco-corona, influenciou positivamente na estabilidade das nanopartículas e mitigou a resposta toxicológica. O córion também apresentou uma função protetora. Os embriões sem córion exibiram taxas maiores de deformação e mortalidade em comparação com o grupo exposto sem a presença de NOM. A dose letal mediana (LC_{50}-96h) foi de 1.5 mg L^{-1}. No terceiro capítulo, foi avaliado os efeitos deste nanohíbrido em uma linhagem de células de fígado do zebrafish (ZFL). A “protein-

corona” decorrente da interação com as proteínas oriundas da suplementação do meio de cultivo com soro fetal bovino melhorou a estabilidade coloidal dos nanomateriais. As concentrações inibitórias média (IC_{50}-24h) observadas em ensaios de viabilidade (AB, MTT, NRU) variaram de 5.7 a 7.0 µg mL^{-1}. Além disso, os ensaios realizados com embrião e com a linhagem de células de fígado mostraram a biocompatibilidade do GO mesmo em alta dosagem (100 $mg.L^{-1}$). Também foi observada a ingestão pelos embriões e a internalização pelas células deste nanomaterial. A dissolução do nanohíbrido teve uma pequena influência na resposta tóxica, sendo a maior parte dela decorrente do nanohíbrido *per se*. Além disso, os efeitos deletérios observados são distintos dos nanomateriais dos quais o nanohíbrido é formado. Assim, os resultados deste trabalho reforçam a importância da avaliação proativa deste promissor nanomaterial minimizando os impactos à saúde humana e ambiental em direção a sustentabilidade e inovação responsável.

Palavras-chave: Toxicologia aquática. Nanotecnologia. Ecotoxicidade. Zebrafish.

SUMMARY

1. INTRODUCTION

Nanoscience is an emerging area of science that involves the study of structures and materials whose size is measured in nanometers (10^{-9} m) and these materials demonstrate unique and interesting properties (BHUSHAN, 2016). With the reduction in nanomaterials (NMs) size, there is an increase in the atomic surface area to the total volume, resulting in new physico-chemical properties compared to conventional bulk materials (NEL et al., 2006).

Silver nanoparticles (AgNPS) have attracted remarkable attention due to their antimicrobial action and unique new physico-chemical properties. The toxicity mechanisms involve cell membrane disruption and DNA transformation via reactive oxygen species (ROS) as the principal agents (DURÁN et al., 2016). Among the engineered nanomaterials, the AgNPs are the most often incorporated in nano-functionalised consumer products. Therefore, they are on the NMs priority list of the Organisation for Economic Co-operation and Development (OECD, 2010) for (eco)toxicological assessment.

The graphene is an important carbon nanomaterial (DE MARCHI et al., 2018; LAWAL, 2019). This nanomaterial consists of a single layer of atoms arranged in a two-dimensional honeycomb lattice with approximately 1nm of thickness (JASTRZEBSKA et al., 2012). Graphene-family nanomaterials (GFNs) include pristine graphene, few-layer-graphene, ultrathin graphite, graphene oxide (GO), reduced graphene oxide (rGO) (SANCHEZ et al., 2012).

GO is the oxygenated form of monolayer graphene. Its oxygenated groups (epoxide, hydroxyl, carboxyl, and carbonyl) lead to a negative surface charge that allows a higher dispersity at polar solvents, like water (GEORGAKILAS et al., 2016; DASARI-SHAREENA et al., 2018). Moreover, the presence of these groups enables the combination with metallic nanoparticles forming graphene–metal nanohybrids (XU et al., 2008, ZHAO et al., 2018).

Among carbon-metallic nanohybrids, the graphene oxide-silver nanoparticle (GO-AgNPs) hybrid material shows potential applications due to its unique physico-chemical properties (YIN et al., 2015). However, due to new characteristics that arise during hybridisation, the environmental behaviour and ecotoxicological effects could be distinct from the sum of their pristine counterparts (SALEH et al., 2014).

Thus, it is necessary to proactively assess the potential risks of these new materials to human and environmental health (PARK et al., 2017; MENG et al., 2018).

In this context, *in vivo* and *in vitro* models could be used on nano(eco)toxicology studies. Together, these assessments have provided important insights into our understanding of nanomaterial-mediated toxicity mechanisms.

1.1. In vivo evaluation: fish embryo test with the zebrafish *(Danio rerio)*

Among the aquatic organisms, zebrafish (*Danio rerio*) is used as an organism model in environmental sciences due to its small body, high fecundity, rapid development with well-characterised stages, and easy handling (CHAKRABORTY et al., 2016; NOYES et al., 2016; ÁVILA et al., 2018). Moreover, the functioning of organ systems like the nervous, cardiovascular, and digestive systems is similar to mamals showing 70% of conserved signalling pathways and high genomic homology with humans (VERMA et al., 2021). Thus, zebrafish can be used in scientific research to replace other models, such as mice (JOHNSTON et al., 2018).

The fish embryo test (FET) is extensively applied at ecotoxicological studies given its excellent correlation with the acute adult fish toxicity test (KNÖBEL et al., 2012; BRAUNBECK et al., 2014; PEREIRA et al., 2019; SIEBER et al., 2019). Furthermore, the embryos may not yet have pain perception due to the incomplete development of their nervous system (LAMMER et al., 2009). Consequently, concerning animal welfare, the utilisation of embryonic stages may be regarded as compatible with the replacement of the 3R’s (Replacement, Reduction and Refinement) principles of animal experimentation (SU et al., 2021).

According to OECD test guideline 236 (OECD, 2013), the newly fertilised zebrafish embryos are exposed to the test chemical for a total of 96 h. Some endpoints could be reported during the test, such as coagulation of fertilised eggs, lack of somite formation, lack of detachment of the tailbud from the yolk sac, and lack of heartbeat. At the end of the exposure period, acute toxicity is determined based on the lethality, and the LC50 (50% *Lethal* Concentration) is calculated (Figure 1).

Figure 1: Fish embryo test (FET) according to OECD TG 236

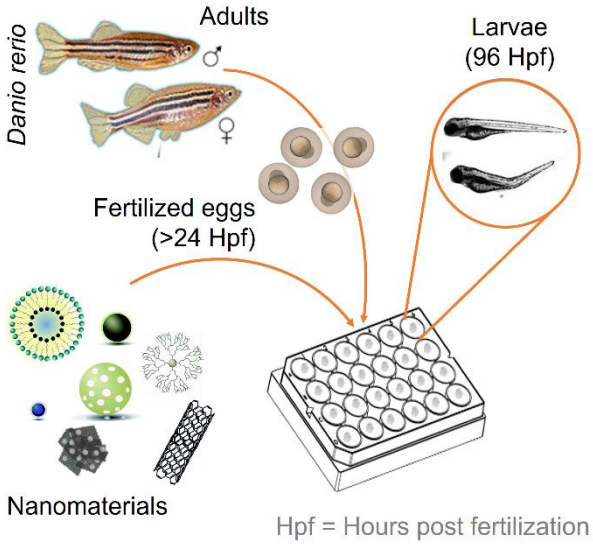

A challenge in this essay for NMs ecotoxicological evaluation is the presence of chorion during the beginning of the test. The chorion membrane has pore channels with 0.5-0.7 mm in diameter, which partly isolates the embryo until the moment of hatching (48 – 72 hours post-fertilization – hpf). In this sense, news protocols have been developed to remove this membrane and exposure direct the “naked” embryo. In this work, a modified FET methodology was utilised to dechorionation the embryos. For this purpose, the chorion of 24 hpf embryos was removed mechanically with tweezers (Figure 2).

Figure 2: Fish embryo test (FET) modified for chorion removal

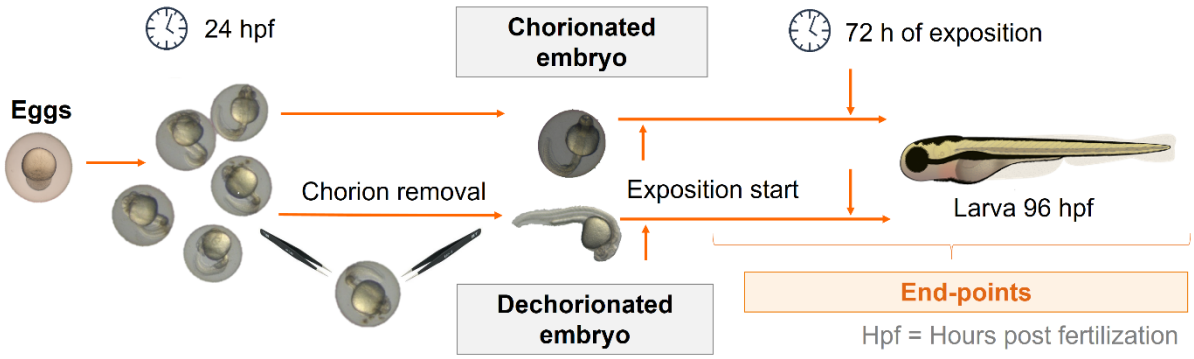

Once in the environment, the NMs are prone to suffer alterations due to their high surface-to-volume ratio and reactivity. For example, the nanomaterials could interact with components present in the environmental matrix and adsorbing biomolecules (such as proteins, metabolites, lipids, polysaccharides, natural organic matter), acquiring a so-called ‘corona’ (NASSER; LYNCH, 2016).

Therefore, the corona formation changes its nano-bio-interface, influencing organismal response and environmental behaviour (DOCTER et al., 2015). For example, the biomolecular-corona composed of biomolecules secreted of *Daphnia magna* (micro-crustacean used as indicator species for toxicant exposure) modify its colloidal stability, dissolution, attractively (as a food source) and, consequently, the toxicity of polystyrene nanoparticles (NASSER; LYNCH, 2016; BRIFFA et al., 2018).

The environmental corona consists primarily of diverse natural organic matter (NOM) and humic acids. These macromolecules are a complex matrix formed during the humification of plant and animal residues (PULIDO-REYES; LEGANES; FERNÁNDEZ-PIÑAS; et al., 2017).

The environmental corona composition is modulated by the nanomaterial surface (e.g. elemental composition, size, shape, surface, functional groups), the medium in which the NM is suspended (e.g. ion strength, pH, temperature), and by biological entities (e.g. biological surface, NOM, biomolecules) (CANESI et al., 2017; PULIDO-REYES et al., 2017).

Therefore, environmental transformations (such as corona formation) play a key role in the toxicity of nanomaterials and must be taken into account in nanosafety assessments towards more realistic scenarios (FADEEL et al., 2018).

1.2. *In vitro* evaluation: cytotoxicity on zebrafish liver cell line

Besides zebrafish embryos, the use of fish cell lines for ecotoxicological assessment is also aligned with 3R’s principles of animal experimentation (MACARTHUR CLARK, 2018). Cell lines could be applied to evaluate the sequence of molecular and cellular pathways that result in adverse outcomes upon nanomaterials exposition (DRASLER et al., 2017).

Herein, zebrafish liver cell line was applied to the investigated of toxicological effects from NHs exposition. This cell line shows general hepatocyte morphology that makes them useful for in vitro toxicological and detoxification investigations.

To provide the optimal conditions for the maintenance of the cells, the basal cell culture is supplemented with serum, commonly fetal bovine serum (FBS), which offers important biomolecules, such as nutritional-related and cell-spreading-related proteins.

Thus, due to the interaction of NMs with these biomolecules, protein will be adsorbed at NMs surface, forming the protein-corona (CEDERVALL et al., 2007, DAWSON; YAN, 2021). Its composition is complex and depends on the intrinsic properties of the nanomaterial (such as size, charge, functional groups) and the medium environment (components of the medium, temperature, pH, interaction time) (NGUYEN; LEE, 2017).

It can be classified into the hard corona and soft corona. The hard corona is composed of proteins with a strong binding affinity of NMs surface. Thus, this layer shows a long residence time, slow exchange time, and high conformational changes. In contrast, the soft corona comprises the layer of proteins bound to the hard corona by weaker interactions and, therefore, its composition is highly dynamic (NGUYEN; LEE, 2017).

Immediately upon interaction, the most abundant molecules in the medium are adsorbed to the surface of the NM and, then, they are gradually replaced as a function of the protein-particle affinity (LIU et al., 2020). Thus, the composition and abundance of the hard corona biomolecules may be different from those present in the biological fluid (Figure 3).

The protein corona modifies the NMs surface that will be in contact with the cell. Thus, the NM-protein complex will determine biological responses, such as cellular absorption, bioavailability and toxicity of NMs (LIU et al., 2020).

Figure 3: Protein corona formation on biological media. (A) Immediately upon interaction; (B) After a longer exposure time, the exchange of proteins among the hard corona, soft corona, and cellular environment; (C) Major factors affecting the protein corona pattern. Abbreviation: NP, nanoparticle (NGUYEN; LEE, 2017)

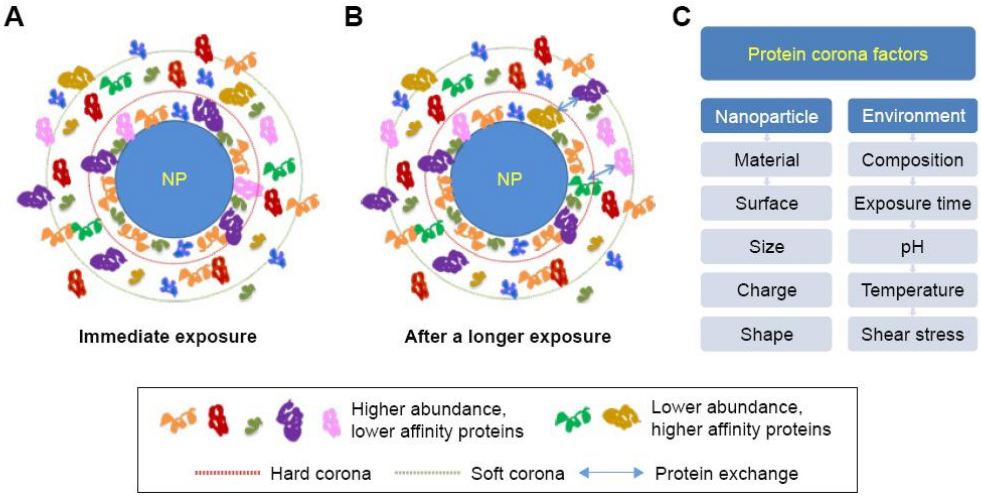

1.3. Structure of the thesis

This thesis comprises an introduction and 3 chapters presented in scientific manuscript format. The supplementary materials indicated in each chapter are available in the Appendix section. The first chapter is a literature review in which the synthesis, applications and ecotoxicology studies about GO-AgNPs nanohybrids was reported. The second chapter is an integrated study that discusses the synthesis, characterization and ecotoxicological assessments on zebrafish embryos. In the third chapter, the effects of this nanohybrid on zebrafish liver cell line (ZFL) were evaluated. Finally, this work is an innovative contribution to environmental nanosafety research of nanohybrid materials towards safe innovation in nanotechnology.

References

ÁVILA, D. S.; RONCATO, J. F.; JACQUES, M. T. Nanotoxicology assessment in complementary/alternative models. **Energy, Ecology and Environment**, v. 3, n. 2, p. 72–80, 2018.

BHUSHAN, B. Introduction to Nanotechnology: History, Status, and Importance of Nanoscience and Nanotechnology Education. In: WINKELMANN, K.; BHUSHAN, B. (eds.). **Global Perspectives of Nanoscience and Engineering Education**. Cham: Springer, 2016. p. 2004-2015. https://doi.org/10.1007/978-3-319-31833-2_1.

BRAUNBECK, T.; KAIS, B.; LAMMER, E.; OTTE, J.; SCHNEIDER, K.; STENGEL, D.;

STRECKER, R. The fish embryo test (FET): origin, applications, and future. **Environmental Science and Pollution Research**, v. 22, p. 16247-16261, 2015.

BRIFFA, S. M.; NASSER, F.; VALSAMI-JONES, E.; LYNCH, I. Uptake and impacts of polyvinylpyrrolidone (PVP) capped metal oxide nanoparticles on Daphnia magna: role of core composition and acquired corona. **Environmental Science Nano**, v. 5, p. 1745–1756, 2018.

CANESI, L.; BALBI, T.; FABBRI, R.; SALIS, A.; DAMONTE, G.; VOLLAND, M.; BLASCO, J. Biomolecular coronas in invertebrate species : Implications in the environmental impact of nanoparticles. **NanoImpact**, v. 8, p. 89–98, 2017.

CHAKRABORTY, C.; SHARMA, A. R.; SHARMA, G.; LEE, S. S. Zebrafish: A complete animal model to enumerate the nanoparticle toxicity. **Journal of Nanobiotechnology**, v. 14, art. 65, 2016.

DASARI SHAREENA, T. P.; MCSHAN, D.; DASMAHAPATRA, A. K.; TCHOUNWOU, P. B. A review on graphene-based nanomaterials in biomedical applications and risks in environment and health. **Nano-Micro Letters**, v. 10, n. 3, p. 1–34, 2018.

DAWSON, K. A.; YAN, Y. Current understanding of biological identity at the nanoscale and future prospects. **Nature Nanotechnology,** v. 16, n. 3, p. 229–242, 2021.

DOCTER, D.; WESTMEIER, D.; MARKIEWICZ, M.; STOLTE, S.; KNAUER, S. K.; STAUBER, R. H. et al. The nanoparticle biomolecule corona: lessons learned - challenge accepted? **Chemical Society Reviews**, v. 44, n. 17, p. 6094–6121, 2015.

DRASLER, B.; SAYRE, P.; STEINHÄUSER, K. G.; PETRI-FINK, A.; ROTHEN-RUTISHAUSER, B. In vitro approaches to assess the hazard of nanomaterials. **NanoImpact**, v. 8, n. August, p. 99–116, 2017.

DURÁN, N.; DURÁN, M.; JESUS, M. B. DE; SEABRA, A. B.; FÁVARO, W. J.; NAKAZATO, G. Silver nanoparticles : A new view on mechanistic aspects on antimicrobial activity. **Nanomedicine: Nanotechnology, Biology, and Medicine**, v. 12, n. 3, p. 789–799, 2016.

FADEEL, B.; FARCAL, L.; HARDY, B.; VÁZQUEZ-CAMPOS, S.; HRISTOZOV, D.; MARCOMINI, A.; LYNCH,I.; VALSAMI-JONES, E.; ALENIUS, H.; SAVOLAINEN, K. Advanced tools for the safety assessment of nanomaterials. **Nature Nanotechnology**, v. 13, p. 537–543, 2018.

GEORGAKILAS, V.; TIWARI, J. N.; KEMP, K. C.; PERMAN, J. A.; BOURLINOS, A. B.; KIM, K. S.; ZBORIL, R. Noncovalent functionalization of graphene and graphene oxide for energy materials, biosensing, catalytic, and biomedical applications. **Chemical Reviews**, v. 116, n. 9, p. 5464–5519, 2016.

JASTRZEBSKA, A. M.; KURTYCZ, P.; OLSZYNA, A. R. Recent advances in graphene family materials toxicity investigations. **Journal of Nanoparticle Research**, v. 14, n. 12, art. 1320, 2012.

JOHNSTON, H. J.; VERDON, R.; GILLIES, S.; BROWN, D. M.; FERNANDES, T. F.; HENRY, T. B.; ROSSI, A. G.; TRAN, L.; TUCKER, C.; TYLER, C. R.; STONE, V. Adoption of in vitro systems and zebrafish embryos as alternative models for reducing rodent use in assessments of immunological and oxidative stress responses to nanomaterials. **Critical Reviews in Toxicology**, v. 48, n. 3, p. 252–271, 2018.

KNÖBEL, M.; BUSSER, F. J. M.; RICO-RICO, Á.; KRAMER, N. I.; HERMENS, J. L. M.; HAFNER, C.; TANNEBERGER, K.; SCHIRMER, C.; SCHOLZ, S. Predicting adult fish acute lethality with the zebrafish embryo: Relevance of test duration, endpoints, compound properties, and exposure concentration analysis. **Environmental Science and Technology**, v. 46, n. 17, p. 9690–9700, 2012.

LAMMER, E.; KAMP, H. G.; HISGEN, V.; KOCH, M.; REINHARD, D.; SALINAS, E. R.; WENDLER, K.; ZOK, S.; BRAUNBECK, Th. Development of a flow-through system for the fish embryo toxicity test (FET) with the zebrafish (Danio rerio). **Toxicology in Vitro**, v. 23, n. 7, p. 1436–1442, 2009.

LAWAL, A. T. Graphene-based nano composites and their applications. A review. **Biosensors and Bioelectronics**, v. 141, art. 111384, 2019.

LIU, N.; TANG, M.; DING, J. The interaction between nanoparticles-protein corona complex and cells and its toxic effect on cells. **Chemosphere**, v. 245, art. 125624, 2020.

MACARTHUR CLARK, J. The 3Rs in research: A contemporary approach to replacement, reduction and refinement. **British Journal of Nutrition**, v. 120, p. S1–S7, 2018. Suppl. 1.

MARCHI, L. DE; PRETTI, C.; GABRIEL, B.; MARQUES, P. A. A. P.; FREITAS, R.; NETO, V. An overview of graphene materials: Properties, applications and toxicity on aquatic environments. **Science of the Total Environment**, v. 631–632, p. 1440–1456, 2018.

MENG, H.; LEONG, W.; LEONG, K. W.; CHEN, C.; ZHAO, Y. Walking the line : The fate of nanomaterials at biological barriers. **Biomaterials**, v. 174, p. 41–53, 2018.

NASSER, F.; LYNCH, I. Secreted protein eco-corona mediates uptake and impacts of polystyrene nanoparticles on Daphnia magna. **Journal of Proteomics**, v. 137, p. 45–51, 2016.

NEL, A.; XIA, T.; MADLER, L.; LI, N. Toxic Potential of Materials at the Nanolevel. **Science**, v. 311, n. 5761, p. 622–627, 2006.

NGUYEN, V. H.; LEE, B. J. Protein corona: A new approach for nanomedicine design. **International Journal of Nanomedicine**, v. 12, p. 3137–3151, 2017.

NOYES, P. D.; GARCIA, G. R.; TANGUAY, R. L. Zebrafish as an in vivo model for sustainable chemical design. **Green Chemistry**, v. 18, n. 24, p. 6410–6430, 2016.

ORGANIZATION FOR ECONOMIC CO-OPERATION AND DEVELOPMENT - OECD. **Guidelines for the testing of chemicals**. Test 236 - Fish embryo toxicity test. Paris, 2013.

PARK, M. V. D. Z.; BLEEKER, E. A. J.; BRAND, W.; CASSEE, F. R.; VAN ELK M.; GOSENS, I.; DE JONG, W. H.; MEESTERS, J. A. J.; PEIJNENBURG, W. J. G. M.; QUIK, J. T. K.; VANDEBRIEL, R. J.; SIPS, A. J. A. M. Considerations for Safe Innovation: The Case of Graphene. **ACS Nano**, v. 11, n. 10, p. 9574–9593, 2017.

PEREIRA, A. C.; GOMES, T.; FERREIRA MACHADO, M. R.; ROCHA, T. L. The zebrafish embryotoxicity test (ZET) for nanotoxicity assessment: from morphological to molecular approach. **Environmental Pollution**, v. 252, p. 1841–1853, 2019.

PULIDO-REYES, G.; LEGANES, F.; FERNÁNDEZ-PINAS, F.; ROSAL, R. Bio-Nano interface and environment: A critical review. **Environmental Toxicology and Chemistry**, v. 36, n. 12, p. 3181–3193, 2017.

PULIDO-REYES, G.; LEGANES, F.; FERNÁNDEZ-PIÑAS, F.; ROSAL, R. Bio-nano interface and environment: A critical review. **Environmental Toxicology and Chemistry**, v. 36, n. 12, p. 3181–3193, 2017.

SALEH, N. B.; AFROOZ, A. R. M. N.; BISESI JUNIOR, J. H.; AICH, N.; PLAZAS-TUTTLE, J.; SABO-ATTWOOD, T. Emergent Properties and Toxicological Considerations for Nanohybrid Materials in Aquatic Systems. **Nanomaterials**, v. 4, n. 2, p. 372–407, 2014.

SANCHEZ, V. C.; JACHAK, A; HURT, R. H.; KANE, A. B. Biological interactions of graphene-family nanomaterials: an interdisciplinary review. **Chemical Research in Toxicology**, v. 25, n. 1, p. 15–34, 2012.

SIEBER, S.; GROSSEN, P.; BUSSMANN, J.; CAMPBELL, F.; KROS, A.; WITZIGMANN, D.; HUWYLER, J. Zebrafish as a preclinical in vivo screening model for nanomedicines. **Advanced Drug Delivery Reviews**, v. 151–152, p. 152–168, 2019.

SU, T.; LIAN, D.; BAI, Y.; WANG, Y. Y. L.; ZHANG, D.; WANG, Z.; YOU, J. The feasibility of the zebrafish embryo as a promising alternative for acute toxicity test using various fish species: A critical review. **Science of The Total Environment**, v. 787, p. 147705, 2021.

VERMA, S. K.; NANDI, A.; SINHA, A.; PATEL, P.; JHA, E.; MOHANTY, S.; PANDA, P. K.; AHUJA, R.; MISHRA, Y. K.; SUAR, M. Zebrafish (Danio rerio) as an ecotoxicological model for Nanomaterial induced toxicity profiling. **Precision Nanomedicine**, v. 4, n. 1, p. 750–781, 2021.

XU, C.; WANG, X.; ZHU, J. Graphene - Metal Particle Nanocomposites. **Journal of Physical Chemistry C**, v. 112, p. 19841–19845, 2008.

YIN, P. T.; SHAH, S.; CHHOWALLA, M.; LEE, K. Design, synthesis, and characterization of graphene − Nanoparticle hybrid materials for bioapplications. **Chemical Reviews**, v. 115, p. 2483–2531, 2015.

ZHAO, N.; YAN, L.; ZHAO, X.; Chen, X.; Li, A.; Zheng, D.; Zhou, X.; Dai, X.; Xu, F.-J. Versatile Types of Organic / Inorganic Nanohybrids : From Strategic Design to Biomedical Applications. **Chemical Reviews**, v. 119, p. 1666–1762, 2018.

2. GRAPHENE OXIDE-SILVER NANOPARTICLE HYBRID MATERIAL: FROM SYNTHESIS TO NANOSAFETY

Graphical abstract

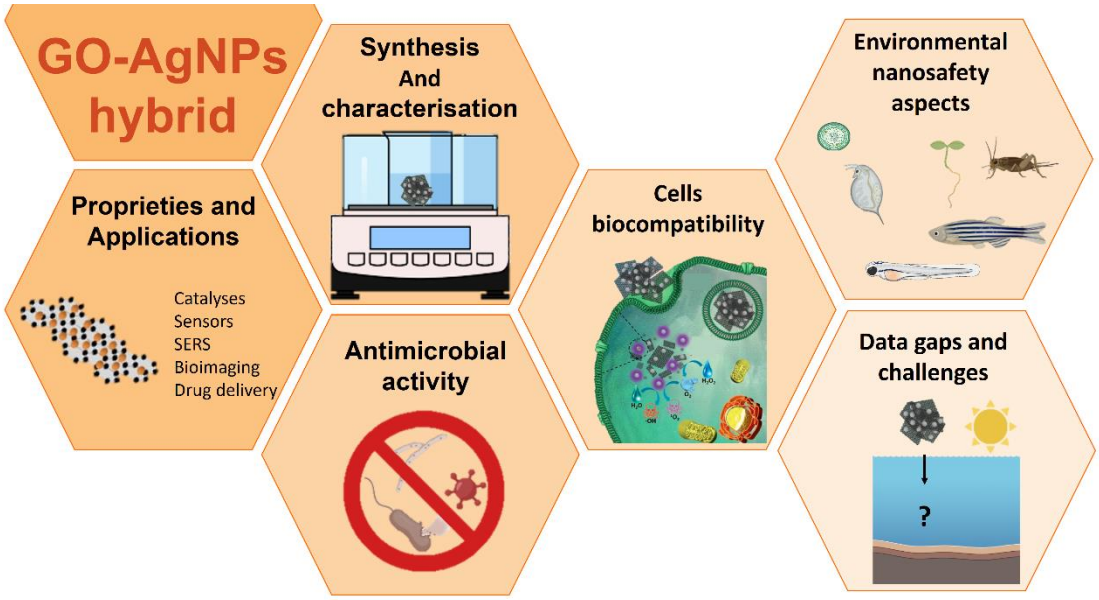

Abstract

The GO-AgNPs nanohybrid has attracted increasing interests of the scientific community due to its unique physicochemical properties that arise from the conjugation of graphene oxide (GO) and silver nanoparticles (AgNPs). This emergent nanomaterial shows the potential to be widely applied, especially in the biomedical field, due to its antimicrobial activities. Although many studies have been conducted on the potential application, limited comprehensive reviews have published on its possible environmental and human health effects. This review aimed to identifies potential environmental uncertainties of these emerging nanohybrid. To this end, we examined and discussed the synthesis and characterisation, the properties and potential applications, *in vitro* biocompatibility and the environmental nanosafety aspects.

Keywords: nanotoxicology, antimicrobial activity, cytotoxicity, safety-by-design

2.1. Introduction

Recently, the material development at the nanoscale shift of single part synthesis towards multi-component assemblages (SALEH et al., 2015). The conjugations of nanomaterials (NMs) could modify inherent physicochemical proprieties such as size, shape, composition, surface chemistry, dissolution properties, sorption characteristics, etc. (AICH et al., 2014). Furthermore, multifunctionality and novel proprieties could rise due to the hybridisation process (SALEH et al., 2014). Thus, this new kind of nanomaterials received significant attention due to their broad potential applications.

These multi-component ensembles of nanomaterials are termed nanohybrids (NHs). Thus, NHs are two or more NMs strongly conjugated (by molecular or macromolecular links and/or physicochemical forces), leading to unique reactivity and property manifestation (SALEH et al., 2015). The NHs could be a combination of carbon NMs (e.g. fullerenes, graphene, carbon nanotubes and derivatives) or metallic nanoparticles (e.g. silver, gold, titanium oxide, etc.) with or without organic coating (WANG et al., 2019). Furthermore, they could be classified based on their parent materials (i.e. carbon-carbon NHs, carbon-metal NHs, metal-metal NHs and organo-metal-carbon NHs) (AICH et al., 2014).

One NHs that have attracted intense attention is GO-AgNPs. This carbon-metallic NH is a combination of graphene oxide (GO) and silver nanoparticles (AgNPs). The graphene is a single atomic thick sheet of carbon atoms in a hexagonal array. Its oxidised form, the graphene oxide (GO), is easily dispersible in water or polar organic media due to its functional groups (DASARI SHAREENA et al., 2018). Moreover, the large surface area due to the two-dimensional structure and the oxygen groups that act as anchoring sites for the attachment of metal NPs provides a good platform for forming nanohybrids based on GO (YIN et al., 2015).

Moreover, due to their unique optical, thermal conductivity, electrical, catalytic properties, and antibacterial capability, AgNPs are an emerging type of NMs with the highest degree of commercialisation. They are constituted by silver metal atoms, varying from small to numerous atoms stabilised by ligands, surfactants, polymers or dendrimers (DARGO et al., 2017). Therefore, they could show variable shape (e.g. spherical, wires, cubes, etc.), size (generally to 1 from 100 nm) and surface charge (YAQOOB et al., 2020).

Thereby, GO is used as a substrate for the growth and stabilisation of AgNPs. Thus, the conjugation between GO and AgNPs prevents them from aggregation. Moreover, the nanohybrid possess unique thermal resistance, electrical conductivity, optical transparency, mechanical strength and chemical versatility that are not available on its single counterparts. These exceptional physicochemical properties indicate its potential for applications in many fields, as materials science, nanomedicine, biotechnology and environmental technology.

The environmental health and safety (EHS) of NHs are primarily unknown. Given the altered physicochemical characteristics and emergent proprieties, the EHS could be distinct from the sum of the component NMs individually. Thus, it is prudent to understand how the hybridisation process influences their environmental risks (PLAZAS-TUTTLE et al., 2015). The scope of the current review is to summarise the potential environmental uncertainties of these emerging nanohybrid.

2.2. Synthesis strategies and characterisation of GO-AgNPs nanohybrids

Generally, graphene-based nanohybrids (Figure 1) could be categorised into two types: (i) nanohybrids formed when nanoparticles are decorated over the GO sheets (Figure 1B,E,H,) or (ii) nanohybrids formed when nanoparticles are encapsulated or coated with graphene sheets (Figure 1D,F,I).

Figure 1: Graphene-nanoparticle hybrid structures: comparison between graphene oxide (A,D,G), GO-decorated with AgNPs (B,E,H) and GO-wrapped AgNPs (C,F,I); Scanning electron microscope (SEM) images (A,B,C); Transmission electron microscopy (TEM) images (D,E,F); schematic illustration of GO and nanohybrids (G,H,I). Panels A and B reprinted with permission from Gurunathan et al. (2016); Panels C,F and I reprinted with permission from Minh et al. (2020). Panels D and E reprinted with permission from Kumari et al. (2020). Panels G and H reprinted with permission from Xiaoli et al. (2020)

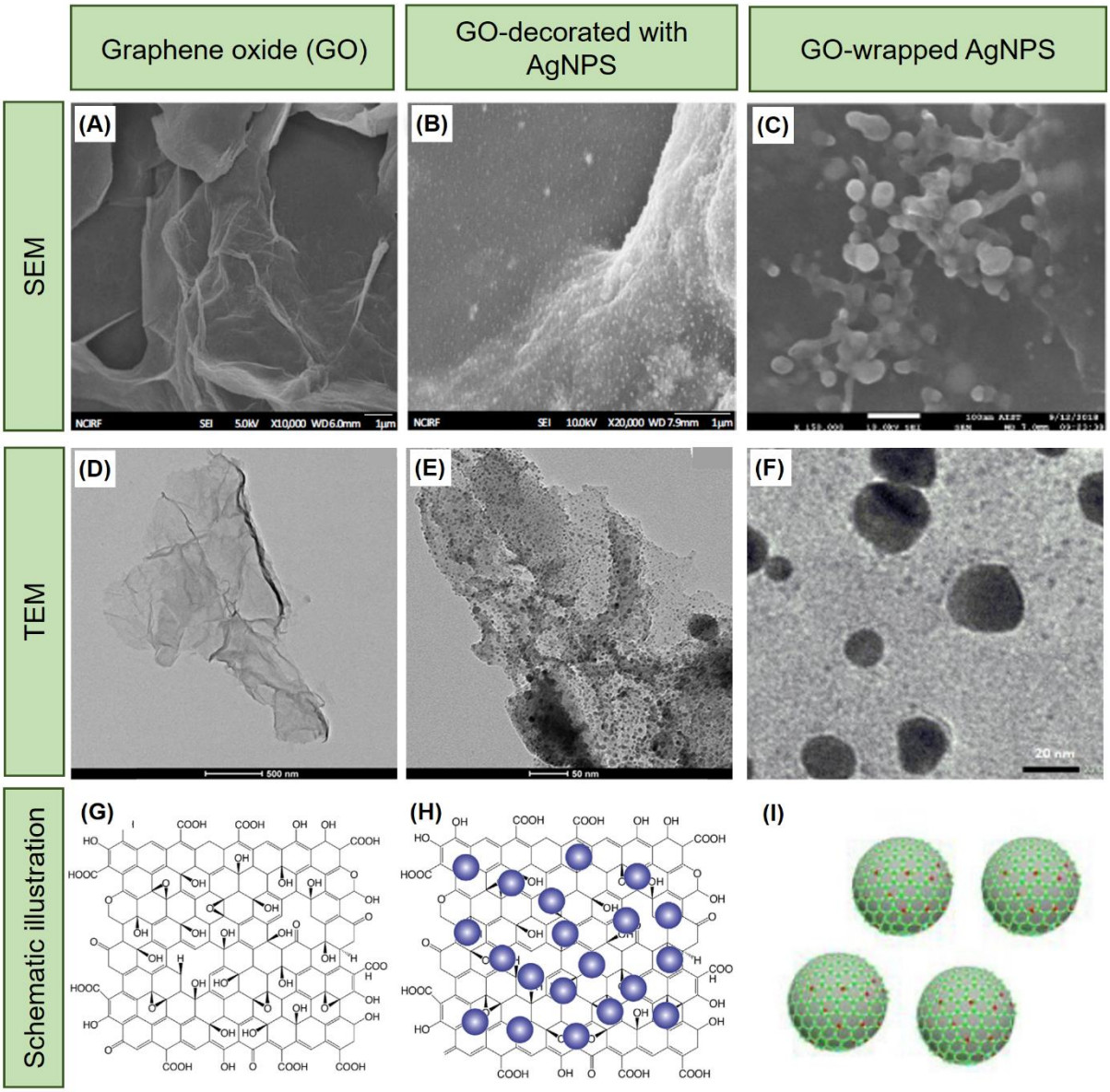

Several methods have been proposed to synthesise GO-AgNPs. Moreover, the most common technic is the chemical reduction of silver ions in GO aqueous dispersion in a bottom-up approach. In this procedure, the metallic salt (commonly $AgNO_3$) is mixed with GO in an aqueous suspension. The negative charge provided by hydrophilic groups (e.g. epoxy and hydroxyl groups) on the GO surface allows

attachment of free metal ions through electrostatic interactions. Subsequently, the reduction agent is added, and silver ions' reduction starts onto the GO surface, forming the GO-AgNPs nanohybrid (Figure 2).

Figure 2: Schematic procedure to synthesis GO-AgNPs nanohybrid by chemical reduction

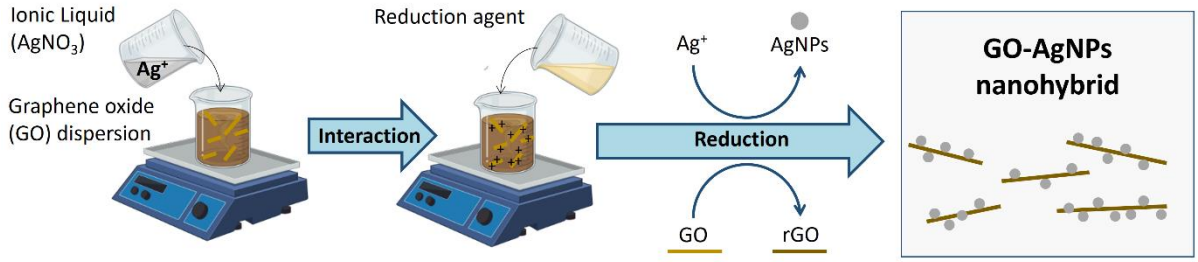

Various reduction agents could be used in this chemical reduction method, such as potassium hydroxide (PASRICHA et al., 2009), sodium citrate (FARIA et al., 2012); sodium borohydride (MAHMOUDI et al., 2015; AHMAD et al., 2020); hydrazine hydrate (ÇIPLAK et al., 2015) or dimethylformamide (LIU, C. et al., 2017). In addition, an environmental-friendly reducing agent could be used, for example, acid ascorbic (SHEN et al., 2011; AZIZ et al., 2017; COBOS et al., 2020), starch-based materials (HAN et al., 2013), sugars (KIM et al., 2018; SHAO et al., 2015) and plant extracts (NAZARI; MOVAFEGHI, 2018; SHI et al., 2018; THOMAS et al., 2020). Moreover, microwave irradiation could be applied to make the reaction faster due to uniform and rapid heating, reducing the barrier to AgNPs reaction, including its reduction, nucleation, and growth (CHOOK et al., 2012; HAN et al., 2013).

Other methods are described in the literature to synthesise GO-AgNPs. For example, strong ultrasonic irradiation (NOOR et al., 2016; KUMARI et al., 2020) or thermal treatment (ZAINY et al., 2012) could also reduce the Ag^+ to Ag in the presence of GO without using a reduction agent or surfactant. The hydrothermal method, a process that uses high temperature and pressure, is also used to induce the growth of AgNPs and reduce GO simultaneously (SHEN et al., 2011). The rotating packed bed reactor was used to create a high-gravity environment that increases mixture and mass transfer and allows the formation of AgNPs onto GO surface (HAN et al., 2016). Besides, due to carbocatalytic properties of GO, the GO-AgNPs could be synthesised using this inherent GO characteristic (GARG et al., 2020). Therefore, GO and $AgNO_3$ were just mixed in ultrapure water with pH 4, and the metallic ion clusters grow on

GO surface in the absence of harmful chemicals or physical methods. Moreover, *ex-situ* methods (i.e. premade colloidal silver nanoparticle which is jointed onto GO sheets) could also be applied (QIAN et al., 2013).

Besides the synthesis strategies, other parameters, such as the ratio between Ag^+ and GO (ÇIPLAK et al., 2015; KAVINKUMAR; MANIVANNAN, 2016, GARG et al., 2020) and the surface chemistry of GO (oxidation rate and debris fragments) (FARIA et al., 2012), critically influence NHs final characteristics, (e.g., AgNPs size, morphology, crystallographic patterns or silver load onto GO sheets).

Therefore, integrated characterisation is a crucial aspect of research in order to provide detailed information about structure and physico-chemical properties of NHs. In this way, chemical and physical techniques can access the NMs characteristics and verify if the material obtained has the desired properties. For example, the UV-Vis spectra of GO-AgNPs could be used to determine the AgNPs formation due to surface plasmon resonance (SPR). This phenomenon is the result of collective oscillations of conduction band electrons due to electromagnetic waves and it is size-dependent. Therefore, small AgNPs will show a peak of absorbance around 400 nm, and it disappears for NPs outside the nanoscale.

The main parameters that control the NH' biological activities are GO and AgNPs size, silver loading onto GO sheets, dissolution behaviour, and colloidal stability at biological media. As NHs characteristics could influence the toxicological outcome, the characterisation techniques play a pivotal role to establish the link between the NHs characteristics and (eco)toxicological profile.

2.3. Proprieties and application

Due to higher performance than singular NMs, NH material possesses an innovation potential and emerges as a promising material in many applications.

The synergetic effects of individual counterparts could be observed during its catalytic performance. Thu et al. (2013) observed a significant enhancement in 4-nitrophenol (4-NP) reduction when in the presence of GO-AgNPs compared to bare AgNPs. The half-life of 4-NP was 2.7 times higher in the presence of AgNPs than that with GO-AgNPs. The catalytic activity against an aromatic pollutant 2-nitroaniline (2- NA) reduction was reported by Naeem et al. (2019). Moreover, they also observed adsorptive removal of cationic and anionic dyes. Similarly, Kumari et al. (2020) have

demonstrated the photocatalytic properties of GO-AgNPs. Under UV-visible radiation, the nanohybrid degraded up to 88% of methylene blue (MB) dye while bare GO degradation is up to 64%. The underlying mechanism of GO-AgNPs photocatalysis can be assigned to the reactive oxygen species (ROS) generation, as shown in Figure 3. Altogether, these findings support the GO-AgNPs application for wastewater treatment.

Figure 3: Schematic overview of photodegradation of methylene blue (MB) dye using GO-AgNPs nanohybrid under UV light irradiation (KUMARI et al., 2020)

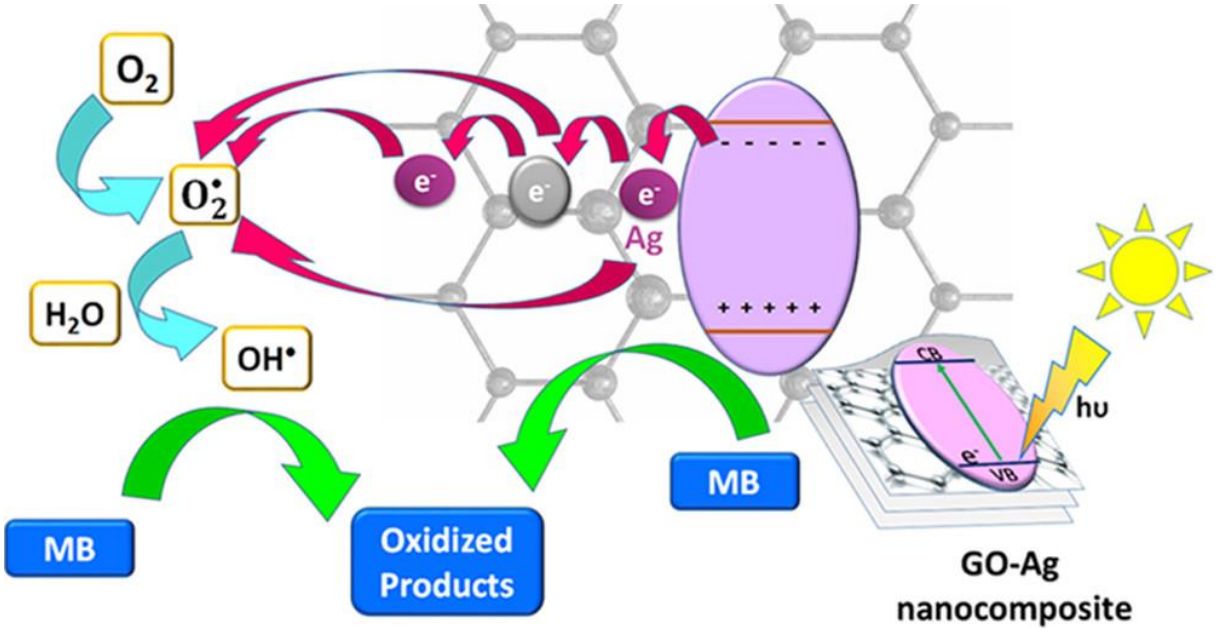

The benefits of GO-AgNPs application could be observed in others fields. For example, AgNPs are applied in forwarding osmosis membrane for water desalination as a biocide agent to prevent biofouling and pomote virus removal (ZODROW et al., 2009; SAWADA et al., 2012). However, the use of AgNPs shows some disadvantages, as agglomeration and detachment from the membrane surface. The attachment of AgNPs onto GO enhances the stability and reduces these problems. In addition, the nanohybrid incorporation increased hydrophilic properties and bacterial inactivation, improving the membrane transport properties (SOROUSH et al., 2015).

Interestingly, GO-AgNPs could also be applied to the removal of organohalides (pesticides). Koushik et al. (2016) showed the degradation (by dehalogenation) of the target pollutants due to the presence AgNPs followed by adsorption onto the GO surface.

Due to its multiple functions and enhanced performance than single components, such as improvements in effective surface area and higher electron transfer rate, the NHs could be applied as electrochemical sensors and biosensors. The GO-AgNPs nanohybrids show less tendency towards self-agglomerations due to the noble metal nanoparticle that acts as spacer and conductor of GO sheets and, consequently, enhances electrical conductivity. For example, the GO-AgNPs could be utilised for the detection of multiple nucleic acid targets (TAO et al., 2012), tryptophan (LI et al., 2013), ammonia (KAVINKUMAR; MANIVANNAN, 2016), hydrogen peroxide (NOOR et al., 2016), glucose (HOA et al., 2017), 4-nitrophenol (AHMAD et al., 2020) and even avian influenza virus H7 (AIV H7) (HUANG et al., 2016).

The detection of biological and chemical molecules by GO-AgNPs could also be mediated by surface-enhanced Raman spectroscopy (SERS). The silver nanoparticle is a promising material for fabricating substrate for SERS detection due to the stability and sensitivity provided by the local surface plasmon resonance effect. Furthermore, GO is an emergent material as SERS substrates due to strong chemical enhancement, extinguishing of target fluorescence, and high adsorption capacity (SHARMA et al., 2017).

Thus, the presence of AgNPS onto GO creates hot spots for strong electromagnetic field enhancement and makes it a potential SERS substrate for ultra-sensitive detection (QIAN et al., 2013). Furthermore, the GO-AgNPs nanohybrid can detect analytes at low concentrations (even if it was a single molecule) due to the synergistic effect between components (FAN et al., 2014). Its application as a SERS-based sensor has been reported for the detection of dye molecules (XIE et al., 2012; SHI et al., 2018; LIU et al., 2020), L-Theanine (essential amino acid) (ZHENG et al., 2017), and paraoxon (an organophosphate pesticide) (JIANG et al., 2018).

Moreover, mediated by SERS, GO-AgNPs could be applied for fast cellular probing and imaging of living cells without cytotoxicity (YIM et al., 2015). This nanoprobe produced an intense Raman signal that makes it possible to detect a target in a complex biological system. For this purpose, Liu et al. (2013) covalently functionalised the nanohybrid with folic acid molecules. Thus, the nanoprobe could achieve selective cancer cells with folate receptors (FR). The Raman intensity was 2 orders of magnitude higher in FR-positive cells (cervical cancer - HeLa) than FR-negative cells (adenocarcinoma human alveolar basal epithelial - A549).

In addition, the uptake is more elevated in HeLa cells, and, consequently, it showed accumulation of NHs on the plasma membrane.

Due to its biocompatibility, others biomedical applications are suitable. Kundu et al. (2017) reported the use of GO-AgNPs NHs with protein capped (human serum albumin and bovine serum albumin) as contrasting agents for X-ray computer tomography (CT). They notice the enhancement of bone tissues of mice models on *in vivo* images. Moreover, they also observed the potential use of this NH as a drug carrier. The K562 cancer cells co-exposure with nanohybrid and Imatinib, a tyrosine kinase inhibitor used in cancer therapy, show a synergistic drug carrier effect that decreases cell viability.

2.3.1. Antibacterial activity

The development of drug resistance (or even multi-resistance), caused by overuse of antibiotics, resulted in inadequate treatment efficacy of bacterial infections. Nanotechnology arises as an alternative in the treatment against (multi) drug-resistant bacterias. It is well known that silver nanoparticles exhibit high toxicity to microorganisms even at small concentrations and could be used as an alternative to antibiotics. Thus, AgNPs were widely applied as antimicrobial agents and are currently being used in many commercial products.

The key mechanism for AgNPs to exert biocidal activity toward bacteria is still not fully understand. However, some possible targets that lead to cell death involve losing membrane integrity and the generation of reactive oxygen species (ROS) and free radical species, which could attack other enzymes and proteins, causing damage to DNA replication (DURÁN et al., 2016).

The colloidal dispersion of AgNPs is stabilised through electrostatic repulsion. A dispersion is stable if particle size continues the same over time, without clumping, and remains in suspension. However, it could become unstable in biological media due to salts' presence, which increases the ionic strength. Furthermore, the aggregation behaviour is undesirable because it decreases the particle/cell surface interaction and negatively affects biocidal activity. Some surfactants (NaDDBS, SDS, TW80, CTAB) or polymers (PVP, PAA, PAH, CMC) could be used as stabiliser agents to increase AgNPs colloidal dispersion stability and avoid aggregation. Nevertheless, the capping agent could influence the toxic profile. Therefore, the GO could be an alternative to

prevent AgNPs aggregation in the absence of the stabilising agent or surface modification.

Additionally, GO also displays antibacterial activity. The sharp edges of GO flakes can act as "nano knife" and "cut" the bacterial membrane. Moreover, GO could generate oxidative stress on bacteria cells. Consequently, the GO exposure towards bacteria results in membrane dysfunction and bacteria inactivation (CHEN et al., 2014).

One example of the application of GO-AgNPs against antibiotic-resistant (methicillin-resistant) microorganisms was reported by De Moraes et al. (2015). In this instance, GO-Ag's minimum inhibitory concentration (MIC) was 15 μg mL^{-1} against methicillin-resistant *Staphylococcus aureus*. The MIC between bacteria with and without antibiotic resistance was almost identical, indicating the resistance mechanism doesn't influence the toxic effects. Moreover, no toxicity was observed for pristine GO or bare-citrate AgNPs, even at the highest concentration of 60 and 80 μg m^{-1}, respectively. Thus, the conjugation between nanoparticles plays an important role in bacteria inactivation.

The synergic effect of the individual components is also observed by Prasad et al. (2017). At the same concentration (100 mg L^{-1}), GO-AgNPs nanohybrid exhibited a higher zone of inhibition by agar diffusion method than reduced GO or AgNPs against Gram-positive *S. aureus* and Gram-negative *E. coli* and *P. mirabilis*. Moreover, the antibacterial activity of GO-AgNPs was superior to nitrofurantoin, a systematic antibiotic.

Looking to enhance the antibacterial activity of AgNPs, Cai et al. (2012) synthesised a polyethyleneimine-GO–AgNPs (PEI-rGO–AgNPs). The nanohybrid showed an extended ion release than PVP-AgNPs and good colloidal stability. After 6 hours of exposure against *E. coli* e *S. aureus*, the bacterial kill rate was higher than the single nanomaterial exposure (AgNPs and GO). The increase in the AgNPs stability and control of Ag^{+} release is an important factor for application as sprayable antibacterial dispersion.

Another design approach to enhance the efficiency of GO-AgNPs was realised by Ullah et al. (2018). They synthesised the GO-based nanohybrid using tobramycin (TOB), an aminoglycoside antibiotic, as a reducing agent of $AgNO_3$. As a result, the nanohybrid TOB-GO-AgNPs displayed the highest antibacterial efficacy of the single counterparts (GO, AgNPS and TOB). The synergetic action of components could be

attributed to the positive charge, which increases the electrostatic interaction with nanoparticles and lipopolysaccharides of the *E. coli* membrane and the controlled release of Ag ions. Moreover, they reported severe bacteria membrane disruption of bacteria treated with the nanohybrid and enhance intracellular reactive oxygen species (ROS), which lead to bacteria cell inactivation.

In general, the peptidoglycan membrane layer (characteristic of gram-negative bacteria strain) could act as an additional layer of protection on bacteria cells from attack by foreign compounds. However, this characteristic does not prevent the GO-AgNPs toxicity since the nanohybrid can kill common gram-negative/gram-positive bacterial strains (SHAO et al., 2015; KELLICI et al., 2016; COBOS et al., 2020; THOMAS et al., 2020).

Due to the surface plasmon resonance of the AgNPs, the photocatalytic activity of nanohybrids could be induced under irradiation, increasing the antimicrobial activities by photoinactivation. GO-AgNPs associated with blue light irradiation (~450 – 470 nm, during 45 min at 9.5 $mW.cm^{-2}$) enhance bacterial inactivation around 90% against *S. aureus*. The possible mechanisms involve disrupting the bacteria cell wall and the DNA damage by oxidation (CAIRES et al., 2020). Similarly, Chen et al. (2020) also reported the synergistic effect of nanohybrid and the enhancement of antibacterial efficiency with photo-thermal assistance (with energy near-infrared laser light) against multi-drug resistant *Escherichia coli*. At 14 mg L^{-1}, GO-AgNPs show a reduction at ~4% of bacteria viability. In association with photo-thermal treatment, the complete cell inactivation could be achieved with an exposure of 7.0 mg L^{-1}. The exposure provoked disruption of bacteria cell integrity as observed by SEM images.

Moreover, the GO size could affect the antibacterial activities, as Truong et al. (2020) reported. They observed a significant enhancement of antibacterial activity against *E. coli* of large GO (> 1 μm) than small GO (~100 nm). The oxygenated groups (–OH and –COOH) of GO could interact with the amino acids of the bacterial wall. Large GO entrap the bacteria cell as observed by TEM and, consequently, induce a higher ROS production.

Similarly, GO-AgNPs produced with larger GO showed higher antibacterial activity. Three possible mechanisms could explain the results: (i) large GO-AgNPs facilitate the contact between NHs and bacterial membrane and produce more damage in bacterial morphology; (ii) larger NHs showed a higher Ag content and, consequently, higher Ag^{+} release and (iii) higher generation of ROS.

Thus, the synergetic effects of NH components could explain the toxicity mechanism towards bacteria (Figure 4). The GO in contact with the bacteria wall could entrap it, and the sharp edges could disrupt the bacterial membrane. The membrane destruction also could occur by the extraction of phospholipids. Moreover, this interaction allows a high local concentration of silver near the bacteria, which increases the permeation of Ag^+ into bacteria. The nanohybrid exposure caused ROS overproduction. The failure to repair oxidative damage (i.e. imbalance between the production of ROS and/or insufficient detoxication by the biological system) could lead to the oxidation of cell membrane lipids and amino acids and, consequently, lead membrane cell and DNA damage and further bacteria inactivation (PRASAD et al., 2017; ABDALLA et al., 2020; TRUONG et al., 2020).

Figure 4: Schematic of the potential antimicrobial mechanism of GO-AgNPs. The absorbing and capturing behaviour of GO sheets might improve the temporary concentration of AgNPs close to the bacterial cells as AgNPs, causing severe damage to bacteria generating Ag^+ and increasing the generation of reactive oxygen species (ROS). (BAKHSHESHI-RAD et al., 2020)

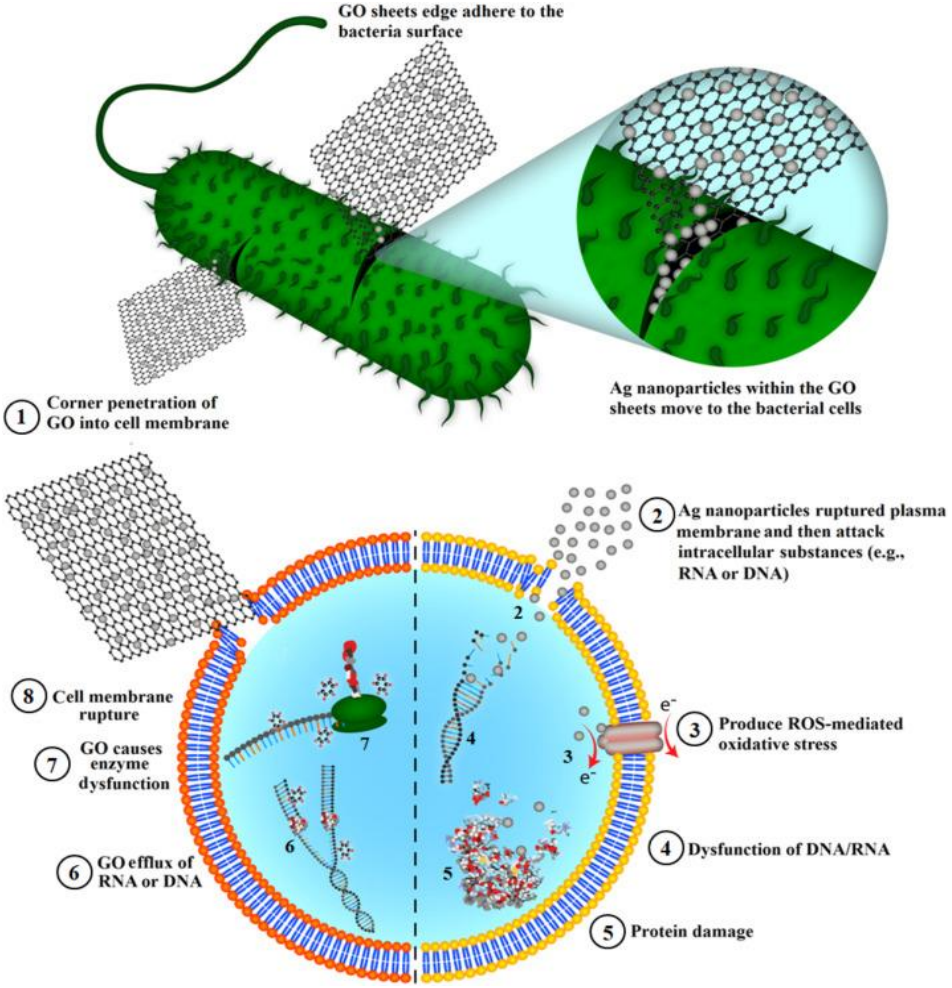

Biocompatibility plays a key role in clinical application of NHs. To address these problem, other substances could be co-incorporated with GO-AgNPs to improve the antibacterial properties and enhance cytocompatibility, aiming for bioapplications.

Thereby, Xie et al. (2017) wrapped the NHs with collagen. They incorporated the nanomaterial on Ti plate treated with dopamine hydrochloride (PDA) towards clinical application as implants. The incorporation of AgNPs on GO sheets increased the bacterial activity against *E. coli* e *S. aureus*. They observed damage to the bacterial membranes. Moreover, after 20 min of irradiation under 660 nm, the antibacterial efficiency achieves 96.3% and 99.4% towards *E. coli* e *S. aureus* due to photocatalytic capability that enhances ROS generation. *In vitro* studies showed the collagen coating increased MC3T3-E1 (osteoblasts) cell viability and *In vivo* studies confirmed the antibacterial activities and the good biocompatibility in mice. After the inserts, the implants with nanohybrids show fewer neutrophils inflammatory cells, indicating antibacterial properties and no tissue necrosis.

Another biomedical application was investigated by Zhou et al. (2016). First, the GO-AgNPs nanohybrid was synthesised and functionalised with poly-diallyldimethylammonium chloride (PDDA). The final AgNPs size anchoring on GO sheet was smaller when the reduction happens in the presence of PDDA. Due to photocatalyst properties, they reported an increase in bactericidal efficiency towards *E. coli* and *S. aureus* under visible light irradiation. Finally, they applied these nanohybrid in burn wounds in mice. The treatment with nanohybrid shows a faster wound closure than the positive control (sterilised deionised water). Beyond the bactericidal activity, the PDDA content could stimulate collagen formation, leading to complete healing after 14 days.

Another reporting demonstrating the potential use of nanohybrid due to its antibacterial performance was provided by Bakhsheshi-Rad et al. (2020). They co-incorporation the hybrid into polylactic acid (PLLA) fibrous for use in orthopaedical applications. Besides the antibacterial activity towards *E. coli* and *S. aureus*, the incorporation of nanohybrid reduced the degradation rate of Mg alloy (which provided a better environment for living bone cells) and enhanced the strength of the implants.

Taken together, GO-AgNPs nanohybrid can bring synergistic advantages to a wide variety of bioapplication because it could act as a biocompatible substrate and provide antibacterial protection.

2.3.2. Antifungal activity

Besides antimicrobial activity, AgNPs also possess antifungal activity. Looking for this promising application in clinical treatment against resistance strains, Li et al. (2013) evaluated the antifungal activities of GO-AgNPs against *Candida albicans* and *Candida tropical*. After incubation of GO-AgNP, an inhibition zone was observed, while GO and AgNPs didn't show inhibition on yeast growth. Moreover, they didn't report changes in yeast morphology after exposure to GO. However, the contact with GO-AgNPs induces loss of membrane integrity and partly releases cytoplasm, as observed in SEM images. Overall, the GO-AgNPs nanohybrid shows a potential application in control yeast infection.

Similarly, Chen and co-workers have demonstrated the antifungal activity of GO-AgNPs nanohybrids against the phytopathogen *Fusarium graminearum* (CHEN et al., 2016). The minimum inhibition concentration (MIC) of spore germination was 4.68 μg $mL^{-1,}$ and it was 3- and 7-fold higher than AgNPs and GO singly exposure. Thus, the GO-AgNPs show a synergistic effect of counterparts on the inhibition efficiency. Moreover, these results show the potential use of GO-AgNPs as an antifungal agent.

2.3.3. Antiviral activity

Viral infections are one of the world's challenges due to their widespread distribution and generation of new pathogens through genetic mutation. The nanomaterials arise as antiviral systems with a broad spectrum action (INNOCENZI; STAGI, 2020; REINA et al., 2020).

The antivirus activity of GO-AgNPs nanohybrids towards feline coronavirus (FCoV), a single-stranded RNA with lipid enveloped virus of Coronaviridae family, and infectious bursal disease virus (IBDV), double-stranded RNA virus without an envelope of Birnaviridae family, was reported by Chen et al. (2016). With 0.1 mg L^{-1} of GO-AgNPs nanohybrids, inhibition of infection by FCoV of 24,8% was observed. Towards IBDV virus, 1 mg L^{-1} exhibited inhibition of 22.7% of infection. Furthermore, pure GO only showed antiviral activity towards FCoV at a non-cytotoxic concentration. The higher antiviral mechanisms of GO and GO-AgNPs towards enveloped viruses could

involve the interaction and rupture of the lipid membrane due to the negative charge of GO and the positive charge of the lipid membrane (Figure 5).

Figure 5: Schematic for the antiviral mechanisms of (A) graphene oxide (GO) against the enveloped virus; (B) graphene-silver nanocomposites (GO-Ag) against the enveloped virus; (C) GO against the non-enveloped virus; (D) GO-Ag against the non-enveloped virus (CHEN et al., 2016)

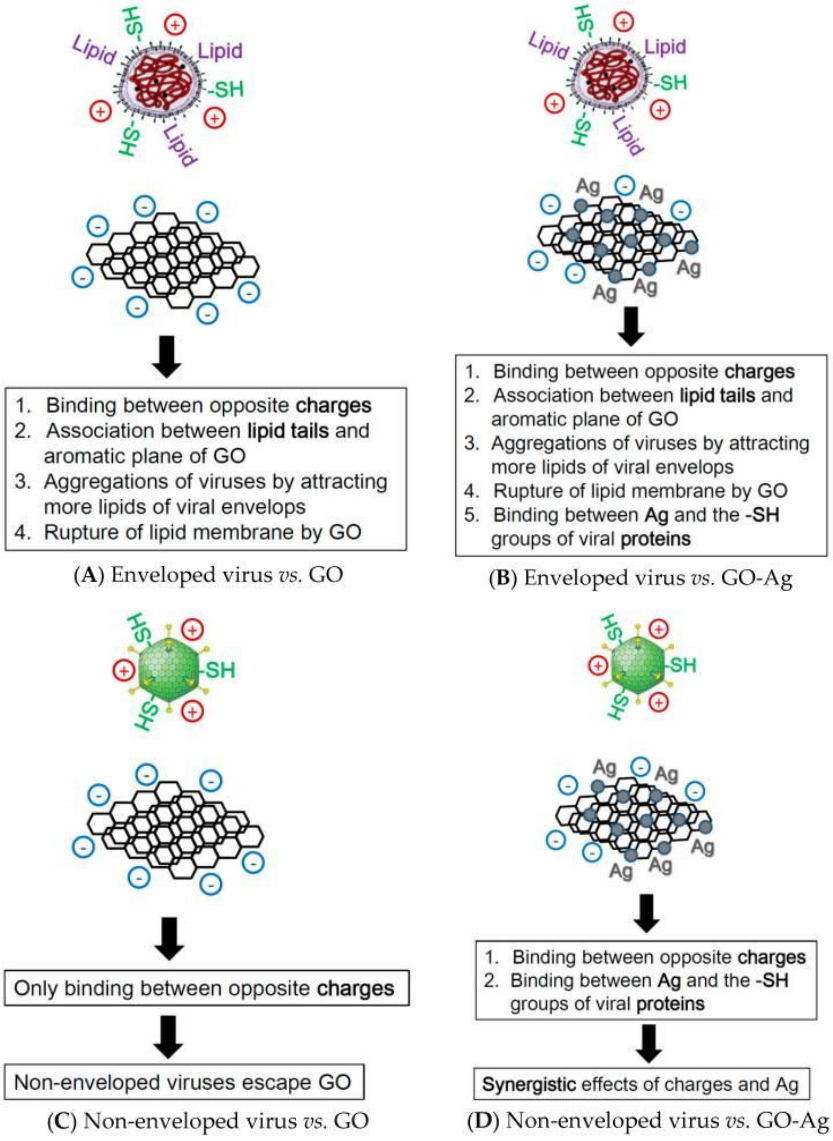

Similarly, the potential application of GO-AgNPs to prevent viral infection was realised by Du et al. (2018). They observed a better inhibitory activity after GO-AgNPs exposure than GO or AgNPs. The inhibition efficiency of 4.0 μg mL^{-1} was 59.2% towards the porcine reproductive and respiratory syndrome virus (PRRSV). Interestingly, besides inhibiting virus entry to host cell and its replication, another

mechanism suggested was activating natural immune response by the up-regulated production of interferon genes.

2.4. Biocompatibility

Biocompatibility refers to the ability of a material to perform an appropriate cell response without toxic or harmful effects. Moreover, it is indispensable for further biological and biomedical appliances. For instance, living cells' response upon NHs exposure is extensively investigated.

The GO-AgNPs nanohybrids can be either biocompatible or toxic to cells. Several groups have reported low cytotoxicity of GO-AgNPs nanohybrids (CAI et al., 2012; SHAO et al., 2015; ANGULO-PINEDA et al., 2019; WIERZBICKI et al., 2019; BAKHSHESHI-RAD et al., 2020). In contrast, other authors reported a loss of cell viability due to oxidative stress generation, loss of membrane integrity (YUAN et al., 2021), DNA damage (ALI et al., 2018) and induction of apoptosis (KHAN et al., 2016). Even enhancing the cell uptake and, consequently, metal intracellular quantity when AgNPs are conjugated to GO sheets than to pristine AgNPs was observed (ZHOU et al., 2014).

These apparently controversial reports could be related to NMs physicochemical proprieties (GO lateral size, purity, silver loading, AgNPs shape, and size), cell media (e.g., presence of biological molecules as fetal bovine serum supplementation, ionic salts), colloidal stability (agglomeration/sedimentation state which influence the NMs dose metrics); mode of exposure (conventional submerged culture, NMs surface presentation, inverted cell culture, air-liquid interface exposure, chip advice) and cell characteristics (cell type, monoculture, co-culture, spheroids, organoid) that critically influence on the response of living cells (DRASLER et al., 2017; GUGGENHEIM et al., 2018; CAO et al., 2021). Thus, a proper understanding of how NHs interact with cells is crucial for further bioapplications.

Once administrated, the NHs will suffer attack by macrophages, a cell involved at the front-line defence mechanism of the innate immune system against foreign objects. Thus, comprehend the toxicity of NHs on immune cells is crucial to graphene-based biomedical applications. For instance, Luna et al. (2016) reported that GO-AgNPs exhibited lower cellular viability than their counterparts against J774 (macrophages tumoral lineage) and peritoneal macrophages collected from Balb/c

mouse. They also observed higher levels of reactive oxygen species (ROS) after the nanohybrids exposure and could be the reason for increased toxicity. Furthermore, transmission electron microscopy (TEM) images showed that GO-AgNPs were internalised and degraded inside J774 macrophages. Interestingly, the cells after GO-AgNPs exposure showed 60% less silver concentration than the cells exposed to pristine AgNPs, indicating a difficult NHs cellular uptake.

Additionally, GO-AgNPs induced late apoptosis/necrosis on J774, while GO mainly induced early apoptosis. Despite its toxicity, the GO-AgNPs did not enhance the production of inflammatory cytokines (e.g. IL-β and TNF-α). Moreover, nitric oxide (NO) production did not affect at sublethal levels of GO-AgNPs exposure, suggesting their response against intracellular invaders remains. Thus, GO-AgNPs show important features for safe nanomedicine applications as their exposure didn't modify in an inflammatory microenvironment (LUNA et al., 2019).

The ability to kill cancer cells selectively is also a desirable feature. As observed by Ali et al. (2018), the human normal (CHANG) and cancerous liver (HepG2) cell lines could respond differently after GO-AgNPs exposure. The GO-AgNPs were able to reduce cellular viability by affecting the integrity of the cellular membrane, increasing ROS production, reducing mitochondrial membrane potential, and enhancing DNA fragmentation. Interestedly, HepG2 cells show be slightly more susceptible than CHANG cells.

Another potential application in cancer therapy is the combination of NMs and chemotherapeutic drugs. To this end, Yuan and Gurunathan (2017) co-exposure GOAgNPs and Cisplatin (CIS) towards human cervical cancer (HeLa) cells. They observed a significant increase of cytotoxicity by ROS-mediated mitochondria-dependent apoptosis, overexpression of pro-apoptotic genes (P53, P21, BAX, BAK, CASP3, and CASP9), a decrease of anti-apoptotic genes (BCL2 and BCL2L1), and an increase of DNA damage when the cell was exposed to a combination of CIS and GO-AgNPs. Therefore, the GO-AgNPs lead to more pronounced effects of CIS in HeLa cells.

Similarly, Choi et al. (2018) reported the cellular response of human ovarian cancer cells and ovarian cancer stem cells (OvCSCs) to GO-AgNPs and its combination with the therapeutic drug salinomycin. The GO-AgNPs exposure significantly reduced the number of colonies, increased ROS generation, led to membrane damage, reduced mitochondrial membrane potential, enhanced pro-

apoptotic gene expression, and down-regulated the anti-apoptotic that trigger cell apoptosis. The combination with salinomycin induced 5-fold higher levels of apoptosis, especially against the cells with high tumorigenic potential (ALDH+CD133+ cells). Thus, the combination treatment with NHs and salinomycin could enhance the treatment efficiency to remove tumour-initiating cells.

Another therapeutic approach against cancer cells is photodynamic therapy. This treatment modality uses a combination of a photosensitiser agent and a specific light source to kill cancer cells. The enhance of effect between the photosensitiser agent and the light source is very desirable. To investigate the application of nanohybrids in chemo-photodynamic therapy, Habiba et al. (2015) tested simultaneously graphene quantum dots decorated with silver nanoparticles (GQDs-AgNPs) as delivery of chemotherapy drug and photosensitiser against HeLa (human cervical cancer) and DU145 (human prostate cancer) cell lines. The cell viability with Vero (normal monkey kidney) cells was also evaluated to compare the cellular response with a normal cell. The increase of apoptosis of cancer cells with enhancements of caspase activity without affecting the viability of normal cells was observed when the cells are co-exposed with nanohybrid and chemotherapy drugs (doxorubicin). The combined exposure with doxorubicin and 425 nm irradiation enhanced the treatment efficacy remarkably compared to treatment by using each modality alone, suggesting the potential application as a photosensitiser in photodynamic therapy against cancer cells.

Therefore, GO-AgNPs could be potentially applied as an adjuvant agent to improve the therapeutic effect of chemotherapy, looking for treatments with lower systemic side effects, higher efficacy, and the reduction of drug resistance. Overall, many promising applications rise of GO-AgNPs nanohybrid in biomedicine applications.

2.5. Environmental nanosafety aspects

With the extensive research and promising applications of NHs in diverse fields, the release of GO-AgNPs into the environment in all stages of the life cycle of products containing the NH is inevitable (PARK et al., 2017). To minimise undesirable hazards impacts on human and environmental health, the idea of "Safer-by-Design" has gained increasing attention in the field of nanoscience and technology (HUTCHISON, 2016).

This approach to developing new nanomaterials at an early stage of their synthetic production and research development involves understanding how physical-chemical proprieties influence toxicity and the ability to modify these factors during synthesis or manufacture (LIN et al., 2018). Thus, the new NHs materials could be a strategy to design new nanomaterials with enhancing multifunctionality and lower ecotoxicity.

The ecotoxicological effects could be distinct from the sum of their pristine counterparts. Thus, understanding the environmental impacts of emerging nanohybrids is mandatory for sustainable nanotechnology (SALEH et al., 2014). However, despite many studies addressing the toxic effects of graphene family and silver nanoparticles in various organisms that have been reported, limited data are available concerning the health risks of nanohybrids exposure. Thus, the modification due to hybridisation on environmental health and safety (EHS) is uncertain.

The toxicity effects of nanomaterials can occur at different trophic levels (microorganisms, invertebrates, and vertebrates). Thereby, the *in vivo* models provided insights into understanding nanoecotoxicology (ÁVILA et al., 2018).

One of these organisms is algae. They are included in hazard assessment as a representative of the primary aquatic producer. To this end, Nazari and Movafeghi (2018) analysed the effects on *Chlorella vulgaris* of exposure GO-AgNPs. To compare, they also expose the microalgae to bare GO. Even though they didn't observe any hazardous effect due to GO exposure, GO-AgNPs reduced the cell viability to 57,82% after treatment at the concentration of 30 mg L^{-1}. Additionally, they observed changes in cell morphology, alterations in the activity on ROS-scavenging systems (e.g., catalase, superoxide dismutase, and ascorbate peroxidase), and the reduction of photosynthetic pigments contents.

As discussed previously, the physical-chemical characteristics could modify the biological response. To analyse it, Nazari et al. (2020) synthesised GO-AgNPs using the micro-wave technique and compared the previous study results that used the hydrothermal method. The characteristics of both GO-AgNPs was very similar, except for the silver loading that was lower in NH synthesised by hydrothermal technic. They observed the same mechanism response. However, these GO-AgNPs owned higher toxicity than NH prepared by conventional techniques. Thus, the silver content is an important factor in the toxicity of NH.

Another study that uses alga to assess the toxic effect of NH exposure was conducted by YIN et al. (2020). They investigated six GO-based nanohybrids (GO-

AgNPs, GO-AuNPs, GO-Pd, GO-Fe_3O_4, GO-Co_3O_4, GO-SnO_2) on two species of algae (Scene*desmus obliquus* and *Chlamydomonas reinhardtii*). They reported the GO-AgNPs lead to higher impairments than other nanohybrids on both algae species, enhancing oxidative stress and membrane permeability and reducing chlorophyll-a pigment even at low concentration (0.2 mg L^{-1}). Moreover, the *C. reinhardtii* was more sensitive than *S. obliquus*. The difference in the biological response could be attributed to higher hydrophobic and abundant components of *C. reinhardtii* cellular surface, which led to more metal ion adsorption and contributed to interaction with NHs. Thus, understanding the mechanisms of interaction between nanomaterials and biological barriers, as cellular membranes, could help design new nanomaterials design looking to modulate the hazardous effects due to its exposure (MENG et al., 2018).

Similarly, Liu et al. (2017) also analysed the impairment of six GO-based nanohybrids (GO-AgNPs, GO-AuNPs, GO-Pd, GO-Fe_3O_4, GO-Co_3O_4, GO-SnO_2) in a transgenerational study on *Daphnia magna*. Due to its well-known ecology and filter feeder behaviour, this planktonic microcrustacean is commonly applied as a water quality indicator. Between all nanohybrids, the GO-AgNPs showed a higher toxic profile. Unfurtelly, the GO-AgNPs exposure induced significant acute toxicity, and almost 100% of daphnids was dead after 24 hours of exposure at the concentrations studied (0.2 to 1 mg L^{-1}). Thus, reproduction, adult size and time of the first brood could not be evaluated for this treatment.

Another extensively applied model in aquatic toxicology is the *Danio rerio* (Zebrafish). The unique set of characteristics it possesses, such as a small body, high fecundity, rapid development with well-characterised stages and easy handling raise it as an up-and-coming promising alternative for *in vivo* toxicity assessments (NOYES et al., 2016). Moreover, the transparency of the embryo allows the visualisation development of major organs. Thus, it makes it possible assessment teratogenic effects induced by nanomaterials exposure (PEREIRA et al., 2019). Among all these advantages, the zebrafish could be used as a model for environmental and human safety due to the high level of resemblance among zebrafish and the human genome (~75 % of similarity) (CHAKRABORTY et al., 2016)

The zebrafish embryo toxicity (FET) test was utilised by De Medeiros et al. (2021) to assess the impairments through initial fish development upon GO-AgNPs exposure. Moreover, they also analysed the influence of co-exposure with natural organic matter (NOM) and chorion egg membrane removal, looking towards more

environmentally realistic scenarios and standardised nanotoxicity testing. The larvae did not show any morphological impairments due to GO exposure, even at high concentration (100 mg L^{-1}). Nevertheless, the larva exposure to GO-AgNPs show notochordal deformation and the presence of edemas. The LC_{50} (concentration that kills 50% of embryos during 96 hours) is 1.5 mg L^{-1}. The presence of NOM mitigated mortality, and LC_{50} changed to 2.3 mg L^{-1}. The removal of chorion allows exposure at the beginning of organogenesis. The naked embryo is more susceptible to GO-AgNPs, and the LC_{50} shifts to 2.3 and 1.2 mg L^{-1} in the presence and absence of NOM.

The interaction with natural macromolecules (such as NOM) forms a unique coating known as corona formation (XU et al., 2020). These transformations inevitably occurs in natural compartments and modify the bioavailability, biocompatibility, and toxicity of pristine nanomaterials (NASSER et al., 2020). The impact of corona on NMs dynamics (i.e., colloidal stability, dissolution, etc) and EHS is a current challenge on nanotoxicology research (WHEELER et al., 2021).

Paranthaman and Das (2018) also analysed the toxicity of GO-AgNPs on zebrafish. They functionalised the GO-AgNPs with Poly-cationic peptides (PCP), looking towards a safe-by-design strategy. The PCP functionalised GO-AgNPS showed higher antibacterial activities and prevent biofilm formation against *E. coli* and *P. aeroginosa* than bare GO-AgNPs. Moreover, the silver ions concentration at supernatant after 120 hours of incubation of NHs in 50 mM phosphate buffer was measured by inductively coupled plasma optical emission spectrometry (ICP-OES) looking towards AgNPs dissolution. The GO-AgNPs reached saturation level (0.6 mg L^{-1}) after 60 h. Conversely, PCP functionalised GO-AgNPs dissolution was not detected.

The dissolution rates reflect on the biological assay. The mortality and histopathological changes in gills and intestines of adult zebrafish were analysed upon supernatant exposure. The GO-AgNPs supernatant lead mortality of fishes within 4 days and abnormal appearance in belly skin was also noticed. They also observed histological abnormalities, such as loss of different primary and secondary gill filaments and alterations in the lamina propria, muscularis externa, and serosa, leading to a thinner epithelial layer of intestine tissue. On the other hand, the supernatant from PCP functionalised GO-AgNPS incubation did not affect fish, probably due to a low dissolution rate. Thus, the authors show a successful strategy towards acquiring more efficient NHs and minimise the toxicological impact.

Upon release, the soil could also be a fate of the nanomaterials, and its presence could impact its biota. Due to GO-AgNPs distinct antibacterial activity, Kim et al. (2018) conducted a study towards its impacts on soil bacteria microbiota. GO-AgNPs modify the soil bacterial community composition. GO-AgNPs enhance the abundance of phylum *Firmicutes*, which bacterias can survive to extreme conditions as soil polluted with metals trace. They observed that GO-AgNPs exposure decreased the relative abundance of Acidobacteria and Cyanobacteria. Acidobacteria use sugars, hemicellulose, and cellulose as carbon sources and could be are involved in nitrogen-cycle processes. Cyanobacteria play a crucial role in N_2-fixation, so it is essential to promote plant growth in soils. In addition, the GO-AgNPs reduce the C-cycling enzyme activity and inhibited nitrification, probably as a consequence of microbiota alteration.

Besides the soil bacteria community, the GO-AgNPs also impact the plants, as Kim et al. (2020) observed. They analysed the effects of GO-AgNPs on seed germination and early growth of crop species (alfalfa, radish and cucumber). The GO-AgNPs lead H_2O_2 accumulation higher than AgNPs exposure. Moreover, the plants exposed to NHs shows Ag accumulated in the seedlings. Thus, concerns transferred to higher trophic levels also need to be explored.

Another terrestrial group of organism that could be affected by the disposable of NHs is the insects. This class of arthropods is found in various environmental conditions and is a crucial component of the food chain. Moreover, some species could be beneficial and act as pollinators, weed killers, productive insects, scavengers, and decomposers. Looking towards the effects of GO-AgNPs against the insects, Alian et al. (2021) availed the impairment due to oral uptake of nanomaterials (GO; 20 μg g^{-1} food; AgNPs; 400 μg g^{-1} food and GO-AgNPs; 20:400 μg g^{-1} food) on female house crickets (*Acheta domesticus*). The GO-AgNPs lead to a disturbance in the energy budget. During 0-3 days, the crickets significantly reduced the consumption of food. However, the digestive enzymes increase their activity and food uptake between 3-6 days of exposure as a compensatory response. Thus, the response profile is typical for a hormetic response. Interestingly, the GO-AgNPs impairments were lower than the individual sum of response from pristine counterparts, showing the potential alternative design to more suitable nanomaterials.

Overall, little information is already available for assessing potential hazards, exposure, and risks of NHs. Moreover, awareness of the hazard potential and a proactive attitude to avoid this promising material's safety issues are necessary.

2.6. Data gaps and challenges for nanohybrid environmental implication studies

The new physical-chemical characteristics that arised during hybridisation modified how this new NM will interact with the environment and, consequently alter its transport, final fate, transformation, and toxicity (Figure 6). Thus, it is highly recommended the nanomaterials characterisation is an essential step in all toxicity studies.

Figure 6: Possible environmental interactions of nanohybrids (NHs): Transport and fate of NHs could be modified due to alteration in porous media transport and changes on colloidal stability (A); The transformation of NHs (e.g. dissolution rate of metallic counterpart, macromolecules adsorption leading to corona formation and degradation), could be distinct than its counterparts. (B); Due to its unique physicochemical properties the toxicity profile of NHs is unknow (C)

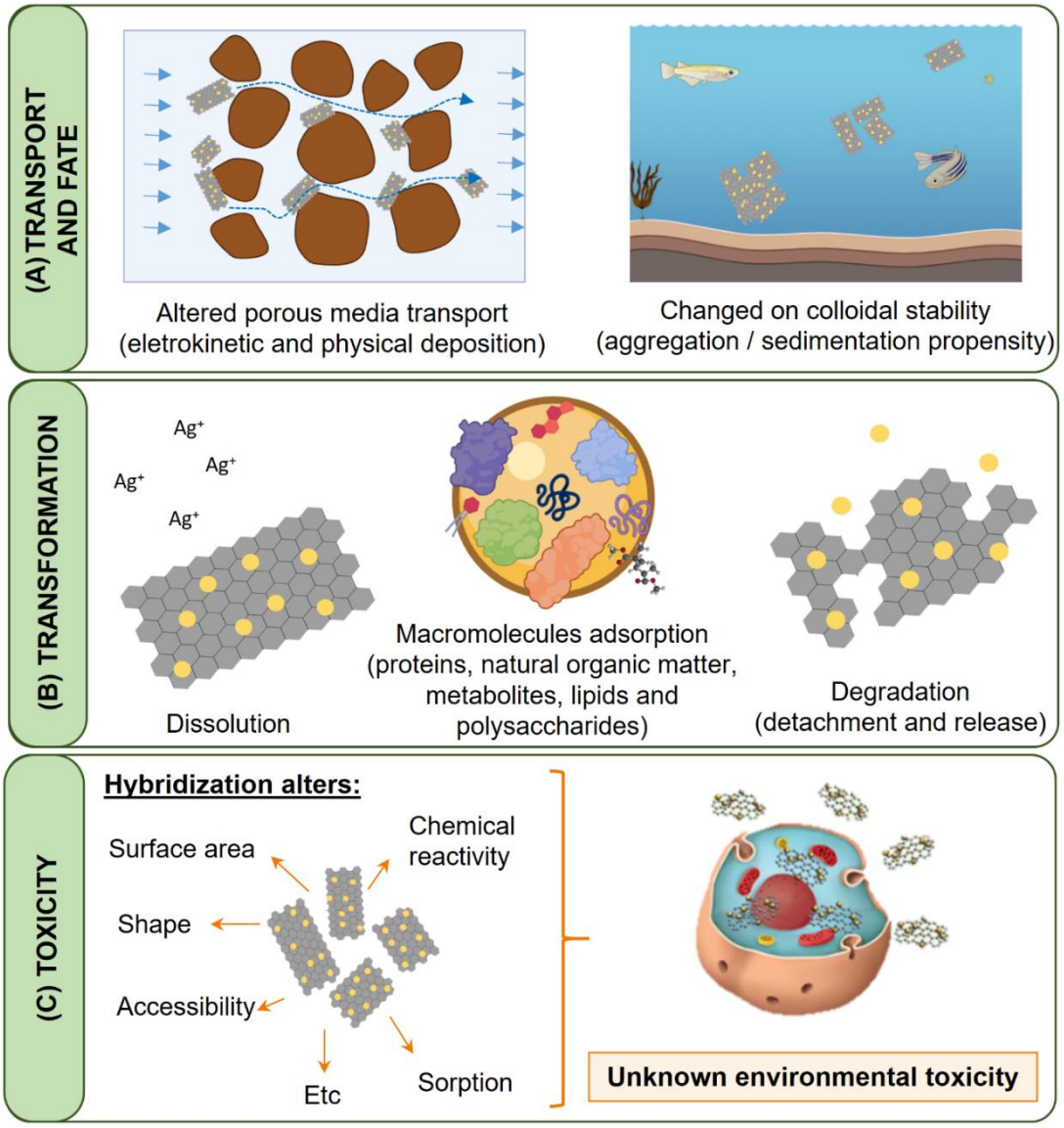

One crucial challenge in the nano-EHS studies is characterising heterogeneity within a particular batch of NMs (i.e., a mixture of different characteristics as differences in particle size distribution, silver loading, etc.) or between batches of NMs. This difference also could occur between synthesis methods. Moreover, the problem with heterogeneity between nanohybrid samples is aggravated compared to single NMs (SALEH et al., 2015). Thus, it is recommended for an accurate characterisation to be possible to compare the toxicological responses.

Moreover, another challenge is to understand how the physical-chemical characteristics modulate the biological response of NHs. The environmental implications of nanostructures (size, shape, surface functionality, coating) have been systematically assessed for bare nanomaterials as GO and AgNPs. However, few studies were conducted considering the nanostructures of nanohybrids. It is fundamental to design new materials with higher efficiency and lower toxicity, looking for a safety-by-design approach.

Another issue in nano-EHS is the interaction with the environment. In fact, NMs fate, transport, transformation, and toxicity could be modified by their intrinsic characteristics and environmental conditions. The environment is a complex matrix that provides a range of conditions (e.g., pH, redox status, ionic strength, organic matter content, bio-fluid conditions, presence of macromolecules, etc.) in which physical-chemical process could occur and result in NMs transformations (LOUIE et al., 2014; ZHAO et al., 2021). Similar to its pristine nanomaterials, these include dissolution of metallic NPs, degradation of coating, change on compositional chemistry speciation, co-existence and possible interaction with other pollutants, modifications on colloid behaviour (aggregation/sedimentation), organic coating due to interaction with natural organic matter and biological macromolecules (i.e., eco-corona formation) (SPURGEON et al., 2020).

The new physical-chemical characteristics that arise during hybridisation modified how this new NM will interact with the environment, and its consequence could be different from its pristine counterparts (SALEH et al., 2015). For example, the changes in van der Waals and electrostatic interactions resulted from GO-AgNps formation modify the aggregation state of nanomaterial. It alters the stability and mobile as larger particles tend to sedimentation on aquatic environmental or electrokinetic and physical deposition at porous media.

Besides changing its fate, the colloidal stability directly influences the dose of NHs to the exposed organism. For example, in the aquatic systems, the NMs aggregates sedimentation leads the benthic organisms as a key receptor of NM (KAHRU; DUBOURGUIER, 2010).

Furthermore, GO and AgNPs could change over time depending on storage, exposure, and condition. However, the effect of the "ageing" of nanohybrids still unknown. Therefore, some questions about hybridisations arise and need to be elucidated. For example, does the conjugate ensemble remain over time and acts as one in the environment or break out into its counterparts? Will the dissolution be altered, and how it mediates the nanotoxicity?

Current biosafety assessments of nanomaterials cannot reach a comprehensive conclusion due to the lack of reliable experimental models, effective detection techniques and recognised evaluation standards

Currently, the graphene-based nanohybrids are not yet at a large scale of production. However, looking towards safer innovations, the toxic profile needs to be assessed during the early innovation stage of development to be aware of its potential risks. Thus, these studies could suggest how potential nanosafety issues can be addressed and increase the chances of success in yielding safe applications of nanohybrids.

2.7. Conclusion

This review summarised the current progress on graphene oxide-silver nanoparticle hybrid material synthesis, applications, and recent progress to understand biological and environmental hazards. Besides the reports on its application, few studies focus on its potential EHS impacts. Thus, the toxicology evaluation within key organisms and its environmental dynamics on relevant scenarios aiming at more efficient material with a lower toxic profile is necessary. The influencing factors and data gaps must be elucidated to design a safer nanomaterial, especially potential environmental risks/damage. Moreover, these systematically collect biosafety data could serve as a first step toward the safety development of GO-AgNPs nanohybrids.

References

ABDALLA, S. S. I.; KATAS, H.; CHAN, J. Y.; GANASAN, P.; AZMI, F.; BUSRA, M. F. Mh. Antimicrobial activity of multifaceted lactoferrin or graphene oxide functionalised silver nanocomposites biosynthesised using mushroom waste and chitosan. **RSC Advances**, v. 10, n. 9, p. 4969–4983, 2020.

AHMAD, N.; AL-FATESH, A. S.; WAHAB, R.; ALAM, M.; FAKEEHA, A. H. Synthesis of silver nanoparticles decorated on reduced graphene oxide nanosheets and their electrochemical sensing towards hazardous 4-nitrophenol. **Journal of Materials Science: Materials in Electronics**, v. 31, n. 14, p. 11927–11937, 2020.

AICH, N.; PLAZAS-TUTTLE, J.; LEAD, J. R.; SALEH, N. B. A critical review of nanohybrids: Synthesis, applications and environmental implications. **Environmental Chemistry**, v. 11, n. 6, p. 609–623, 2014.

ALI, D.; ALARIFI, S.; ALKAHTANI, S.; ALMEER, R. S. Silver-doped graphene oxide nanocomposite triggers cytotoxicity and apoptosis in human hepatic normal and carcinoma cells. **International Journal of Nanomedicine**, v. 13, p. 5685–5699, 2018.

ALIAN, R. S.; DZIEWIĘCKA, M.; KĘDZIORSKI, A.; MAJCHRZYCKI, Ł.; AUGUSTYNIAK, M. Do nanoparticles cause hormesis? Early physiological compensatory response in house crickets to a dietary admixture of GO, Ag, and GOAg composite. **Science of The Total Environment**, v. 788, art. 147801, 2021.

ANGULO-PINEDA, C.; PALMA, P.; BEJARANO, J.; RIVEROS, A.; KOGAN, M.; PALZA, H. Antibacterial Silver Nanoparticles Supported on Graphene Oxide with Reduced Cytotoxicity. **Jom**, v. 71, n. 10, p. 3698–3705, 2019.

ÁVILA, D. S.; RONCATO, J. F.; JACQUES, M. T. Nanotoxicology assessment in complementary/alternative models. **Energy, Ecology and Environment**, v. 3, p. 72–80, 2018.

AZIZ, N. S. A.; AZMI, M. K. N.; HASHIM, A. M. One-pot green synthesis of highly reduced graphene oxide decorated with silver nanoparticles. **Sains Malaysiana**, v. 46, n. 7, p. 1083–1088, 2017.

BAKHSHESHI-RAD, H. R.; ISMAIL, A. F.; AZIZ, M.; AKBARI, M.; HADISI, Z.; KHOSHNAVA, S. M.; PAGAN, E.; CHEN, X. Co-incorporation of graphene oxide/silver nanoparticle into poly-L-lactic acid fibrous: A route toward the development of cytocompatible and antibacterial coating layer on magnesium implants. **Materials Science and Engineering C**, v. 111, art. 110812, 2020.

CAI, X.; LIN, M.; TAN, S.; MAI, W.; ZHANG, Y.; LIANG, Z.; LIN, Z.; ZHANG, X. The use of polyethyleneimine-modified reduced graphene oxide as a substrate for silver nanoparticles to produce a material with lower cytotoxicity and long-term antibacterial activity. **Carbon**, v. 50, n. 10, p. 3407–3415, 2012.

CAIRES, C. S. A.; FARIAS, L. A. S.; GOMES, L. E.; PINTO, B. P.; GONÇALVES, D. A.; ZAGONEL, L. F.; NASCIMENTO, V. A.; ALVES, D. C. B.; COLBECK, I.; WHITBY, C.; CAIRES, A. R. L.; WENDER, H. Effective killing of bacteria under blue-light irradiation promoted by green synthesised silver nanoparticles loaded on reduced graphene oxide sheets. **Materials Science and Engineering C**, v. 113, n. December 2019, p. 110984, 2020.

CAO, Y.; LI, S.; CHEN, J. Modeling better in vitro models for the prediction of nanoparticle toxicity: a review. **Toxicology Mechanisms and Methods**, v. 31, n. 1, p. 1–17, 2021. .

CHAKRABORTY, C.; SHARMA, A. R.; SHARMA, G.; LEE, S. S. Zebrafish: A complete animal model to enumerate the nanoparticle toxicity. **Journal of Nanobiotechnology**, v. 14, art. 65, 2016.

CHEN, J.; PENG, H.; WANG, X.; SHAO, F.; YUANA, Z.; HAN, H. Graphene oxide exhibits broad-spectrum antimicrobial activity against bacterial phytopathogens and fungal conidia by intertwining and membrane perturbation. **Nanoscale**, v. 6, n. 3, p. 1879–1889, 2014.

CHEN, J.; SUN, L.; CHENG, Y.; LU, Z.; SHAO, K.; LI, T.; HU, C.; HAN, H. Graphene Oxide-Silver Nanocomposite: Novel Agricultural Antifungal Agent against Fusarium graminearum for Crop Disease Prevention. **ACS Applied Materials and Interfaces**, v. 8, n. 36, p. 24057–24070, 2016.

CHEN, Y. N.; HSUEH, Y. H.; HSIEH, C. TE; TZOU, D. Y.; CHANG, P.-L. Antiviral activity of graphene-silver nanocomposites against non-enveloped and enveloped viruses. **International Journal of Environmental Research and Public Health**, v. 13, n. 4, art. 430, 2016.

CHEN, Y.; WU, W.; XU, Z.; JIANG, C.; HAN, S.; RUAN, J.; WANG, Y. Photothermal-assisted antibacterial application of graphene oxide-Ag nanocomposites against clinically isolated multi-drug resistant Escherichia coli. **Royal Society Open Science**, v. 7, n. 7, 2020. https://doi.org/10.1098/rsos.192019.

CHOI, Y. J.; GURUNATHAN, S.; KIM, J. H. Graphene oxide-silver nanocomposite enhances cytotoxic and apoptotic potential of salinomycin in human ovarian cancer stem cells (OvCSCs): A novel approach for cancer therapy. **International Journal of Molecular Sciences**, v. 19, n. 3, art. 710, 2018.

CHOOK, S. W.; CHIA, C. H.; ZAKARIA, S.; AYOB, M. K.; CHEE, K. L.; HUANG, N. M.; NEOH, H. M.; LIM, H. M.; JAMAL, R.; RAHMAN, R. M. F. R. A. Antibacterial performance of Ag nanoparticles and AgGO nanocomposites prepared via rapid microwave-assisted synthesis method. **Nanoscale Research Letters**, v. 7, art. 541, 2012.

COBOS, M.; DE-LA-PINTA, I.; QUINDÓS, G.; FERNÁNDEZ, M. D.; FERNÁNDEZ, M. J. Graphene oxide-silver nanoparticle nanohybrids: Synthesis, characterization, and antimicrobial properties. **Nanomaterials**, v. 10, n. 2, art. 376, 2020.

DARGO, H.; AYALIEW, A.; KASSA, H. Synthesis paradigm and applications of silver nanoparticles (AgNPs): a review. **Sustainable Materials and Technologies**, v. 13, p. 18-23, 2017.

DASARI SHAREENA, T. P.; MCSHAN, D.; DASMAHAPATRA, A. K.; TCHOUNWOU, P. B. A review on graphene-based nanomaterials in biomedical applications and risks in environment and health. **Nano-Micro Letters**, v. 10, n. 3, p. 1–34, 2018.

DE MEDEIROS, A. M. Z.; KHAN, L. U.; SILVA, G. H. DA; OSPINA, C. A.; ALVES, O. L.; CASTRO, V. L. DE; MARTINEZ, D. E. T. Graphene oxide-silver nanoparticle hybrid material: an integrated nanosafety study in zebrafish embryos. **Ecotoxicology and Environmental Safety**, v. 209, art. 111776, 2021.

DRASLER, B.; SAYRE, P.; STEINHÄUSER, K. G.; PETRI-FINK, A.; ROTHEN-RUTISHAUSER, B. In vitro approaches to assess the hazard of nanomaterials. **NanoImpact**, v. 8, p. 99–116, 2017.

DU, T.; LU, J.; LIU, L.; DONG, N.; FANG, L.; XIAO, S.; HAN, H. Antiviral Activity of Graphene Oxide-Silver Nanocomposites by Preventing Viral Entry and Activation of the Antiviral Innate Immune Response. **ACS Applied Bio Materials**, v. 1, n. 5, p. 1286–1293, 2018.

DURÁN, N.; DURÁN, M.; JESUS, M. B. DE; SEABRA, A. B.; FÁVARO, W. J.; NAKAZATO, G. Silver nanoparticles : A new view on mechanistic aspects on antimicrobial activity. **Nanomedicine: Nanotechnology, Biology, and Medicine**, v. 12, n. 3, p. 789–799, 2016.

FARIA, A. F.; MARTINEZ, D. S. T.; MORAES, A. C. M.; COSTA, M. E. H. M. DA; BARROS, E. B.; SOUZA FILHO, A. G.; PAULA, A. J.; ALVES, O. L. Unveiling the role of oxidation debris on the surface chemistry of graphene through the anchoring of ag nanoparticles. **Chemistry of Materials**, v. 24, n. 21, p. 4080–4087, 2012.

GARG, K.; PAPPONEN, P.; JOHANSSON, A.; PUTTARAKSA, N.; GILBERT, L. Preparation of graphene nanocomposites from aqueous silver nitrate using graphene oxide's peroxidase-like and carbocatalytic properties. **Scientific Reports**, v. 10, n. 1, p. 1–13, 2020.

GUGGENHEIM, E. J.; MILANI, S.; RÖTTGERMANN, P. J. F.; DUSINSKA, M.; SAOUT, C.; SALVATI, A.; RÄDLER, J. O.; LYNCH, I. Refining in vitro models for nanomaterial exposure to cells and tissues. **NanoImpact**, v. 10, p. 121–142, 2018.

GURUNATHAN, S.; HYUN PARK, J.; CHOI, Y.-J.; WOONG HAN, J.; KIM, J.-H. Synthesis of graphene oxide-silver nanoparticle nanocomposites: An efficient novel antibacterial agent. **Current Nanoscience**, v. 12, n. 6, p. 762–773, 2016.

HABIBA, K.; ENCARNACION-ROSADO, J.; GARCIA-PABON, K.; VILLALOBOS-SANTOS, J. C.; MAKAROV, V.; AVALOS, J. A.; WEINER, B. R.; MORELL, G. Improving cytotoxicity against cancer cells by chemo-photodynamic combined modalities using silver-graphene quantum dots nanocomposites. **International Journal of Nanomedicine**, v.11, p.107-119, 2015.

HAN, X.-W.; MENG, X.-Z.; ZHANG, J.; WANG, J.-X.; HUANG, H.-F.; ZENG, X.-F.; CHEN, J.-F. Ultrafast Synthesis of Silver Nanoparticle Decorated Graphene Oxide by a Rotating Packed Bed Reactor. **Industrial & Engineering Chemistry Research**, v. 55, p. 11622–11630, 2016.

HAN, Y.; LUO, Z.; YUWEN, L.; TIAN, J.; ZHU, X.; WANG, L. Synthesis of silver nanoparticles on reduced graphene oxide under microwave irradiation with starch as an ideal reductant and stabiliser. **Applied Surface Science**, v. 266, p. 188–193, 2013.

HOA, L. T.; LINH, N. T. Y.; CHUNG, J. S.; HUR, S. H. Green synthesis of silver nanoparticle-decorated porous reduced graphene oxide for antibacterial non-enzymatic glucose sensors. **Ionics**, v. 23, n. 6, p. 1525–1532, 2017.

HUANG, J.; XIE, Z.; XIE, Z.; LUO, S.; XIE, L.; HUANG, L.; FAN, Q.; ZHANG, Y.; WANG, S.; ZENG, T. Silver nanoparticles coated graphene electrochemical sensor for the ultrasensitive analysis of avian influenza virus H7. **Analytica Chimica Acta**, v. 913, p. 121–127, 2016.

HUTCHISON, J. E. The road to sustainable nanotechnology: Challenges, progress and opportunities. **ACS Sustainable Chemistry and Engineering**, v. 4, p. 5907–5914, 2016.

INNOCENZI, P.; STAGI, L. Carbon-based antiviral nanomaterials: Graphene, C-dots, and fullerenes. A perspective. **Chemical Science**, v. 11, n. 26, p. 6606–6622, 2020.

JIANG, Y.; WANG, J.; MALFATTI, L.; CARBONI, D.; SENES, N.; INNOCENZI, P. Highly durable graphene-mediated surface enhanced Raman scattering (G-SERS) nanocomposites for molecular detection. **Applied Surface Science**, v. 450, p. 451–460, 2018.

KAHRU, A.; DUBOURGUIER, H. From ecotoxicology to nanoecotoxicology. **Toxicology**, v. 269, n. 2–3, p. 105–119, 2010.

KAVINKUMAR, T.; MANIVANNAN, S. Uniform decoration of silver nanoparticle on exfoliated graphene oxide sheets and its ammonia gas detection. **Ceramics International**, v. 42, n. 1, p. 1769–1776, 2016.

KELLICI, S.; ACORD, J.; VAUGHN, A.; POWER, N. P.; MORGAN, D. J.; HEIL, T.; FACQ, S. P.; LAMPRONTI, G. I. Calixarene Assisted Rapid Synthesis of Silver-Graphene Nanocomposites with Enhanced Antibacterial Activity. **ACS Applied Materials and Interfaces**, v. 8, n. 29, p. 19038–19046, 2016.

KHAN, M.; KHAN, M.; AL-MARRI, A. H.; AL-WARTHAN, A.; ALKHATHLAN, H. Z.; SIDDIQUI, M. R. H.; NAYAK, V. L.; KAMAL, A.; ADIL, S. F. Apoptosis inducing ability of silver decorated highly reduced graphene oxide nanocomposites in A549 lung cancer. **International Journal of Nanomedicine**, v. 11, p. 873–883, 2016.

KIM, M. J.; KO, D.; KO, K.; KIM, D.; LEE, J.-Y.; WOO, S. M.; KIM, W.; CHUNG, H. Effects of silver-graphene oxide nanocomposites on soil microbial communities. **Journal of Hazardous Materials**, v. 346, p. 93–102, 2018.

KOUSHIK, D.; SEN, S.; MALIYEKKAL, S. M.; PRADEEP, T. Rapid dehalogenation of pesticides and organics at the interface of reduced graphene oxide – silver nanocomposite. **Journal of Hazardous Materials**, v. 308, p. 192–198, 2016.

KUMARI, S.; SHARMA, P.; YADAV, S.; KUMAR, J.; VIJ, A.; RAWAT, P.; KUMAR, S.; SINHA, C.; BHATTACHARYA, J.; SRIVASTAVA, C. M. A Novel Synthesis of the Graphene Oxide-Silver (GO-Ag) Nanocomposite for Unique Physiochemical Applications. **ACS Omega**, v. 5, n. 10, p. 5041–5047, 2020.

KUNDU, N.; MUKHERJEE, D.; MAITI, T. K.; SARKAR, N. Protein-Guided Formation of Silver Nanoclusters and Their Assembly with Graphene Oxide as an Improved Bioimaging Agent with Reduced Toxicity. **Journal of Physical Chemistry Letters**, v. 8, p. 2291–2297, 2017.

LI, C.; WANG, X.; CHEN, F.; ZHANG,C.; ZHI, X.; WANG, K.; CUI, D. The antifungal activity of graphene oxide-silver nanocomposites. **Biomaterials**, v. 34, n. 15, p. 3882–3890, 2013.

LI, J.; KUANG, D.; FENG, Y.; ZHANG, F.; XU, Z. Biosensors and Bioelectronics Green synthesis of silver nanoparticles – graphene oxide nanocomposite and its application in electrochemical sensing of tryptophan. **Biosensors and Bioelectronic**, v. 42, p. 198–206, 2013.

LIN, S.; YU, T.; YU, Z.; HU, X.; YIN, D. Nanomaterials Safer-by-Design: An Environmental Safety Perspective. **Advanced Materials**, v. 30, n. 17, p. 1–5, 2018.

LIU, C.; SHEN, J.; YEUNG, K. W. K.; TJONG, S. C. Development and Antibacterial Performance of Novel Polylactic Acid-Graphene Oxide-Silver Nanoparticle Hybrid Nanocomposite Mats Prepared By Electrospinning. **ACS Biomaterials Science & Engineering**, v. 3, n. 3, p. 471-486, 2017.

LIU, L.; HOU, S.; ZHAO, X.; LIU, C.; LI, Z.; LI, C.; XU, S.; WANG, G.; YU, J.; ZHANG, C.; MAN, B. Role of graphene in constructing multilayer plasmonic sers substrate with graphene/agnps as chemical mechanism—electromagnetic mechanism unit. **Nanomaterials**, v. 10, n. 12, art. 2371, 2020.

LIU, Y.; FAN, W.; XU, Z.; PENG, W.; LUO, S. Transgenerational effects of reduced graphene oxide modified by Au, Ag, Pd, Fe3O4, Co3O4 and SnO2 on two generations of Daphnia magna. **Carbon**, v. 122, p. 669–679, 2017.

LIU, Z.; GUO, Z.; ZHONG, H.; QIN, X.; WANA, M.; YANGA, B. Graphene oxide based surface-enhanced Raman scattering probes for cancer cell imaging. **Physical Chemistry Chemical Physics**, v. 15, n. 8, p. 2961–2966, 2013.

LOUIE, S. M.; MA, R.; LOWRY, G. V. Transformations of Nanomaterials in the Environment. **Frontiers of Nanoscience**, v. 7, p. 55–87, 2014.

LUNA, L. A. V. DE; MORAES, M. D. A. C.; CONSONNI, S. R.; PEREIRA, C. D.; CADORE, S.; GIORGIO, S.; ALVES, O. L. Comparative in vitro toxicity of a graphene oxide - silver nanocomposite and the pristine counterparts toward macrophages. **Journal of Nanobiotechnology**, v. 14, art. 12, 2016.

LUNA, L. A. V. DE; ZORGI, N. E.; MORAES, A. C. M. DE; SILVA, D. S. DA; CONSONNI, S. R.; GIORGIO, S.; ALVES, O. L. In vitro immunotoxicological assessment of a potent microbicidal nanocomposite based on graphene oxide and silver nanoparticles. **Nanotoxicology**, v. 13, n. 2, p. 189–203, 2019.

MAHMOUDI, E.; NG, L. Y.; BA-ABBAD, M. M.; MOHAMMAD, A. W. Novel nanohybrid polysulfone membrane embedded with silver nanoparticles on graphene oxide nanoplates. **Chemical Engineering Journal**, v. 277, p. 1–10, 2015.

MENG, H.; LEONG, W.; LEONG, K. W.; CHEN, C.; ZHAO, Y. Walking the line : The fate of nanomaterials at biological barriers. **Biomaterials**, v. 174, p. 41–53, 2018.

MINH, P. N.; HOANG, V.-T.; DINH, N. X.; VAN HOANG, O.; VAN CUONG, N.; BICH HOP, D. T.; TUAN, T. Q.; KHI, N. T.; HUY, T. Q.; LE, A.-T. Reduced graphene oxide-wrapped silver nanoparticles for applications in ultrasensitive colorimetric detection of Cr(vi) ions and the carbaryl pesticide. **New Journal of Chemistry**, v. 44, n. 18, p. 7611–7620, 2020.

MORAES, A. C. M. DE. Graphene oxide-silver nanocomposite as a promising biocidal agent against methicillin- resistant Staphylococcus aureus. **International Journal of Nanomedicine**, v. 10, p. 6847–6861, 2015.

NAEEM, H.; AJMAL, M.; QURESHI, R. B.; MUNTHA, S. T.; FAROOQ,M.; SIDDIQ, M. Facile synthesis of graphene oxide–silver nanocomposite for decontamination of water from multiple pollutants by adsorption, catalysis and antibacterial activity. **Journal of Environmental Management**, v. 230, p. 199–211, 2019.

NASSER, F.; CONSTANTINOU, J.; LYNCH, I. Nanomaterials in the Environment Acquire an "Eco-Corona" Impacting their Toxicity to Daphnia Magna—a Call for Updating Toxicity Testing Policies. **Proteomics**, v. 20, n. 9, e1800412, 2020. doi: 10.1002/pmic.201800412.

NAZARI, F.; MOVAFEGHI, A. Synthesis of Reduced Graphene Oxide-Silver Nanocomposites and Assessing Their Toxicity on the Green Microalga Chlorella vulgaris. **BioNanoScience**, v. 8, p. 997-1007, 2018.

NOOR, A. M.; SHAHID, M. M.; RAMESHKUMAR, P.; HUANG, N. M. A glassy carbon electrode modified with graphene oxide and silver nanoparticles for amperometric determination of hydrogen peroxide. **Microchimica Acta**, v. 183, n. 2, p. 911–916, 2016.

NOYES, P. D.; GARCIA, G. R.; TANGUAY, R. L. Zebrafish as an in vivo model for sustainable chemical design. **Green Chemistry**, v. 18, n. 24, p. 6410–6430, 2016.

PARK, M. V. D. Z.; BLEEKER, E. A. J.; BRAND, W.; CASSEE, F. R.; VAN ELK, M.; GOSENS, I.; DE JONG, W. H.; MEESTERS, J. A. J.; PEIJNENBURG, W. J. G.M.; QUIK, J. T. K.; VANDEBRIEL, R. J.; SIPS, A. J. A. M. Considerations for Safe Innovation: The Case of Graphene. **ACS Nano**, v. 11, n. 10, p. 9574–9593, 2017.

PEREIRA, A. C.; GOMES, T.; FERREIRA MACHADO, M. R.; ROCHA, T. L. The zebrafish embryotoxicity test (ZET) for nanotoxicity assessment: from morphological to molecular approach. **Environmental Pollution**, v. 252, p. 1841–1853, 2019.

PLAZAS-TUTTLE, J.; ROWLES, L.; CHEN, H.; BISESI JUNIOR, J. H.; SABO-ATTWOOD, T.; SALEH, N. B. Dynamism of Stimuli-Responsive Nanohybrids: Environmental Implications. **Nanomaterials**, v. 5, n. 2, p. 1102–1123, 2015.

PRASAD, K.; LEKSHMI, G. S.; OSTRIKOV, K.; LUSSINI, V.; BLINCO, J.; MOHANDAS, M.; VASILEV, K.; BOTTLE, S.; BAZAKA, K.; OSTRIKOV, K. Synergic bactericidal effects of reduced graphene oxide and silver nanoparticles against Gram-positive and Gram-negative bacteria. **Scientific Reports**, v. 7, art. 1591, 2017.

QIAN, Z.; CHENG, Y.; ZHOU, X.; WU, J.; XU, G. Fabrication of graphene oxide / Ag hybrids and their surface-enhanced Raman scattering characteristics. **Journal of Colloid And Interface Science**, v. 397, p. 103–107, 2013.

REINA, G.; PENG, S.; JACQUEMIN, L.; ANDRADE, A. F.; BIANCO, A. Hard Nanomaterials in Time of Viral Pandemics. **ACS Nano**, v. 14, n. 8, p. 9364–9388, 2020.

SALEH, N. B.; AFROOZ, A. R. M. N.; BISESI JUNIOR, J. H.; AICH, N.; PLAZAS-TUTTLE, J.; SABO-ATTWOOD, T. Emergent Properties and Toxicological Considerations for Nanohybrid Materials in Aquatic Systems. **Nanomaterials**, v. 4, n. 2, p. 372–407, 2014.

SALEH, N. B.; AICH, N.; PLAZAS-TUTTLE, J.; LEAD, J. R.; LOWRY, G. V. Research strategy to determine when novel nanohybrids pose unique environmental risks. **Environmental Science: Nano**, v. 2, n. 1, p. 11–18, 2015.

SAWADA, I.; FACHRUL, R.; ITO, T.; OHMUKAI, Y.; MARUYAMA, T.; MATSUYAMA, H. Development of a hydrophilic polymer membrane containing silver nanoparticles with both organic antifouling and antibacterial properties. **Journal of Membrane Science**, v. 387–388, n. 1, p. 1–6, 2012.

SHAO, W.; LIU, X.; MIN, H.; DONG, G.; FENG, Q.; ZUO, S. Preparation, Characterization, and Antibacterial Activity of Silver Nanoparticle-Decorated Graphene Oxide Nanocomposite. **ACS Applied Materials & Interfaces**, v. 7, n. 12, p. 6966–6973, 2015.

SHARMA, S.; PRAKASH, V.; MEHTA, S. K. Graphene/silver nanocomposites-potential electron mediators for proliferation in electrochemical sensing and SERS activity. **TrAC - Trends in Analytical Chemistry**, v. 86, p. 155–171, 2017.

SHEN, J.; SHI, M.; YAN, B.; MA, H.; LI, N.; YE, M. One-pot hydrothermal synthesis of Ag-reduced graphene oxide composite with ionic liquid. **Journal of Materials Chemistry**, v. 21, n. 21, p. 7795–7801, 2011.

SHI, G.; WANG, M.; ZHU, Y.; WANG, Y.; XU, H. A novel natural SERS system for crystal violet detection based on graphene oxide wrapped Ag micro-islands substrate fabricated from Lotus leaf as a template. **Applied Surface Science**, v. 459, p. 802–811, 2018.

SOROUSH, A.; MA, W.; SILVINO, Y.; RAHAMAN, M. S. Surface modification of thin film composite forward osmosis membrane by silver-decorated graphene-oxide nanosheets. **Environmental Science: Nano**, v. 2, n. 4, p. 395–405, 2015.

SPURGEON, D. J.; LAHIVE, E.; SCHULTZ, C. L. Nanomaterial Transformations in the Environment: Effects of Changing Exposure Forms on Bioaccumulation and Toxicity. **Small**, v. 16, n. 36, art. 2000618, 2020. Special issue.

TAO, Y.; LIN, Y.; HUANG, Z.; REN, J.; QU, X. DNA-templated silver nanoclusters-graphene oxide nanohybrid materials: A platform for label-free and sensitive fluorescence turn-on detection of multiple nucleic acid targets. **Analyst**, v. 137, n. 11, p. 2588–2592, 2012.

THOMAS, R.; UNNIKRISHNAN, J.; NAIR, A. V; DANIEL, E. C.; BALACHANDRAN, M. Antibacterial performance of GO – Ag nanocomposite prepared via ecologically safe protocols. **Applied Nanoscience**, v. 10, p. 4207-4219, 2020.

THU, T. V.; KO, P. J.; PHUC, N. H. H.; SANDHU, A. Room-temperature synthesis and enhanced catalytic performance of silver-reduced graphene oxide nanohybrids. **Journal of Nanoparticle Research**, v. 15, n. 10, p. 1975, 2013.

TRUONG, T. T. V.; KUMAR, S. R.; HUANG, Y.-T.; CHEN, D. W.; LIU, Y.-K.; LUE, S. J. Size-dependent antibacterial activity of silver nanoparticle-loaded graphene oxide nanosheets. **Nanomaterials**, v. 10, n. 6, p. 1–18, 2020.

ULLAH, S.; AHMAD, A.; SUBHAN, F.; JAN, A.; RAZA, M.; KHAN, A. U.; RAHMAN, A.-U.; KHAN, U. A.; TARIQ, M.; YUAN, Q. Tobramycin mediated silver nanospheres/graphene oxide composite for synergistic therapy of bacterial infection. **Journal of Photochemistry and Photobiology B: Biology**, v. 183, p. 342–348, 2018.

WANG, D.; SALEH, N. B.; SUN, W.; PARK, C. M.; SHEN, C.; AICH, N.; PEIJNENBURG, W. J. G. M.; ZHANG, W.; JIN, Y.; SU, C. Next-Generation Multifunctional Carbon − Metal Nanohybrids for Energy and Environmental Applications. **Enviromental Science & Technology**, v. 53, n. 13, p. 7265–7287, 2019.

WHEELER, K. E.; CHETWYND, A. J.; FAHY, K. M.; HONG, B. S.; TOCHIHUITL, J. A.; FOSTER, L. A.; LYNCH, I. Environmental dimensions of the protein corona. **Nature Nanotechnology**, v. 16, n. 6, p. 617–629, 2021.

WIERZBICKI, M.; JAWORSKI, S.; SAWOSZ, E.; JUNG, A.; GIELERAK, G.; JAREMEK, H.; ŁOJKOWSKI, W.; WOŹNIAK, B.; STOBIŃSKI, L.; MAŁOLEPSZY, A.; CHWALIBOG, A. Graphene Oxide in a Composite with Silver Nanoparticles Reduces the Fibroblast and Endothelial Cell Cytotoxicity of an Antibacterial Nanoplatform. **Nanoscale Research Letters**, v. 14, n. 1, art. 320, 2019.

XIAOLI, F.; QIYUE, C.; WEIHONG, G.; YAQING, Z.; CHEN, H.; JUNRONG, W.; LONGQUAN, S. Toxicology data of graphene-family nanomaterials: an update. **Archives of Toxicology**, v. 94, n. 6, p. 1915–1939, 2020.

XIE, X.; MAO, C.; LIU, X.; ZHANG, Y.; CUI, Z.; YANG, X.; YEUNG, K. W. K.; PAN, H.; CHU, P. K.; WU, S. Synergistic Bacteria Killing through Photodynamic and Physical Actions of Graphene Oxide/Ag/Collagen Coating. **ACS Applied Materials and Interfaces**, v. 9, n. 31, p. 26417–26428, 2017.

XIE, Y.; LI, Y.; NIU, L.; WANG, H.; QIAN, H.; YAO, W. A novel surface-enhanced Raman scattering sensor to detect prohibited colorants in food by graphene/silver nanocomposite. **Talanta**, v. 100, p. 32–37, 2012.

XU, L.; XU, M.; WANG, R.; YIN, Y.; LYNCH, I.; LIU, S. The crucial role of environmental coronas in determining the biological effects of engineered nanomaterials. **Small**, art. 2003691, 2020. https://doi.org/10.1002/smll.202003691.

YAQOOB, A. A.; UMAR, K.; IBRAHIM, M. N. M. Silver nanoparticles: various methods of synthesis, size affecting factors and their potential applications–a review. **Applied Nanoscience (Switzerland)**, v. 10, n. 5, p. 1369–1378, 2020.

YIM, D. BIN; KANG, H.; JEON, S.-J.; KIM, H.-I.; YANG, J.-K.; KANG, T. W.; LEE, S.; CHOO, J.; LEE, Y.-S.; KIM, J. W.; KIM, J.-H. Graphene oxide-encoded Ag nanoshells with single-particle detection sensitivity towards cancer cell imaging based on SERRS. **Analyst**, v. 140, n. 10, p. 3362–3367, 2015.

YIN, J.; DONG, Z.; LIU, Y.; WANG, H.; LI, A.; ZHUO, Z.; FENG, W.; FAN, W. Toxicity of reduced graphene oxide modified by metals in microalgae: Effect of the surface properties of algal cells and nanomaterials. **Carbon**, v. 169, p. 182–192, 2020.

YIN, P. T.; SHAH, S.; CHHOWALLA, M.; LEE, K. Design, Synthesis, and Characterisation of Graphene − Nanoparticle Hybrid Materials for Bioapplications. **Chemical Reviews**, v. 115, p. 2483–2531, 2015.

YUAN, Y.-G.; CAI, H.-Q.; WANG, J.-L.; MESALAM, A.; REZA, A. M. MD. T.; LI, L.; CHEN, L.; QIAN, C. Graphene oxide–silver nanoparticle nanocomposites induce oxidative stress and aberrant methylation in caprine fetal fibroblast cells. **Cells**, v. 10, n. 3, p. 682, 2021.

YUAN, Y. G.; GURUNATHAN, S. Combination of graphene oxide-silver nanoparticle nanocomposites and cisplatin enhances apoptosis and autophagy in human cervical cancer cells. **International Journal of Nanomedicine**, v. 12, p. 6537–6558, 2017.

ZAINY, M.; HUANG, N. M.; VIJAY KUMAR, S.; LIM, H. N.; CHIA, C.H.; HARRISON, I. Simple and scalable preparation of reduced graphene oxide-silver nanocomposites via rapid thermal treatment. **Materials Letters**, v. 89, p. 180–183, 2012.

ZHAO, Y.; LIU, Y.; ZHANG, X.; LIAO, W. Environmental transformation of graphene oxide in the aquatic environment. **Chemosphere**, v. 262, n. 26, art. 127885, 2021.

ZHENG, H.; NI, D.; YU, Z.; LIANG, P. Preparation of SERS-active substrates based on graphene oxide/silver nanocomposites for rapid zdetection of L-Theanine. **Food Chemistry**, v. 217, p. 511–516, 2017.

ZHOU, X.; DORN, M.; VOGT, J.; SPEMANN, D.; YU, W.; MAO, Z.; ESTRELA-LOPIS, I.; DONATH, E.; GAO, C. A quantitative study of the intracellular concentration of graphene/noble metal nanoparticle composites and their cytotoxicity. **Nanoscale**, v. 6, p. 8535–8542, 2014.

ZHOU, Y.; CHEN, R.; HE, T.; XU, K.; DU, D.; ZHAO, N.; CHENG, X.; YANG, J.; SHI, H.; LIN, Y. Biomedical Potential of Ultrafine Ag / AgCl Nanoparticles Coated on Graphene with Special Reference to Antimicrobial Performances and Burn Wound Healing. **Acs Applied Materials & Interfaces**, v. 8, n. 24, p. 15067–15075, 2016.

ZODROW, K.; BRUNET, L.; MAHENDRA, S.; LI, D.; ZHANG, A.; LI, Q.; ALVAREZ, P. J. J. Polysulfone ultrafiltration membranes impregnated with silver nanoparticles show improved biofouling resistance and virus removal. **Water Research**, v. 43, n. 3, p. 715–723, 2009.

3. GRAPHENE OXIDE-SILVER NANOPARTICLE HYBRID MATERIAL: AN INTEGRATED NANOSAFETY STUDY IN ZEBRAFISH EMBRYOS[1]

Highlights

- Nanoecotoxicity of GO-AgNPs on zebrafish embryos is dose-response manner.
- Silver nanoparticles drives the toxicity of GO-AgNPs nanohybrid.
- The chorion embryo membrane critically impacts the toxicity of GO-AgNPs.
- NOM is not effective to avoid the agglomeration of GO-AgNPs in exposure medium.
- NOM mitigates the toxicity of GO-AgNPs.

Graphical abstract

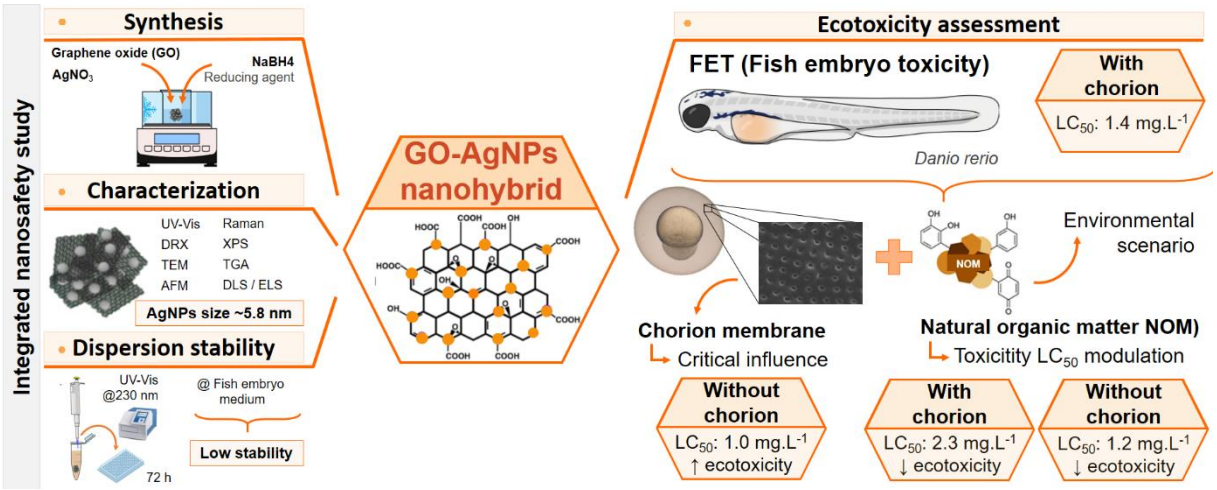

[1] This chapter was published in “Ecotoxicology and Environmental Safety” (https://doi.org/10.1016/j.ecoenv.2020.111776)

Abstract

This work reports an integrated nanosafety study including the synthesis and characterization of the graphene oxide-silver nanoparticle hybrid material (GO-AgNPs) and its nano-ecotoxicity evaluation in the zebrafish embryo model. The influences of natural organic matter (NOM) and a chorion embryo membrane were considered in this study, looking towards more environmentally realistic scenarios and standardized nanotoxicity testing. The nanohybrid was successfully synthesized using the $NaBH_4$ aqueous method, and AgNPs (~ 5.8 nm) were evenly distributed over the GO surface. GO-AgNPs showed a dose-response acute toxicity: the LC_{50} was 1.5 mg L^{-1} for chorionated embryos. The removal of chorion, however, increased this toxic effect by 50%. Furthermore, the presence of NOM mitigated mortality, and LC_{50} for GO-AgNPs changed respectively from 2.3 to 1.2 mg L^{-1} for chorionated and de-chorionated embryos. Raman spectroscopy confirmed the ingestion of GO by embryos; but without displaying acute toxicity up to 100 mg L^{-1}, indicating that the silver drove toxicity down. Additionally, it was observed that silver nanoparticle dissolution has a minimal effect on these observed toxicity results. Finally, understanding the influence of chorion membranes and NOM is a critical step towards the standardization of testing for zebrafish embryo toxicity in safety assessments and regulatory issues.

Keywords: nanohybrids; chorion; nanoecotoxicology; nanotoxicity; alternative methods

3.1. Introduction

Graphene oxide (GO) is a two-dimensional carbon nanomaterial. It is composed of carbon atoms organized in a hexagonal lattice, forming one flat sheet, containing oxygenated groups. Due to its extraordinary properties (e.g., thermal resistance, electrical conductivity, optical transparency, mechanical strength and chemical versatility), GO has been explored for many applications in materials science, nanomedicine, biotechnology and environmental technology (REN; CHENG, 2014; DIDEIKIN; VUL, 2019). GO-metal hybrid materials make up an emerging class of advanced materials based on graphene oxide. The goal of synthetizing new GO-based nanohybrid materials, coupling different metallic nanoparticles, is to enhance material functionality and/or to obtain multifunctional properties, working towards superior performance and new applications (YIN et al., 2015; FONSECA et al., 2018; HASSANDOOST et al., 2019).

Silver nanoparticles (AgNPs) are collectively one of the most extensively used types of nanomaterial, this being due to their antibacterial capability, catalytic activity, and optical and photo-thermal properties (MCGILLICUDDY et al., 2017).

To this end, the GO-AgNPs hybrid material possesses a substantial potential for innovation; demonstrating promising applications in different sectors, such as environmental engineering (KOUSHIK et al., 2016), electrochemical sensing and catalysis (SHARMA et al., 2017; XU et al., 2017), agriculture (CHEN et al., 2016) and biomedicine (MORAES, 2015; ZHOU et al., 2016). Interestingly, GO-AgNPs may possess a use as a membrane material for seawater desalination and treatment, due to their hydrophobicity and antimicrobial properties (SOROUSH et al., 2015). This nanohybrid might also be applied in a wide variety of electrochemical sensors and biosensors for the detection of tryptophan (LI et al., 2013), ammonia (KAVINKUMAR; MANIVANNAN, 2016), glucose (HOA et al., 2017) and 4-nitrophenol (AHMAD et al., 2020). In addition, GO-AgNPs have also been explored for the development of drug-delivery systems (ENCARNACION-ROSADO et al., 2016) and novel bio-imaging materials (KUNDU et al., 2017). Due to their promising applications, it is imperative to support studies that comprise the risk and toxicity evaluation of nanohybrid materials at an early stage of their synthetic production and research development, to minimize undesirable impacts on human and environmental health towards sustainable nanotechnology and responsible innovation (HUTCHISON, 2016). In fact, the safety-

by-design of this nanomaterial needs to include a minimum amount of information on the tested materials (i.e. physical-chemical characterization), the influence of the surrounding environment (i.e. colloidal behaviour and natural organic matter) and the biological model organism, for a toxicity assessment (LIN et al., 2018). However, and although many studies have reported on the toxic effects of exposure to the graphene family and metallic nanoparticles (as silver nanoparticles) in various biological models, the nano-ecotoxicology and environmental safety aspects of GO-based nanohybrids are poorly understood (LUNA et al., 2016; KIM et al., 2018). Special attention to the environmental risks of nanohybrids is therefore required (SALEH et al., 2014; PLAZAS-TUTTLE et al., 2015; SALEH et al., 2015).

Nanomaterial can be transported in aquatic ecosystems, which makes them available for uptake by aquatic organisms (PARK et al., 2017). The predicted environmental concentrations (PECs) for carbon-based nanomaterial and AgNPs in an aquatic compartment lie in the 0.02-6.0 ηg.L^{-1} range (MOTTIER et al., 2017; ZHAO et al., 2020). Furthermore, natural organic matter (NOM) is one crucial factor that influences the aggregation state of nanomaterial in aquatic systems (GRILLO et al., 2015; MARKIEWICZ et al., 2018) therefore it should be considered in the nano-ecotoxicological evaluation towards more environmentally realistic scenarios (LOWRY et al., 2014). Nanomaterial-NOM interactions are a fundamental issue in the understanding of nanomaterial mobility and consequently bioavailability for different organisms (SU et al., 2017; CASTRO et al., 2018). The presence of NOM may modify the dissolution rate of metallic nanoparticles, including AgNPs (ZHANG et al., 2018). Thus, NOM interaction with the AgNP surface might improve the colloidal stability and decrease the Ag^{+} release, which would have a direct influence on the toxicological profile of AgNPs (GUNSOLUS et al., 2015). It is therefore important to study the effects of NOM during the ecotoxicity assessment of GO-AgNP nanohybrids.

The Zebrafish (*Danio rerio*) is a promising model for environmental and human health studies because it presents an exceptional set of characteristics (CHAKRABORTY et al., 2016; LEE et al., 2017; HAQUE; WARD, 2018). A recent critical challenge for nanotoxicity assessments using zebrafish embryos is the presence of a chorion membrane (SIEBER et al., 2019). This biological structure presents pore channels of 0.5-0.7 mm in diameter, which partly isolate the larvae from the environment until hatching (LIN et al., 2013). The membrane penetration ability is strongly correlated with nanoparticle size, and in most cases, this characteristic may

block the entrance of nanomaterial (CHEN et al., 2020). For example, should GO adhere to this membrane, a gas exchange will be prevented from occurring. This hypoxic microenvironment can then induce hatching delay and malformation (SU et al., 2017). The removal of this membrane commences the direct exposition of the embryo to nanomaterial and simultaneously guarantees that the effects are provoked by nanoparticles, and not by the hypoxic environment – which potentially causes secondary morphological deformations (PANZICA-KELLY et al., 2015; KHAN et al., 2019).

Other parameters such as lipophilicity, charges, and specific molecular conformations, may also play an important role in the definition of the uptake of chemicals across the chorion of zebrafish embryos (PELKA et al., 2017). The removal of the chorion protection enables us to begin exposition of the embryo at an early life stage when the fish has begun its organogenesis (CHEN et al., 2015), and consequently to change its toxicological profile. For example, TiO_2 and graphitic carbon nitride (g-C_3N_4) nanomaterial showed no acute toxicity to zebrafish embryos with chorion protection. Nevertheless, de-chorionated embryos exhibited an increase in mortality due to direct nano-bio interaction between the nanomaterial and the embryonic epidermis (HE et al., 2020). It is therefore fundamental to understand the influence of chorion on the toxicity of nanohybrids in order to support the development of standardized nanotoxicity testing.

The synthetic method used to produce GO-AgNPs critically influences their final material properties. The reducing agent used in the reaction (ÇIPLAK et al., 2015), different ratios of GO and Ag^+ (ÇIPLAK et al., 2015; KAVINKUMAR; MANIVANNAN, 2016) or surface microchemicals (quantity of oxygen function groups or debris) present in raw GO (FARIA et al., 2012) could provide distinct nanohybrid material. Therefore, it is necessary to use an integrated approach (chemical and physical techniques) to better understand the different aspects related to chemical composition (e.g., functional surface groups, oxidation states, silver loading) and structure (e.g., metal particle size and shape, crystalline phase, chemical bonds); especially, when considering nano-toxicological studies (FLAHAUT et al., 2018).

In this work, we performed an integrated nanosafety study for an ecotoxicity assessment of the emerging GO-AgNPs nanohybrid using zebrafish embryos as a biological model. The following aspects were studied: i) GO-Ag nanohybrid synthesis and characterization; ii) nanohybrid dispersion stability and silver dissolution in the

zebrafish medium; and iii) toxicity assessment on the zebrafish embryos. The influences of chorion membrane removal and NOM on the toxicity of GO-AgNPs were reported towards more realistic and standardized methods for nano-ecotoxicology research and regulatory issues.

3.2. Material and methods

3.2.1. Synthesis of nanomaterial

3.2.1.1. Graphene oxide

GO sheets were synthesized from graphite flakes (purchased from Sigma-Aldrich, Lot#MKBW0432V) by the modified Hummers method (BECERRIL et al., 2008). Briefly, a graphite flake (5.0g) and $NaNO_3$ (3.75 mg) were placed in a round-bottomed flask and H_2SO_4 (370 mL; A.R) was added in an ice bath under continuous stirring for 20 minutes. Then $KMnO_4$ (22.5g) was slowly added over about one hour. The mixture reaction was stirred for 72 hours at room temperature, which was then diluted with ultrapure water (300 mL). The mixture was stirred again for one more hour at 95°C. After the temperature fell to 60°C, H_2O_2 (15 ml; 30%) was added to reduce the $KMnO_4$ residual and the liquid was left to stand overnight. The resultant mixture was brilliant yellow.

The mixture was centrifuged (6,000 rpm; 15 min) and rinsed with 1.0 L of an aqueous H_2SO_4 solution (3%) and H_2O_2 (0.5%) to remove oxidant ions and inorganic impurities. The resulting product was dialyzed (cut-off: 14,000 kDa) against deionized water for 3 days. The graphene oxide dispersion was lyophilized to produce GO powder, which was stored in a sealed vessel at room temperature. Stock-suspensions of 1 mg mL^{-1} were prepared in ultrapure water by sonication in an ultrasonic bath (CPXH; Cole-Parmer) at 40 Hz for 80 min.

3.2.1.2. Graphene oxide-silver nanoparticle hybrid material

A GO-AgNPs nanohybrid was obtained using $NaBH_4$ as a reducing agent for the $AgNO_3$ (MAHMOUDI et al., 2015). Previously prepared GO (20 mg) was dispersed in ultrapure water (40 mL) using an ultrasonic bath (1 hour). This suspension was

mixed with $AgNO_3$ (purchased from Sigma Aldrich, purity > 99.0% per 0.004 mol L^{-1}; 20 ml) in an ice bath under continuous stirring for 1 hour. Then $NaBH_4$ (63 mg) was slowly added and the reaction was kept under stirring overnight to ensure that the silver was reduced entirely. The GO-AgNP stock dispersion was stored in a sealed vessel protected from light.

3.2.2. Characterization of nanomaterial

The absorbance of GO and GO-AgNP dispersions was recorded using UV-vis spectroscopy (micro plate spectrophotometer; MultiskanTM; Thermo Scientific). The appearance of a Plasmon resonance band at 390-410 nm was used to confirm the formation of AgNPs. The high-resolution X-ray diffraction (XRD) patterns (XDR6000, Shimadzu) of dry samples were measured using Cu Kα1 radiation (λ: 1.5406 Å) at 40 kV in the range of 2θ = 5–90°. The shape, surface morphology and thickness of the graphene sheets were evaluated through topography images from atomic force microscopy (AFM). This analysis was conducted in ambient conditions using a Multimode 8 microscope with a Nano Scope 5 controller, with Peakforce tapping (Bruker). Images were treated on Gwyddion software. We obtained size distributions of GO sheets by measuring ~130 flakes on ImageJ software.

Transmission Electron Microscopy (TEM) analyses were carried out using a JEM-2100 microscope, operating in TEM mode at 200 kV and a Double Aberration Corrected Titan Cubed Themis, performing an 80 and 300 kV. TEM samples were prepared by dropping 3 mL of diluted dispersion on Cu grids with a Lacey carbon film. The size distributions of AgNPs on GO sheets we obtained by measuring 100 nanoparticles, using ImageJ software.

Raman spectra were measured using XploRA™ PLUS Confocal Raman Microscope (Horiba Jobin Yvon). The excitation wavelength was 638 nm. The scanned spectral range was 400-4000 cm^{-1} with a spectral resolution of >1.4 cm^{-1} and accumulation times were typically five collections of 5s. The samples were prepared by spreading a small quantity of solid powder on glass microscope slides and Raman spectra were collected at random points under a magnification of 100X the objective.

X-ray photoelectron spectroscopic (XPS) analysis was performed to verify the surface chemistry of GO and its nanohybrid material. This analysis was carried out at

K-Alpha XPS (Thermo Fisher Scientific). Survey spectra were measured (i.e., full-range) to identify the elemental composition of materials. High-resolution spectra of carbon and silver (only to nanohybrid) were acquired to determine the functional groups and silver state. The data were analysed using Thermo Advantage software (version 5.957).

Thermo gravimetric analysis (TGA) was performed using a thermogravimetric analyzer (STA 449 F3Jupiter@; NETZSCH,; 10°C min^{-1}; synthetic air flow rat of 50 mL min^{-1}).

3.2.3. Dispersion stability monitoring

The dispersion stability of nanomaterial (100 mg L^{-1}) in the absence and presence of NOM (Suwannee River NOM; International Humic Substances Society; fixed concentration: 20 mg L^{-1}) was pursued by spectrophotometric analyses (micro plate spectrophotometer; Multiskan GO; Thermo Scientific). The absorbance of samples at 230 nm was used to compare stabilities. Surface charges (zeta potentials) of the material were measured by electrophoretic light scattering (ELS) at Zetasizer Nano ZS (Model ZEN3600, Malvern). The dispersion was prepared in ultrapure water (as a reference control) and the zebrafish embryo medium (used in a biological assay). The samples were maintained static for 72 hours, and 100-µL aliquot was removed every 24 hours from the surface of the dispersion. Each measurement was carried out with three independent measures. We used the OECD 318 guideline (OECD, 2017), with modifications, when monitoring the colloidal dispersion stability of nanomaterial in ultrapure water and the zebrafish medium.

The NOM concentration used in the present study presented itself in the US EPA test guidelines (USEPA, 1996) due to being representative of surface and groundwater environmental conditions (JANKNECHT et al., 2009; WANG et al., 2015; CLEMENTE et al., 2017).

3.2.4. Zebrafish embryo toxicity testing

In vivo assays are based on the fish embryo acute toxicity (FET) test (OECD 236, 2013) (OECD, 2013) modified for chorion removal. Briefly, zebrafish eggs were collected one hour after a natural mating of wild-type adults, and washed with

reconstituted water. The eggs were selected under microscopy for their viability to assay. The egg was considered non-viable if the embryo was delayed, not correctly developed, or dead (a coagulated egg). 24 hours post-fertilization (HPF), the eggs were de-chorionated mechanically with forceps (Dumont™ no.5) according to the reported procedure (HENN; BRAUNBECK, 2011).

The exposition commenced at 24 hpf and was performed for 72 hours (24-96 hpf) without any renovation in the medium. The two groups of embryos were exposed to the same range of concentrations, as follows. Salts/nanomaterial (5 different expositions): the control (medium only); $AgNO_3$; GO; GO-AgNPs; and a filtrate-only control.

Moreover, the co-exposure with NOM (Suwannee River NOM, International Humic Substances Society, fixed concentration at 20 mg L^{-1}) was also evaluated and all experiments were carried out in triplicate. Thus, the breakdown for the number of treatments was as follows: two groups of embryos (with and without chorion) in five different substances or nanomaterial types, multiplied by two (presence or absence of NOM), giving us 20 treatments in total.

The filtrate-only control was also performed to assess either impairment caused by dissolved ions throughout the assay. The dispersion then of GO-AgNPs in the zebrafish media (100 mg L^{-1}) was kept under the same conditions (test media, photoperiod, temperature) and time (72h) of the assay; after this, the dispersion was filtrated (Millipore; 0,1 nm; Ptfe). The remaining filtrate was diluted and used in a FET assay (PETERSEN, 2015). The dilution factor was similar to making 0.5; 1; 2 and 4 mg L^{-1}; that is, 200; 100; 50 and 25 times. The test was performed under the same conditions as the OECD standard test, as described below. For every group, 10 embryos (3 replicates) were exposed to 20 ml of dispersion (2 ml/egg) and incubated in Petri dishes at 28°C and a 14h:10h, light : dark cycle until after 96 HPF, live larvae are photographed with a stereomicroscope (Stereo Discovery V20, Zeiss). The fish embryo was kept in reconstituted water (fish embryo medium), prepared as moderately hard water (USEPA, 2002). Briefly, into distilled water was added $NaHCO_3$ (96 mg L^{-1}), $MgSO_4$ (60 mg L^{-1}), KCl (4 mg L^{-1}), $CaSO_4$ (60 mg L^{-1}), and pH 7.5±0.5. The parameters assessed in FET were: i) mortality, ii) malformation, iii) edema, iv) hatching, v) total length and vi) yolk sac size. The lethal concentration (LC_{50}) value (i.e. a concentration that kills 50% of the embryos during the observation period) was calculated based on the mortality rate and was used when comparing the two groups.

The Embrapa Environment's Ethics Commission approved the animal handling procedures for Animal Use (CEUA-Embrapa Environment, protocol number 004/2017).

3.2.5. Chemical transformation of the GO-AgNP nanohybrid in the zebrafish culture medium

Chemical changes due to exposure to the environment (i.e. light, temperature, test media, presence of NOM) were assessed in the GO-AgNPs during the toxicity assay. For this, a dispersion (100 mg L^{-1}) of GO-AgNPs in the medium test was prepared and maintained in the same conditions as the test. After 72 hours, the liquid was centrifuged (14,000 rpm; 1 hour) and the supernatant was discarded. The pellet was re-suspended in ultrapure water and the chemistry surface analysed by XPS. The control experiment was performed using the same procedure, but the dispersion (100 mg L^{-1} of GO-AgNPs in medium test) was centrifuged immediately. In addition to this, the contribution of the presence of NOM (20 mg L^{-1}) was also evaluated.

3.2.6. Data analysis

The lethal concentration (LC_{50}) values (i.e. a concentration that kills 50% of the embryos during the observation period) and 95% confidence intervals were calculated using Probit analyses of dose-mortality data from bioassay studies in PriProbit software. Data were analysed regarding normality distribution and homogeneity of variance (homoscedasticity) using (respectively) Shapiro-Wilk's and Levene's tests. As the results were normal and homoscedastic, differences between means of treatments were evaluated using variance analysis (ANOVA-one way). Differences between embryos with and without chorion were analysed using ANOVA-two way. The tests were followed by Dunnet's multiple comparisons test with a confidence interval of $p < 0.05$. Statistical analyses and graphs were generated on Origin software (version 8.5). All data are presented as the means ± SD.

3.3. Results and discussion

The GO-AgNPs nanohybrid demonstrated the ability to be synthetized through *in situ* methods, in which the growth of the metal nanoparticle occurs directly on the graphene oxide flake, or through *ex situ* methods, in which a premade nanoparticle is

attached to the graphene oxide surface. Different methods may be applied for each approach. The *in situ* approach, for example, includes reduction by chemical agents, and hydrothermal and electrochemical techniques (YIN et al., 2015). In this study, the one-step aqueous methods using the reduction method to form a GO-AgNP nanohybrid were chosen. In general, this technique uses a metal precursor (e.g. $AgNO_3$) mixture with GO dispersion, and a chemical agent simultaneously reduces it. The defects and oxygen-functional groups provide the attachment of free Ag^+ onto a GO surface through electrostatic interactions, and the addition of reducing agents, enabling the synthesis of AgNPs (FARIA et al., 2012). The synthesis of nanohybrids in this study used $NaBH_4$ as a reduction agent and the growth of AgNPs was controlled by the low temperature (ice bath).

Several substances may be used to reduced Ag^+ in the presence of GO for synthesis of the nanohybrid, such as sodium citrate (FARIA et al., 2012, TANG et al., 2013), potassium hydroxide (PASRICHA et al., 2009), or hydrazine hydrate (ÇIPLAK et al., 2015). Environmentally friendly (green) synthesis has also been developed: *Hibiscus sabdariffa* extract (NAZARI; MOVAFEGHI, 2018), glucose (SHAO et al., 2015, Kim et al., 2018), and ascorbic acid (KAVINKUMAR; MANIVANNAN, 2016) have each been used to form the GO-AgNP nanohybrid.

However, the mechanism of silver nanoparticle nucleation and growth on GO surfaces needs to be elucidated in more detail by exploring advanced characterization methods. Furthermore, graphene-metal nanohybrids exhibit emergent properties, which might be able to modify the characteristics of its precursor (WANG et al., 2019). Thus, a complete nanohybrid characterization is crucial to elucidate the interactions of nanomaterial within biological and environmental systems (FLAHAUT et al., 2018).

3.3.1. Graphene oxide characterization

The final GO stock-dispersion (1.0 g L^{-1}) shows a light brown colour (Figure 1-A). The optical characteristics of GO were verified by UV-Vis spectroscopy in the range of 200-800 nm. The absorption spectrum of GO exhibited an absorption band centred at 230 nm, which is characteristic of π-π* electronic transitions of C-C aromatic bonds (MORAES, 2015) (Figure 1-B). The XRD pattern (Figure 1-C) exhibits diffraction peaks at 2θ values of 10.9 and 42.3 that may be indexed as (002) and (100) diffraction plans of hexagonal structure graphene oxide.

AFM images of GO reveals size distribution from 50 to 650 nm, the mean size being 180 nm. A histogram of particle sizes was constructed by counting more than one hundred flakes. Besides this, the topography images showed their average thickness to be around 1 nm, which reveals a single-layer structure of GO sheets. However, this was larger than that for pure graphene (0.335 nm), probably because of oxygenated groups present in GO (LIU et al., 2017) (Figure 1-D, E, F).

Raman spectroscopy is a useful technique that provides remarkable information on the structural disorder in sp^2 hybridized carbon materials, such as graphene. The Raman scattering spectrum (Figure 1-G) of GO typically presents two peaks: the D-Band and G-Band. The first band, D, was located at ~1332 cm^{-1} and assigned to the breathing mode of κ-point phonons, with A1g symmetry. This band has thus resulted in a disordered structure of graphene. The prominent D peak originates from the structural imperfections created by introducing hydroxyl and epoxide groups in the carbon structure during the oxidation of graphene flakes. The G band (~1590 cm^{-1}) is attributed to the tangential stretching mode of the E2g phonon in the sp^2 carbon atoms (DRESSELHAUS et al., 2010). In this way, the ratio between intensities of the D-Band (I_D) and G-Band (I_G) could indicate the proportion of defects in flakes. In GO flakes, the calculated ratio was 1.15, which shows a high presence of defects that confirm the presence of oxygenated groups in graphene flakes.

The chemical composition of the GO surface was determined by X-ray photoelectron spectroscopy (XPS). Survey spectrum (Figure 1-H) showed the presence of carbon (66.5 ± 0.9%), oxygen (31.4 ± 0.6%) and nitrogen (2.0 ± 0.6%). A high percentage of oxygen confirmed the oxidation of GO. The high-resolution C1s spectrum (Figure1-I) reveals the functional groups (C-O and COO) present on the surface of GO. Table 3.1 shows the respective percent contents of each group derived from the de-convoluted C1s spectrum.

Thermogravimetric analysis was acquired in order to access the thermal stability of GO and the result is presented in the supplementary material (Figure S1 - Appendix A). GO displays a two steps decomposition. The first mass loss, that occur in the range of 150 – 200°C, is attributed to the decomposition of oxygenated groups and the second, at 500°C is assigned to the decomposition of the graphitic portion.

Figure 1: Graphene oxide (GO) characterization. Stock dispersion at 1.0 g L^{-1} (A), UV-Vis absorption spectrum (B). XRD pattern (C). AFM topography image (D). AFM topography image zoomed in (E). Histogram of size distribution of GO flakes (F). Raman Spectrum, D and G bands (G). Survey XPS spectrum (H). High-resolution C1s XPS spectrum (I)

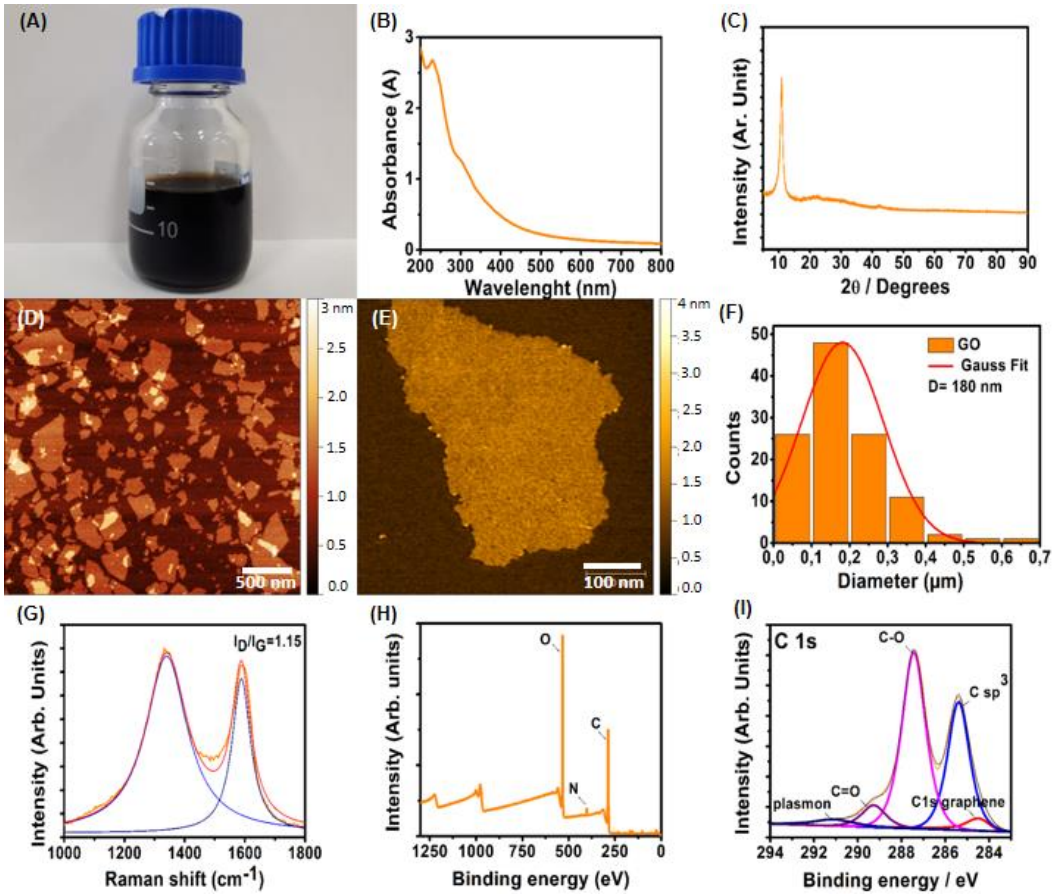

Table 1: Surface chemistry elemental analysis in high-resolution C1s of GO by X-ray photoelectron spectroscopy

Chemical groups	Binding energy (eV)	% Atomic
Graphitic / aromatic carbon (-C=C-)	284.1	5.34
Aliphatic carbon (-C-C-)	285.0	31.97
Epoxy/hydroxyl groups (C-O)	286.9	45.52
Carbon / ester (COO)	288.7	9.11
π- π * transition in aromatic	290.7	8.07

3.3.2. Graphene oxide silver nanoparticle characterization

GO-AgNP stock dispersion presents a black-green colour (Figure 2-A). The UV-Vis absorption spectrum (Figure 2-B) shows an absorption band at 400 nm that refers to the plasmon resonance due to the formation of AgNPs. The XRD pattern of the

GO-AgNP nanohybrid material exhibits a broad diffraction peaks at a 2θ value of 25.0 that corresponds to the (002) graphene diffraction plan. This result suggests that graphene oxide is partially reduced to graphene during nanohybrid material synthesis. In addition, the XRD pattern of GO-AgNPs also presents diffraction reflections at 2θ values of 38, 44.1, 64.3 and 77.4, corresponding to the (111), (200), (220) and (311) diffraction planes of the Ag cubic phase (ICDD/PDF 01-1167), confirming that decoration of the graphene sheet with Ag nanoparticles occurs (Figure 2-C).

TEM images of GO-AgNPs show the formation of uniformly distributed AgNPs (black dots) on the surface of the GO sheet. The AgNPs are of a mean size of 5.8 nm (Figure 2-D,E,F,G). Furthermore, Das et al. (2011) and Mahmoudi et al. (2015) prepared GO-AgNPs nanohybrid using borohydride as a reducing agent of silver nitrate in a GO dispersion. The distribution size of AgNPs was very similar (5-10 nm and 2-5 nm, respectively).

Negative surface charges carried by functional groups in the GO flakes allowed electrostatic interaction with the Ag^+ ion and provided a platform for the nucleation and growth of nanoparticles. The Raman spectrum of the GO-AgNPs nanohybrid (Figure 2-I) displays a considerable increase in the ratio of the intensities of the D and G bands (I_D/I_G) from 1.15 to 1.35, after decorating GO nanoflakes with AgNPs. This increase in the I_D/I_G value may be attributed to a rise in degree of disorder in the graphene matrix due to the interaction of GO with AgNPs. Similarly, Chen et al. (2018) observed an enhancement of the I_D/I_G ratio after AgNPs anchored into GO flakes, due to an increase in the structural defects of graphene. In this case, they found an I_D/I_G value of 1.098 for GO; after hybrid formation, the ratio modified to 1.31.

The XPS survey spectrum (Figure 2-J) revealed that the surface chemistry of GO-AgNPs is composed of 67.45% carbon, 29.67% oxygen, and 2.88% silver. The high-resolution de-convoluted C1s spectrum (Figure 2-K) showed the peaks at binding energies of 285, 286.9, and 288.7 eV, attributing to the C–C, C–O and O–C═O bonds, as exhibited respectively in Table 2. The lowering of the epoxy/hydroxyl group content in the hybrid material manifested that sodium borohydride also reduced the epoxy and aldehyde groups present in the GO sheet. Furthermore, the Ag spectrum (Figure 2-L) shows the characteristic peaks for Ag3d at 368.3 and 374.3 eV corresponding to the $Ag3d_{5/2}$ and $Ag3d_{3/2}$, respectively, suggesting an interaction of AgNPs with graphene oxide sheets. Furthermore, the Ag spectrum (Figure 2-L) was composed mostly of Ag metal (~99%). The presence of silver mostly in metallic form indicates that the growth

of AgNPs in GO sheets has also been observed in previous studies (DE MORAES, 2015; SHAO et al., 2015; KELLICI et al., 2016).

The thermal gravimetric analysis (TGA) shows the two steps decomposition similarity to GO (Supplementary Material; Figure S1 – Appendix A). However, the nanohybrid displays reduction of decomposition temperatures. This behaviour suggest that AgNPs act as catalysts (FARIA et al., 2014; MORAES, 2015). Moreover, the residuals content, approximately 60%, could be related to the silver mass proportion on GO-AgNPs.

Figure 2: GO-AgNP nanohybrid characterization. Stock-dispersion at 0.5 g L^{-1} (A), UV-Vis absorption spectrum with plasmon resonance @ 400 nm (B). XRD pattern (C). Typical TEM images (D). TEM image, high resolution (E). TEM image of AgNPs (F). Histogram AgNP size distribution decorated on a GO flake (G); AFM topography image (H). Raman Spectrum, D and G bands (I). Survey XPS spectrum (J). High-resolution C1s XPS spectrum (K). High-resolution Ag spectrum (L)

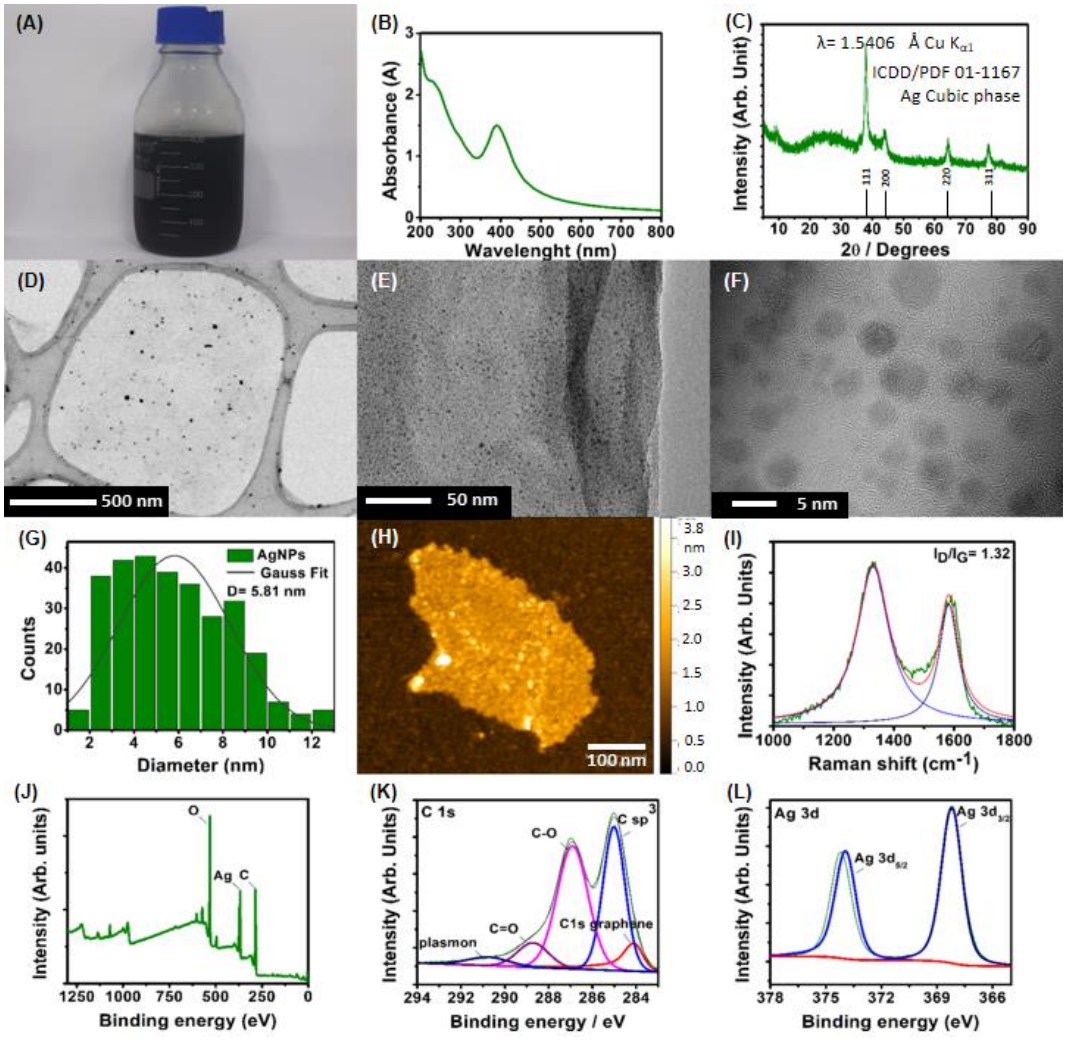

Table 2: Surface chemistry elemental analysis in high-resolution C1s and of GO-AgNPs by X-ray photoelectron spectroscopy

Chemical groups	Binding energy (eV)	% Atomic
Graphitic / aromatic carbon (-C=C-)	284.1	9.78
Aliphatic carbon (-C-C-)	285.0	33.65
Epoxy/hydroxyl groups (C-O)	286.9	35.97
Carbon / ester (COO)	288.7	11.88
π- π * transition in aromatic	290.7	8.73

3.4. The influence of nom on the dispersion stability of GO and GO-AgNPs in ultrapure water and the fish embryo medium

The fish embryo medium is a type of standard synthetic water recommended by USEPA in order to simulate natural surface water. In this way, the medium exhibits characteristics of a real water environment where features of multiple salts coexist. Each ion in the medium affects nanomaterial aggregation and sedimentation behaviour.

Moreover, in the aquatic environment, the nanomaterial's stability can also be affected by interaction with Natural Organic Matter (NOM). It interacts with nanomaterial and increases the steric repulsive force between nanoparticles (BUNDSCHUH et al., 2018). Consequently, the surface coating formed in nanoparticles can increase stability and its bioavailability (JIANG et al., 2017).

The dispersion stability of GO and the GO-AgNP nanohybrid was studied in ultrapure water and a fish embryo medium in the presence and absence of NOM (Figure 3-A, B). The GO and GO-AgNPs in ultrapure water feature desirable stability demonstrated by a small decrease in absorbance (less than 20% for all samples) and a high surface charge (ζ_{GO} = -47,9 ± 2,9 mV and $\zeta_{GO\text{-}AgNPs}$ = -46,6 ± 2,5 mV) (OECD, 2017) (Figure 3-C). This probably occurred due to high surface oxygen contents and small particle size. However, in the zebrafish embryo medium, after 24h the samples decreased absorbance to less than 40% of the initial, and the surface charge reduced to ζ_{GO} = -24,8 ± 2,2 mV and $\zeta_{GO\text{-}AgNPs}$ = -18,8 ± 0,7 mV (Figure 3-D). The lower colloidal stability was brought about by the ionic strength of medium and salt types (cationic salts like Na^+, Ca^{2+} e Mg^{2+}) that compete for adsorption with protons on the colloidal surface and reduced ionic strength (HE et al., 2017). Consequently,

aggregation and/or destabilization of flakes occur; it is possible to observe, however, nanomaterial floating, separating the dispersion into two phases as seen through a visual inspection (Figure 3-B).

The presence of NOM has the potential to change stability due to hydrogen bonds, Lewis acid-base interactions, π– π interactions, and steric repulsions (JIANG et al., 2017). Similar to Clemente et al. (2017), an enhancement of colloidal stability in the presence of NOM was observed for GO in the zebrafish medium, which maintained ~90% initial absorbance throughout 72 hours. However, the NOM at 20 mg mL^{-1} was not sufficient to produce stable dispersions for GO-AgNPs due to the lower amount of oxygen groups promoted by the partial reduction of graphene oxide caused by borohydride, as demonstrated by the lower surface charge (Zeta potential), XRD patterns and decrease of total percentage of C-O (High resolution C1s XPS spectra). In this way, the number of functional sites that NOM may interact with is not enough to enhance the colloidal stability of a nanohybrid in the fish embryo medium. However, it is very difficult to probe the stability of GO-based materials with much precision. Due to flocculent settling, the supernatant phase and the sedimentation/coagulation phase demonstrates different nanomaterial behaviours/concentrations. Thus, the collected material for the UV-Vis studied only reflects the condition of the upper layer (Figure 3).

Figure 3: Monitoring the dispersing stability of GO and GO-AgNPs in ultrapure water and fish embryo media in the presence and absence of NOM (Final concentration: 20 mg L-1). Visual inspection in ultrapure water (A) and fish embryo media (B) for 72h. Percentage of initial absorbance @ 235 nm of samples at ultrapure water (C) and fish embryo media (D)

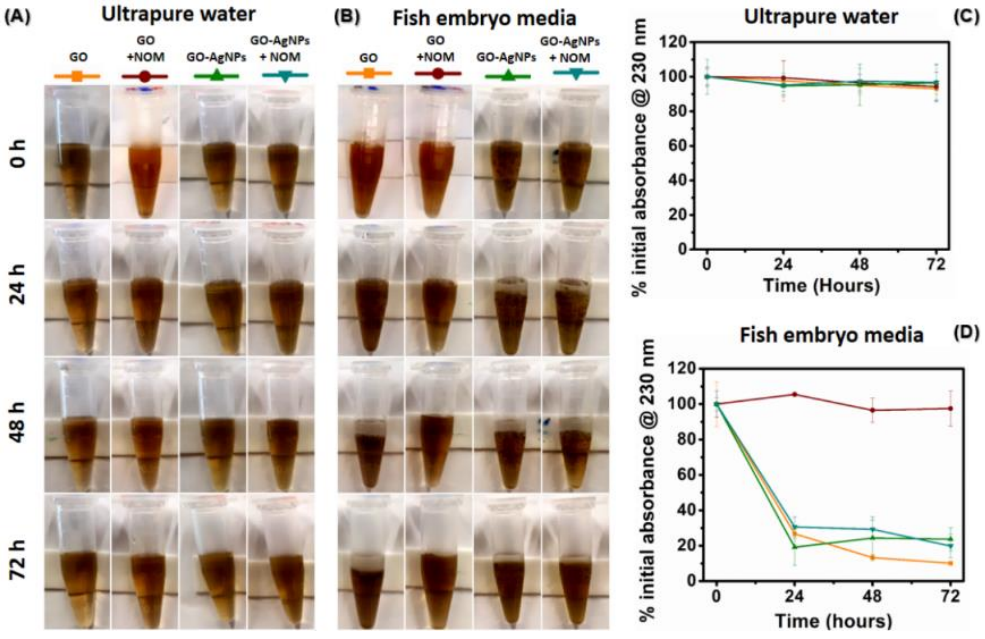

3.5. Toxicity on zebrafish embryos

Chorion is a polypeptide structure that protects the embryo from exposure to external agents until hatching and represents a biological barrier to protect embryos. In this way, the effects observed after exposition are directly related to the permeability of chorion to this chemical compound (HENN; BRAUNBECK, 2011).

Protocols for chorion membrane removal are emerging to overcome this matter, and high throughput screening systems using embryos without chorion are already being exploited for nanomaterial toxicity studies (PELKA et al., 2017). Additionally, nanomaterial physicochemical properties might allow us to determine how it would interact with biological membranes, (i.e. chorion) and consequently, determine the effects observed in organisms (PAATERO et al., 2017; MENG et al., 2018). Its removal seems to make the organism more susceptible. For example, Olasagasti et al. (2014) observed the influence of chorion membrane in the deleterious exposition effects (i.e. changes in gene expression and in the uptake of NPs) of commercial AgNPs (18 mm) in zebrafish. When an embryo was surrounded by chorion (e.g. exposition begins with 4 HPF and finishes with 48 HPF), it did not show changes in comparison to the control. On the other hand, when the exposition started after hatching (72 HPF) they noted overexpression in Mt (considered as a specific biomarker for metal toxicity) and Il1β genes (that are activated in response to inflammation and involved in the innate immune response) and in the uptake of NPs after 48 hours. Hatched embryos therefore provide an assessment potential of real toxic nanoparticle effects, without the influence of a chorion membrane. The ability of nanoparticles to penetrate chorion then is a key factor in the experimental design that influences toxicology profiles (PAATERO et al., 2017; HAMM et al., 2019). The chorion-off approach for the embryo toxicity assay was developed to ensure the contact of naked embryos with nanoparticles and eliminate differences with the chorion barrier (PANZICA-KELLY et al., 2015). It is an important step in knowledge towards the development of nanosafety studies.

The exposure of $AgNO_3$ to chorionated and de-chorionated embryos results in LC_{50} values of 69.8 (61.1–78.8) and 38.1 (33.3–41.0) μg L^{-1}, respectively. LC_{50} in the presence of NOM reduced toxicity, changing this to a higher value. In this case, the LC_{50} was 172.1 (162.1–183.6) and 94.0 (79.1–119.0) μg L^{-1} for exposition with and without chorion, respectively (Figure 4). Survival embryos presented a bigger yolk sac size than the control for exposure to 50, 60, and 75 μg L^{-1}, and 35, 40, and 50 μg L^{-1}

$AgNO_3$ (absence of NOM) for chorionated and de-chorionated embryos respectively (Figure 4-C). This deleterious effect did not occur in larvae exposure to $AgNO_3$ in the presence of NOM (at 20 mg L^{-1}) (Figure 4-D).

Considering LC_{50} values, the deleterious effects are more pronounced when embryos are de-chorionated and $AgNO_3$ exposure occurs in the absence of NOM. In the control group, all animals showed normal development. It is likely that the sulfhydryl groups present in the chorion were able to absorb cations, leading to low Ag^+ penetration into chorionic space.

These effects agree with those reported by Powers et al. (2010), who observed a small aggregation of chorion in embryos exposed to $AgNO_3$. Chorion might have been acting then as a major barrier to entry into the perivitelline space of metal cations (BURNISON et al., 2006). The toxicological profiles of the nanoparticle might thus be influenced by surface charges; it would then modify the capacity to penetrate through biological barriers such as chorion (PATERO et al., 2017).

The physical deformities caused by the exposure of zebrafish embryos to AgNPs have already been reported (LEE et al., 2007; ASHARANI et al., 2008; MASSARSKY et al., 2013; RIBEIRO et al., 2014; CÁCERES-VÉLEZ et al., 2018). It has also been documented that AgNPs can increase the production of reactive oxidative species (ROS) (MASSARSKY et al., 2013) and consequently, induce significant structural damage (ALE et al., 2018). Moreover, Ag^+ can cross the gill membrane and unbalance the ionoregulatory system because it replaces the Na^+ of the Na^+/K^+ATPase pump which is present in this organ (KWOK et al., 2016). Thus, this process has the potential to lead to the accumulation of fluid under the skin (edema).

Furthermore, NOM acted as a natural antidote for Ag^+. Ionic Ag was able to interact with NOM thought carboxylic groups and mitigated its deleterious effects on embryos (GAO et al., 2015). In this way, NOM may reduce toxicity because it can work as a free-radical scavenger.

Figure 4: Toxicity of $AgNO_3$ on zebrafish embryos in the presence and absence of NOM (20 mg L^{-1}). Visual inspection of larvae with 96 hpf (A). Deleterious effects (percentage) observed at final of exposure (B). Total length and yolk sac size for larvae exposure to $AgNO_3$ in absence of NOM (C). Total length and yolk sac size for larvae exposure to $AgNO_3$ in presence of NOM (D). Asterisks indicate groups that statistically differed from the control (one-way ANOVA, followed by Dunnet's: * $p < 0.05$, ** $p < 0.01$ and *** $p < 0.01$)

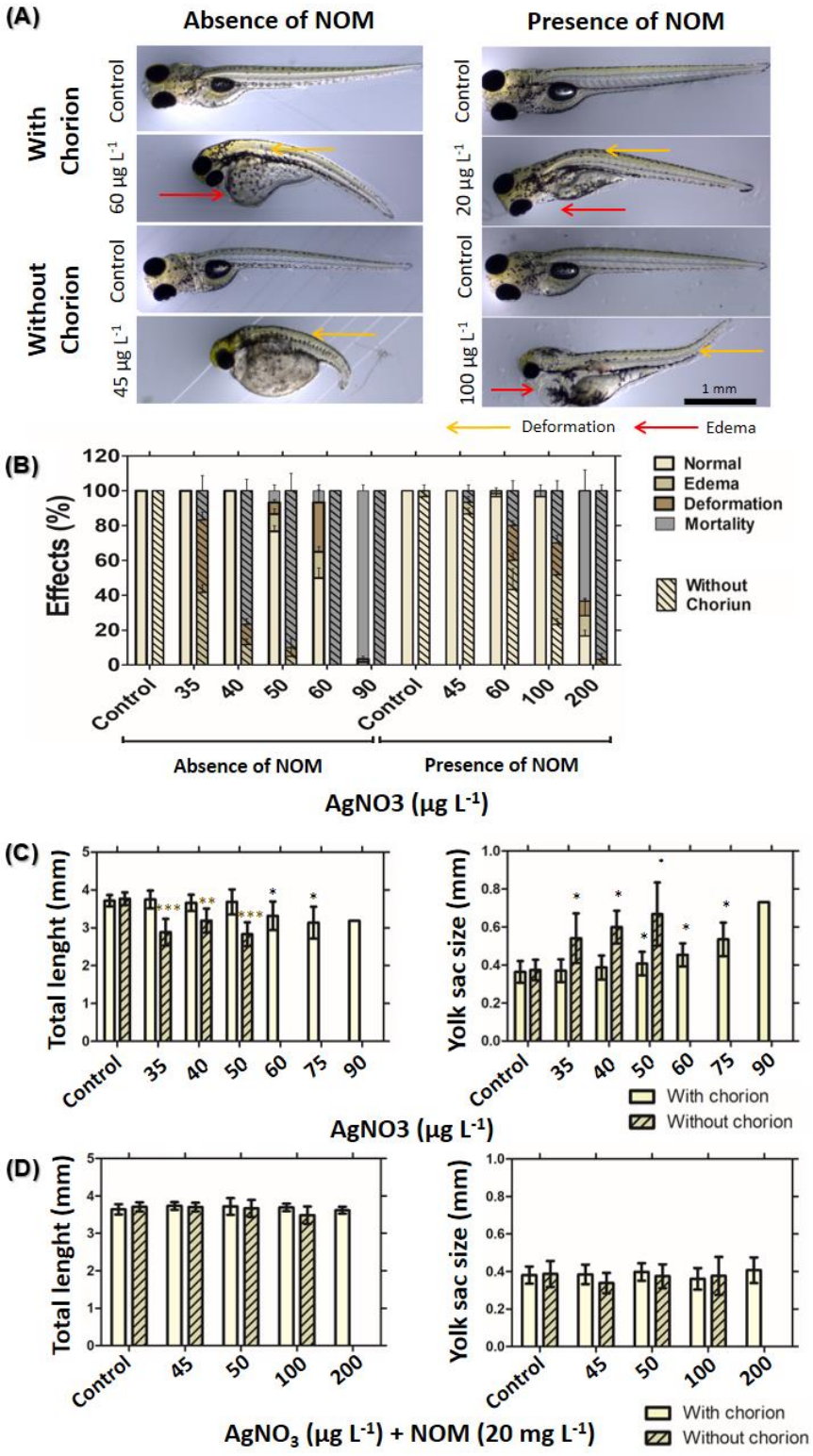

The embryos exposed to GO (in the presence or absence of NOM) did not present any deleterious effects, although we were able to observe the presence of GO inside the digestive tract (Figure 5-A) and in the gills (Figure 5-B) of larvae as observed by Raman spectroscopy (Supplementary Material; Figure S2 – Appendix A). Through this technique, it is possible to see the D and G bands (signal spectra pattern characteristic of GO) inside the organism exposed, which confirms the internalization of carbon nanomaterial (HU et al., 2015). Unfortunately, analysis for the bio-distribution of GO-AgNPs in the embryos through Raman spectroscopy was not possible due to the low concentration dose necessary to maintain the organism alive. Therefore, the nanohybrid was not sufficiently concentrated for Raman measurements to detect it.

Figure 5: Visual inspection of larvae with 96 HPF exposure to GO (100 mg L^{-1}) and the accumulation of nanomaterial as confirmed by Raman spectroscopy in gill (A) and stomach (B)

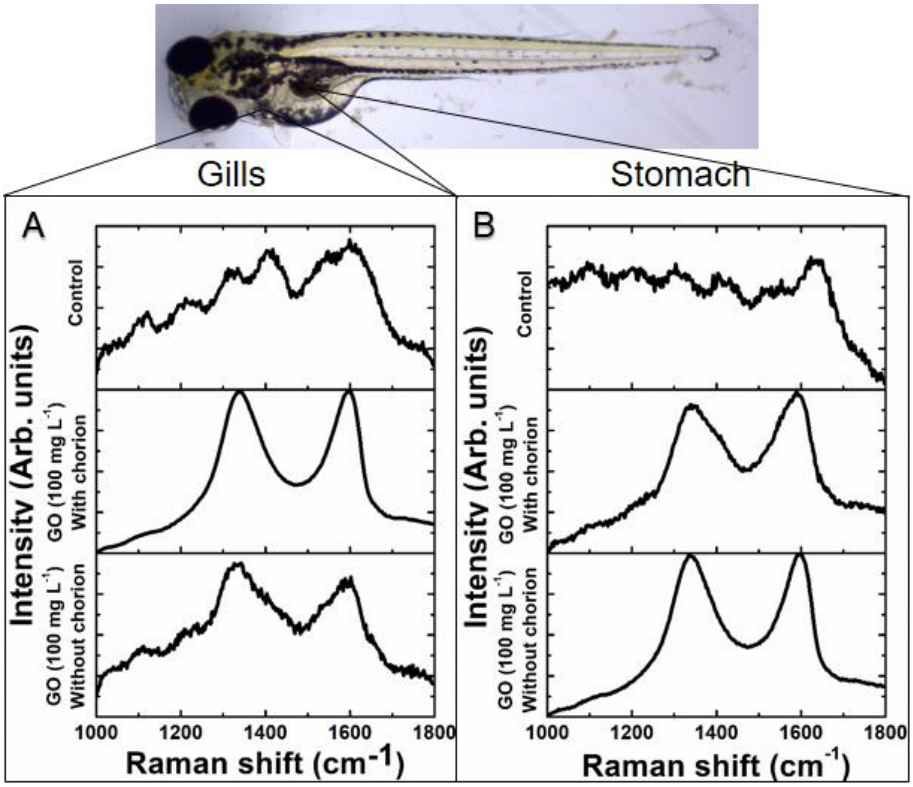

Prior to 120 hpf, the embryos did not actively eat, but were able to start gaping from the protruding-mouth embryo stage (72 hpf) (KIMMEL et al., 1995) allowing the accumulation of nanomaterial along the digestive tract. Moreover, the epidermal route (i.e. epidermis and gills) also plays an important role in the uptake and bio-distribution of nanoparticles (VAN POMEREN et al., 2017).

For the GO-AgNP hybrid, LC_{50} values for chorionated and de-chorionated embryos were, respectively, 1.4 (1.3–1.7) and 1.0 (0.9–1.2) mg L^{-1}. The presence of NOM rose to a higher value, indicating a mitigation of ecotoxicity. In this case, the LC_{50} was 2.3 (2.2–2.5) mg L^{-1} for chorionated embryos and 1.2 (1.1–1.4) mg L^{-1} for de-chorionated embryos (Figure 6-A, B). The LC_{50} for all groups appears in Table 3, below.

Table 3: LC_{50} values (mg L^{-1}) for fish exposed to $AgNO_3$, GO and GO-AgNPs in the absence and presence of NOM (20 mg L^{-1})

		Absence of NOM	**Presence of NOM**
With chorion	$AgNO_3$	0.069 (0.061 – 0.079)	0.172 (0.162 – 0.183)
	GO	>100	>100
	GO-AgNPs	1.4 (1.3 – 1.7)	2.3 (2.2 – 2.5)
Without chorion	$AgNO_3$	0.038 (0.033 – 0.041)	0.094 (0.079 – 0.119)
	GO	>100	>100
	GO-AgNPs	1.0 (0.9 – 1.2)	1.2 (1.1 – 1.4)

Deleterious effects for survival embryos (pericardial edema, notochord malformation as scoliosis, and shortened body) demonstrated the dose-dependent response for exposition to GO-AgNPs. At a higher GO-AgNP concentration, some embryos failed to absorb the yolk sac (Figure 6-C,D). The lack of intake nutrients, then, may compromise the normal development of embryos.

The implications of NOM on the environmental risk assessment of nanomaterial and realistic exposure scenarios involve understanding NOM's environmental interactions and its influence on ecotoxicity (CASTRO et al., 2018). The nanomaterial can interact with organic ligands, thus forming a spontaneous molecular coating: the "NOM-corona" (NASSER; LYNCH, 2016). NOM-coronas have the capacity to influence nanomaterial modification processes in the environment, including dissolution (for metallic nanoparticles), colloidal stability and bio-distribution (CLEMENTE et al., 2017; JIANG et al., 2017; BAALOUSHA et al., 2018; CÁCERES-VÉLEZ et al., 2018). Additionally, corona formation promotes a surface modification that alters the nano-bio-eco-interface, and provides a new biological and environmental entity for nanomaterial (DOCTER et al., 2015).

Figure 6: Toxicity of GO-AgNPs on zebrafish embryos in the presence and absence of NOM (20 mg L^{-1}). Visual inspection of larvae with 96hpf (A). Deleterious effects (percentage) observed at final of exposure (B). Total length and yolk sac size for larvae exposure to GO-AgNPs in absence of NOM (C). Total length and yolk sac size for larvae exposure to GO-AgNPs in presence of NOM (D). Asterisks indicate groups that statistically differed from the control (one-way ANOVA, followed by Dunnet's: * $p < 0.05$, ** $p < 0.01$ and *** $p < 0.01$)

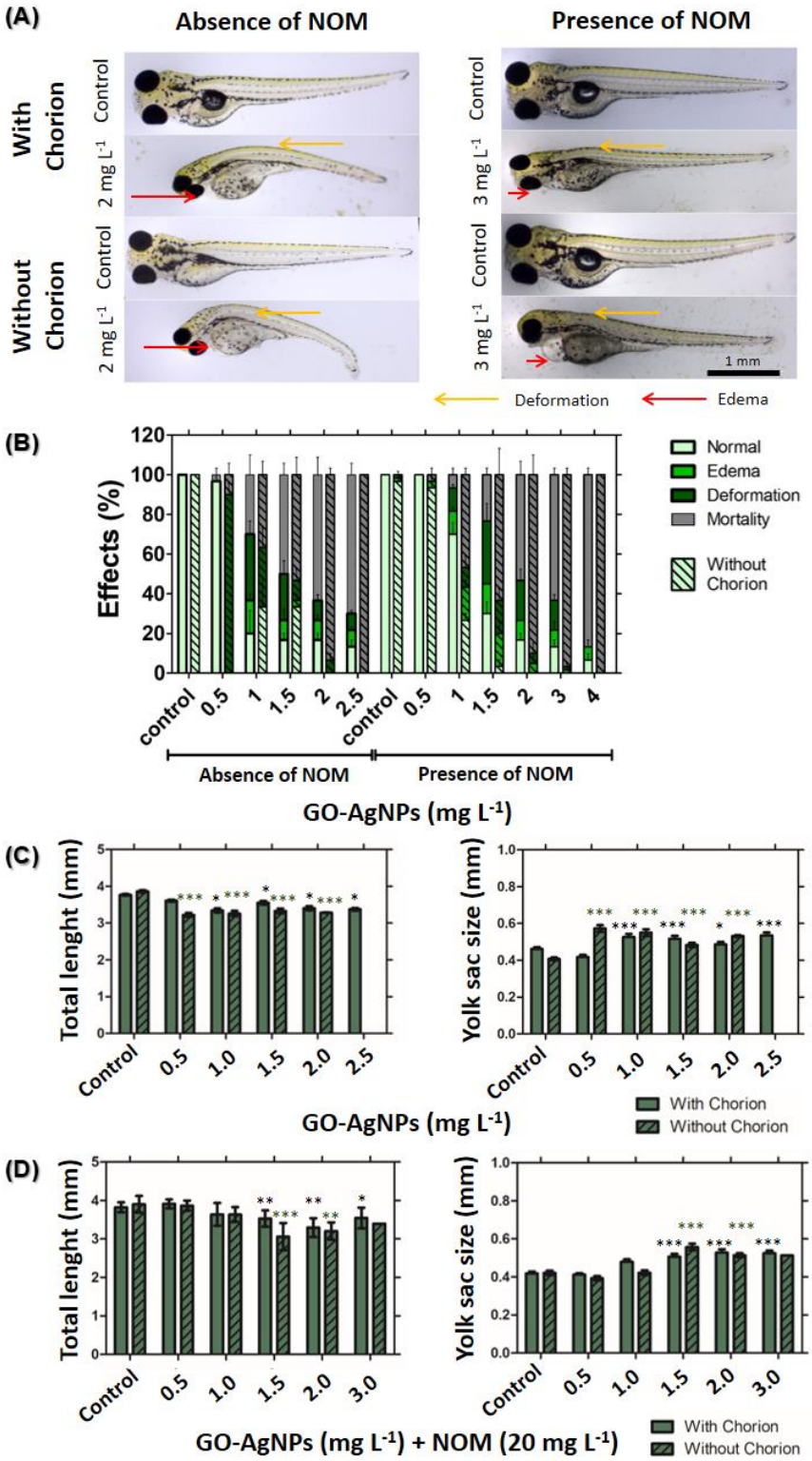

The presence of NOM might in fact modulate toxicity by adsorption on the AgNP surface, forming a corona that provides the reducing dissolution rates from AgNPs into Ag^+ (GUNSOLUS et al., 2015; WANG et al., 2016; CÁCERES-VÉLEZ et al., 2018), and consequently, could reduce ecotoxicity. Hence, the eco-toxicological profiles are determined by intrinsic features and by surrounding environmental conditions (TORTELLA et al., 2019). For this reason, many studies are considering this co-exposure scenario (nanoparticles + NOM) in order to reach more environmentally relevant scenarios (CHEN et al., 2015; GAO et al., 2015; CLEMENTE et al., 2017). The presence of NOM might be able to mediate the adsorption and reduction of free Ag^+ into AgNPs on the GO surface, thus generating a GO-AgNP hybrid (DONG et al., 2019) and decreasing free silver ions in dissolution. Therefore, the amount of free silver ions may be said to affect bioavailability in aqueous media depending on the dissolution rate and adsorption processes of metal NPs (WANG et al., 2016).

As reported in the literature, the primary toxicity of AgNPs is caused by the release of silver ions, but is also influenced by the nanoparticles themselves (VAN AERLE et al., 2013; ABRAMENKO et al., 2018). Therefore, the dissolution of nanoparticles plays a pivotal role in metal nanoparticle fate, bio-distribution and toxicity and needs to be taken into consideration as a decision criterion in a regulatory context (KLAESSIG, 2018). In fact, there is a correlation between dissolution behaviour and the toxicity of AgNPs in different ionic environments, especially when mediated by the presence of chloride ions (LEE et al., 2018).

Furthermore, differences between observed exposure effects of GO-AgNPs nanohybrids and each nanomaterial isolated (GO and AgNPs) was also observed by Wierzbicki et al. (2019). They observed an enhancement of antibacterial properties in the nanohybrids and an inhibition of AgNP toxic effects – such as cytotoxicity towards fibroblasts, human umbilical vein endothelial cells, and chicken embryo chorioallantois membranes. Similarly, they also demonstrated the good biocompatibility between GO and the nanohybrid GO-AgNPs.

In order to understand the effects from the dissolution of silver nanoparticles on toxicity, filtrate-only control was performed. The idea was to observe the potential effects of the remaining filtrates and assess the influence of dissolved ions in the ecotoxicity assay (PETERSEN, 2015). The filtrate-only control did not reveal any deleterious effects in chorionated embryos. Conversely, for embryo exposure without chorion, it was possible to observe an enhancement of impairment effects on

development. However, it was not possible to calculate the LC_{50} value because it was higher than the maximum value studied (Supplementary Material, Figure S3 – Appendix A). According to this, the silver nanoparticle dissolution promoted low ion releases and the major cause of impairments observed in GO-AgNP exposure seems to have been mainly produced by the nanohybrids themselves.

The XPS high-resolution spectra for Ag with GO-AgNPs after 72h in the same conditions as those of the FET assay did not reveal any alteration in silver speciation at surface level in comparison to the control (Supplementary Material, Table 1 and Figure S4 – Appendicx A). Similarly, Intrchom et al. (2018) observed a reduced dissolution in Ag^+ from carbon nanotube-AgNP nanohybrids, and consequently, a decline of ecotoxicity in freshwater algae (*Chlamydomonas reinhardtii*). Moreover, it is important to emphasize that the nanohybrid effects cannot have been attributed to AgNPs alone. In this case, a potentiation effect might have been present. For example, Liu et al. (2017) studied the impact of GO-AgNPs on bacterial biofilm formation. The inhibition was attributed to ROS formation and physical damage. The observed effect of the nanohybrid was stronger than that observed in a single exposure to GO or AgNPs. These findings reinforce the importance of studying the nanohybrid as a new material because the effect may be distinct from the isolated material.

It was not possible to evaluate the toxic effects of isolated AgNPs because it proved too challenging to synthesize nanoparticles in an aqueous solution with the same characteristics (e.g. shape, size, surface chemistry and structural defects). For example, Faria et al. (2014) synthesized AgNPs anchored in GO-AgNPs and produced nanoparticles with an average size of 7.5 nm and spherical morphology. Whereas, in the absence of GO, the AgNPs produced showed variable shape and a bigger diameter (~ 60 nm). Further, the presence of GO in an aqueous solution modified the environment in which the reduction of Ag^+ would occur, and the presence of functional groups made an ideal scaffold grown from AgNPs, providing an anchor to begin nucleation and prevent aggregation (PERREAULT et al., 2015). Therefore, the presence of GO plays a pivotal role in the nucleation and growth of AgNPs, enabling the generation of smaller nanoparticles. A GO scaffold, then, is important for modifying the silver nanoparticles' toxic characteristics (ABRAMENKO et al., 2018; GEORGE et al., 2012; LIU et al., 2019).

It is, in fact, very hard to establish a direct comparison among isolated materials and nanohybrids because their chemical and physical properties may be distinct one from the other. According to results in the literature, the LC_{50} for AgNPs ranges from 0.050 to 17 mg L^{-1} (ORBEA et al., 2017; BOYLE; GOSS, 2018). Therefore, the immobilization of silver nanoparticles on a graphene oxide surface might decrease the adverse effects of AgNPs on zebrafish embryos as demonstrated by the higher LC_{50} value. Finally, in this work, the LC_{50} of $AgNO_3$ (69 µg L^{-1}) was 20 times less than the LC_{50} of GO-AgNPs (1.4 mg L^{-1}) under the same conditions (embryos with chorion and in the absence of NOM), demonstrating that a silver ionic is more toxic than a nanohybrid.

Overall, an important factor in our findings, which distinguishes the GO-AgNPs over isolated AgNPs, may be the reduction in the nanoparticles' dynamics, due to an attachment of the silver particle to the GO surface. This leads to a hybrid material with reduced dissolution behaviour and interaction with biological tissues, both having a critical impact on the toxicity of nanohybrids when compared with isolated AgNPs. However, one should pay attention to the fact that GOs present huge variability regarding their toxicological effects on zebrafish embryos, potentially leading to results very different from those found in our present assessment (D'AMORA et al., 2017; CHEN et al., 2017; BANGEPPAGARI et al., 2019). Therefore, it is not possible to generalize the toxicological profile of GO-AgNP hybrids for the moment. With this in mind, it is mandatory to provide a complete nanohybrid physicochemical characterization during ecotoxicity testing, which should be geared towards future comparative studies and the harmonization of methodologies for the safety-by-design of various types of nanomaterial.

3.6. Conclusions

Herein, GO-AgNPs nanohybrid was synthesized through Ag^{+} reducing to AgNPs, using $NaBH_4$ as reducing agent. In addition, the GO-AgNP hybrid was well characterized, considering the requirements for nanotoxicology studies. The natural organic matter (20 mg L^{-1}) enhanced the dispersion stability of GO in a zebrafish medium for up to 72 hours, though this effect was not observed for GO-AgNPs. The ecotoxicity of $AgNO_3$ and the nanohybrid on zebrafish embryos was observed in a dose-response manner, in the presence and absence of chorion. GO did not affect the

embryos with any toxicity, with or without chorion, even at a higher exposure concentration (100 mg L^{-1}); indicating that silver drives down toxicity in the nanohybrid. Furthermore, it was verified that the chorion embryo membrane critically influences toxicity. NOM mitigated the ecotoxicity effect of Ag^{+} and GO-AgNPs on the embryos, suggesting implications for risk assessment involving these materials. The positive biocompatibility of GO and the inhibition of silver dissolution, as observed in the filtrate-only control, both suggest that GO may be used as a platform for the reduction of silver toxicity. Furthermore, these results indicate the GO-AgNPs might also be used as a platform to increase the safe use of AgNPs.

In light of the above, this work is an important contribution toward proactive ecotoxicological evaluation involving the emerging nanohybrid materials. Finally, the approach used for chorion membrane removal guarantees the direct exposure of embryos, reducing the sources of variability and contributing to the standardization of fish embryo toxicity testing.

References

ABRAMENKO, N. B.; DEMIDOVA, T. B.; ABKHALIMOV, E. V.; ERSHOV, B. G.; KRYSANOV, E. Y.; KUSTOV, L. M. Ecotoxicity of different-shaped silver nanoparticles: Case of zebrafish embryos. J **Journal of Hazardous Materials**, v. 347, p. 89-94, 2018.

AHMAD, N.; AL-FATESH, A. S.; WAHAB, R.; ALAM, M.; FAKEEHA, A. H. Synthesis of silver nanoparticles decorated on reduced graphene oxide nanosheets and their electrochemical sensing towards hazardous 4-nitrophenol. **Journal of Materials Science: Materials in Electronics**, v. 31, n. 14, p. 11927–11937, 2020.

CASTRO, V. L.; CLEMENTE, Z.; JONSSON, C.; SILVA, M.; VALLIM, J. H.; DE MEDEIROS, A. M. Z.; MARTINEZ, D. S. T. Nanoecotoxicity Assessment of Graphene Oxide and Its Relationship with Humic Acid. **Environmental Toxicology and Chemistry**, v. 37, n. 7, p. 1998–2012, 2018.

CHAKRABORTY, C.; SHARMA, A. R.; SHARMA, G.; LEE, S. S. Zebrafish: A complete animal model to enumerate the nanoparticle toxicity. **Journal of Nanobiotechnology**, v. 14, art. 65, 2016.

CHEN, J.; SUN, L.; CHENG, Y.; LU, Z.; SHAO, K.; LI, T.; HU, C.; HAN, H. Graphene Oxide-Silver Nanocomposite: Novel Agricultural Antifungal Agent against Fusarium graminearum for Crop Disease Prevention. **ACS Applied Materials and Interfaces**, v. 8, n. 36, p. 24057–24070, 2016.

DIDEIKIN, A. T.; VUL, A. Y. Graphene Oxide and Derivatives : The Place in Graphene Family. **Frontiers in Physics**, v. 6, art. 149, 2018.

FARIA, A. F.; MARTINEZ, D. S. T.; MORAES, A. C. M.; COSTA, M. E. H. M. DA; BARROS, E. B.; SOUZA FILHO, A. G.; PAULA, A. J.; ALVES, O. L. Unveiling the role of oxidation debris on the surface chemistry of graphene through the anchoring of ag nanoparticles. **Chemistry of Materials**, v. 24, n. 21, p. 4080–4087, 2012.

FONSECA, L. C.; ARAÚJO, M. M. DE; MORAES, A. C. M. DE; SILVA, D. S. DA; FERREIRA, A.G.; FRANQUI, L. S.; MARTINEZ, D. S, T.; ALVES, O. L. Nanocomposites based on graphene oxide and mesoporous silica nanoparticles: Preparation, characterization and nanobiointeractions with red blood cells and human plasma proteins. **Applied Surface Science**, v. 437, p. 110–121, 2018.

GRILLO, R.; ROSA, A. H.; FRACETO, L. F. Engineered nanoparticles and organic matter : A review of the state-of-the-art. **Chemosphere**, v. 119, p. 608–619, 2015.

GUNSOLUS, I. L.; MOUSAVI, M. P. S.; HUSSEIN, K.; BÜHLMANN, P.; HAYNES, C. L. Effects of Humic and Fulvic Acids on Silver Nanoparticle Stability, Dissolution, and Toxicity. **Environmental Science and Technology**, v. 49, n. 13, p. 8078–8086, 2015.

HABIBA, K.; ENCARNACION-ROSADO, J.; GARCIA-PABON, K.; VILLALOBOS-SANTOS, J. C.; MAKAROV, V. I.; AVALOS, J. A.; WEINER, B. R.; MORELL, G. Improving cytotoxicity against cancer cells by chemo-photodynamic combined modalities using silver-graphene quantum dots nanocomposites. **International Journal of Nanomedicine**, v. 11, p. 107-119, 2015.

HAQUE, E.; WARD, A. C. Zebrafish as a Model to Evaluate Nanoparticle Toxicity. **Nanomaterials**, v. 8, n. 7 art. 561, 2018.

HASSANDOOST, R.; POURAN, S. R.; KHATAEE, A.; OROOJI, Y.; JOO, S. W. Hierarchically structured ternary heterojunctions based on Ce^{3+}/ Ce^{4+} modified Fe_3O_4 nanoparticles anchored onto graphene oxide sheets as magnetic visible-light-active photocatalysts for decontamination of oxytetracycline. **Journal of Hazardous Materials**, v. 376, p. 200-211, 2019.

HE, Y.; PENG, G.; JIANG, Y.; ZHAO, M.; WANG, X.; CHEN, M.; LIN, S. Environmental Hazard Potential of Nano-Photocatalysts Determined by Nano-Bio Interactions and Exposure Conditions. **Small**, v. 16, n. 21, art. 1907690, 2020. Special issue.

HOA, L. T.; LINH, N. T. Y.; CHUNG, J. S.; HUR, S. H. Green synthesis of silver nanoparticle-decorated porous reduced graphene oxide for antibacterial non-enzymatic glucose sensors. **Ionics**, v. 23, n. 6, p. 1525–1532, 2017.

HU, X.; OUYANG, S.; MU, L.; AN, J.; ZHOU, Q. Effects of Graphene Oxide and Oxidized Carbon Nanotubes on the Cellular Division, Microstructure, Uptake, Oxidative Stress, and Metabolic Profiles. **Environmental Science and Technology**, v. 49, n. 18, p. 10825–10833, 2015.

HUTCHISON, J. E. The road to sustainable nanotechnology: Challenges, progress and opportunities. **ACS Sustainable Chemistry and Engineering**, v. 4, n. 11, p. 5907–5914, 2016.

KAVINKUMAR, T.; MANIVANNAN, S. Uniform decoration of silver nanoparticle on exfoliated graphene oxide sheets and its ammonia gas detection. **Ceramics International** , v. 42, n. 1, p. 1769–1776, 2016.

KIM, M. J.; KO, D.; KO, K.; KIM, D.; LEE, J.-Y.; WOO, S. M.; KIM, W.; CHUNG, H. Effects of silver-graphene oxide nanocomposites on soil microbial communities. **Journal of Hazardous Materials**, v. 346, p. 93–102, 2018.

KOUSHIK, D.; SEN, S.; MALIYEKKAL, S. M.; PRADEEP, T. Rapid dehalogenation of pesticides and organics at the interface of reduced graphene oxide – silver nanocomposite. **Journal of Hazardous Materials**, v. 308, p. 192–198, 2016.

KUNDU, N.; MUKHERJEE, D.; MAITI, T. K.; SARKAR, N. Protein-Guided Formation of Silver Nanoclusters and Their Assembly with Graphene Oxide as an Improved Bioimaging Agent with Reduced Toxicity. **Journal of Physical Chemistry Letters**, v. 8, n. 10, p. 2291–2297, 2017.

LEE, K. Y.; JANG, G. H.; BYUN, C. H.; JEUN, M.; SEARSON, P. C.; LEE, K. H. Zebrafish models for functional and toxicological screening of nanoscale drug delivery systems : promoting preclinical applications. **Bioscience Reports**, v. 37, n. 3, art. BSR20170199, 2017.

LI, J.; KUANG, D.; FENG, Y.; ZHANG, F.; XU, Z. Green synthesis of silver nanoparticles – graphene oxide nanocomposite and its application in electrochemical sensing of tryptophan. **Biosensors and Bioelectronic**, v. 42, p. 198–206, 2013.

LOWRY, G. V.; GREGORY, K. B.; APTE, S. C.; LEAD, J. R. Transformations of Nanomaterials in the Environment. **Frontiers of Nanoscience**, v. 7, p. 55–87, 2014.

LUNA, L. A. V. DE; MORAES, M. D. A. C.; CONSONNI, S. R.; PEREIRA, C. D.; CADORE, S.; GIORGIO, S.; ALVES, O. L. Comparative in vitro toxicity of a graphene oxide - silver nanocomposite and the pristine counterparts toward macrophages. **Journal of Nanobiotechnology**, v. 14, art. 12, 2016.

MARKIEWICZ, M.; KUMIRSKA, J.; LYNCH, I.; MATZKE, M.; KÖSER, J.; BEMOWSKY, S.; DOCTER, D.; STAUBER, R.; WESTMEIER, D.; STOLTE, S. Changing environments and biomolecule coronas: Consequences and challenges for the design of environmentally acceptable engineered nanoparticles. **Green Chemistry**, v. 20, p. 4133-4168, 2018.

MCGILLICUDDY, E.; MURRAY, I.; KAVANAGH, S.; MORRISON, L.; FOGARTY, A.; CORMICAN, M.; DOCKERY, P.; PRENDERGAST, M.; ROWAN, N.; MORRIS, D. Silver nanoparticles in the environment: Sources, detection and ecotoxicology. **Science of the Total Environment**, v. 575, p. 231–246, 2017.

MORAES, A. C. M. DE. Graphene oxide-silver nanocomposite as a promising biocidal agent against methicillin- resistant Staphylococcus aureus. **International Journal of Nanomedicine**, v. 10, p. 6847–6861, 2015.

MOTTIER, A.; MOUCHET, F.; PINELLI, É.; GAUTHIER, L.; FLAHAUT, E. Environmental impact of engineered carbon nanoparticles: from releases to effects on the aquatic biota. **Current Opinion in Biotechnology**, v. 46, p. 1–6, 2017.

ORGANIZATION FOR ECONOMIC CO-OPERATION AND DEVELOPMENT - OECD. **Guidance document on aquatic and sediment toxicological testing of nanomaterials**. Paris, 2020. 68 p. (Series on Testing and Assessment, n. 317).

PARK, M. V. D. Z.; BLEEKER, E. A. J.; BRAND, W.; CASSEE, F. R.; VAN ELK M.; GOSENS, I.; DE JONG, W. H.; MEESTERS, J. A. J.; PEIJNENBURG, W. J. G. M.; QUIK, J. T. K.; VANDEBRIEL, R. J.; SIPS, A. J. A. M. Considerations for Safe Innovation: The Case of Graphene. **ACS Nano**, v. 11, n. 10, p. 9574–9593, 2017.

PLAZAS-TUTTLE, J.; ROWLES, L.; CHEN, H.; BISESI JUNIOR, J. H.; SABO-ATTWOOD, T.; SALEH, N. B. Dynamism of Stimuli-Responsive Nanohybrids: Environmental Implications. **Nanomaterials**, v. 5, n. 2, p. 1102–1123, 2015.

REN, W.; CHENG, H. M. The global growth of graphene. **Nature Nanotechnology**, v. 9, n. 10, p. 726–730, 2014.

SALEH, N. B.; AFROOZ, A. R. M. N.; BISESI JUNIOR, J. H.; AICH, N.; PLAZAS-TUTTLE, J.; SABO-ATTWOOD, T. Emergent Properties and Toxicological Considerations for Nanohybrid Materials in Aquatic Systems. **Nanomaterials**, v. 4, n. 2, p. 372–407, 2014.

SALEH, N. B.; AICH, N.; PLAZAS-TUTTLE, J.; LEAD, J. R.; LOWRY, G. V. Research strategy to determine when novel nanohybrids pose unique environmental risks. **Environmental Science: Nano**, v. 2, n. 1, p. 11–18, 2015.

SHARMA, S.; PRAKASH, V.; MEHTA, S. K. Graphene/silver nanocomposites-potential electron mediators for proliferation in electrochemical sensing and SERS activity. **TrAC - Trends in Analytical Chemistry**, v. 86, p. 155–171, 2017.

SIEBER, S.; GROSSEN, P.; BUSSMANN, J.; CAMPBELL, F.; KROS, A.; WITZIGMANN, D.; HUWYLER, J. Zebrafish as a preclinical in vivo screening model for nanomedicines. **Advanced Drug Delivery Reviews**, v. 151–152, p. 152–168, 2019.

SOROUSH, A.; MA, W.; SILVINO, Y.; RAHAMAN, M. S. Surface modification of thin film composite forward osmosis membrane by silver-decorated graphene-oxide nanosheets. **Environmental Science: Nano**, v. 2, n. 4, p. 395–405, 2015.

SU, Y.; YANG, G.; LU, K.; PETERSEN, E. J.; MAO, L. Colloidal properties and stability of aqueous suspensions of few-layer graphene: Importance of graphene concentration. **Environmental Pollution**, v. 220, p. 469–477, 2017.

XU, J.; WANG, Y.; HU, S. Nanocomposites of graphene and graphene oxides: Synthesis, molecular functionalization and application in electrochemical sensors and biosensors. A review. **Microchimica Acta**, v. 184, n. 1, p. 1-44, 2017.

YIN, P. T.; SHAH, S.; CHHOWALLA, M.; LEE, K. Design, Synthesis, and Characterization of Graphene − Nanoparticle Hybrid Materials for Bioapplications. **Chemical Reviews**, v. 115, p. 2483–2531, 2015.

ZHANG, J.; GUO, W.; LI, Q.; WANG, Z.; LIU, S. The effects and the potential mechanism of environmental transformation of metal nanoparticles on their toxicity in organisms. **Environmental Science: Nano**, v. 5, n. 11, p. 2482–2499, 2018.

ZHAO, J.; LIN, M.; WANG, Z.; CAO, X.; XING, B. Engineered nanomaterials in the environment: Are they safe? **Critical Reviews in Environmental Science and Technology**, v. 51, n. 14, p. 1443–1478, 2020.

ZHOU, Y.; CHEN, R.; HE, T.; XU, K.; DU, D.; ZHAO, N.; CHENG, X.; YANG, J.; SHI, H.; LIN, Y. Biomedical Potential of Ultrafine Ag / AgCl Nanoparticles Coated on Graphene with Special Reference to Antimicrobial Performances and Burn Wound Healing. **Acs Applied Materials & Interfaces**, v. 8, n. 24, p. 15067–15075, 2016.

4. TOXICITY ASSESSMENT OF GRAPHENE OXIDE-SILVER NANOPARTICLES HYBRID MATERIAL ON ZEBRAFISH LIVER CELLS

Highlights

- GO-AgNPs hard protein corona shows a similar profile of GO.
- The LC_{50}-24h of GO-AgNPs ranged from 5.7 to 7.0 ug ml^{-1} across all endpoints
- GO shows high biocompatibility and is a promising platform for assembling hybrids
- GO-AgNPs is more toxic than AgNPs pristine but much less toxic than $AgNO_3$.
- GO-AgNPs can be internalised in ZFL cells as confirmed by Raman spectroscopy.

Graphical Abstract

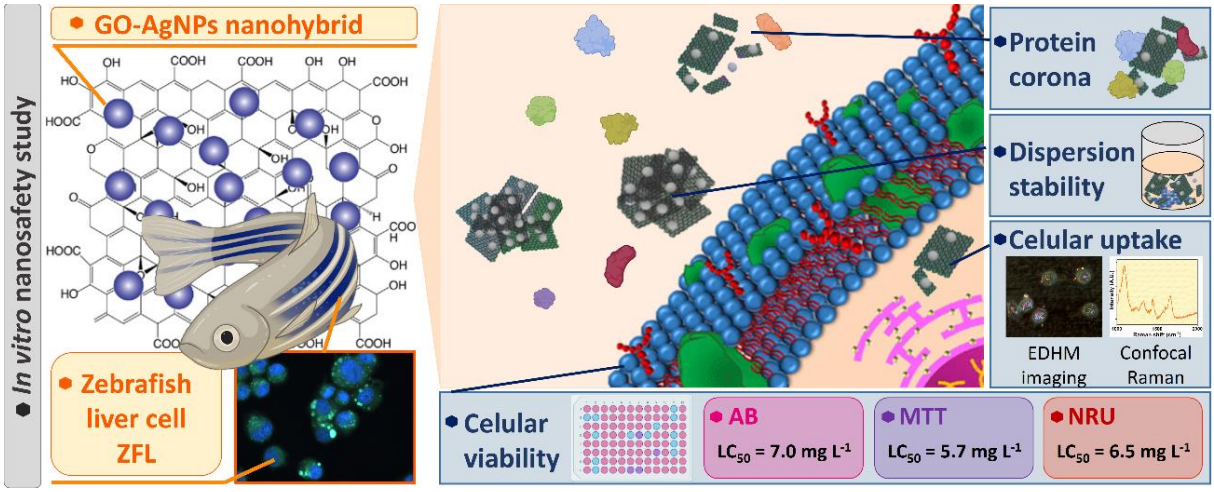

Abstract

Graphene oxide-silver nanoparticles hybrid material (GO-AgNPs) has been explored for innovation and applications in sensors, drug delivery, catalysis, and new antimicrobial platforms. Therefore, it is crucial to evaluate proactively its environmental, health and safety aspects. In this work, we assessed the toxicity of GO-AgNPs and its pristine counterparts (GO and AgNPs) on Zebrafish liver cell line (ZFL) associated with the protein corona characterisation and cellular internalisation studies. Atomic force microscopy and SDS-PAGE analysis confirmed the fetal bovine serum (FBS)-protein corona formation on these materials after incubation with ZFL culture medium. AFM analysis demonstrated an increase in GO surface roughness after decoration with silver nanoparticles and protein corona formation. However, it was not possible to identify relevant differences (protein bands) in the protein corona profile by SDS-PAGE analysis between GO-AgNPs and GO pristine. Furthermore, FBS-corona enhanced the colloidal stability of both materials in the cell culture medium. The cytotoxicity was assessed using AB, MTT and NR classical *in vitro* assays. Considering AB assay, the IC_{50}-24h values observed to GO-AgNPs, AgNPs, and $AgNO_3$ were 7.0, 25.8 and 1.3 μg mL^{-1}, respectively. Similar cytotoxicity tendency was also observed in MTT and NR assays, indicating dose-response toxic effects to these materials. These results suggest that ZFL cells are more susceptible to GO-AgNPs than AgNPs pristine. However, $AgNO_3$ was much more toxic to ZFL cells and GO pristine did not show any toxicity against these cells up to 100 μg mL^{-1}, indicating that silver is driving the toxicity effects observed. Additionally, enhanced dark-field hyperspectral microscopy and Raman spectroscopy were used as complementary techniques to demonstrate the interaction of GO-AgNPs with the cellular membrane and its internalisation capacity on this cell line. Finally, this work is a novel contribution towards *in vitro* approaches to the safety evaluation of emerging graphene-nanoparticles hybrid materials for responsible nanotechnology innovations.

Keywords: nanomaterials, nanoecotoxicity, protein corona, nanosafety.

4.1. Introduction

Nanohybrids are promising multifunctional materials due to their novel or synergistic physico-chemical proprieties (AICH et al., 2014; PLAZAS-TUTTLE et al., 2015; SALEH et al., 2015). In particular, the metallic-carbon nanohybrids based on graphene can be obtained by incorporation of metallic nanoparticles, such as silver nanoparticles (AgNPs), onto graphene oxide (GO) sheets (HUANG et al., 2011; FARIA et al., 2012; BAI et al., 2013; YIN et al., 2015; DE MEDEIROS et al., 2021). Graphene oxide- silver nanoparticles hybrid material (GO-AgNPs) is a very special kind of nanohybrid considering its huge number of applications in health, energy, catalysis, composites and the environment (ZHAO et al., 2018; WANG et al., 2019; AMIR et al., 2020; FU et al., 2020; LIANG et al., 2020). For example, it has been applied for water treatment and desalinisation (VICENTE-MARTÍNEZ et al., 2020), catalysis (NAEEM et al., 2019), membrane composites (FONSECA et al., 2017), bioremediation (SOROUSH et al., 2015; KOUSHIK et al., 2016), sensor/biosensor (SHARMA et al., 2017), drug delivery (HABIBA et al., 2016; ULLAH et al., 2018) and bioimaging (KUNDU et al., 2017). Due to its high antibacterial activity, GO-AgNPs can be an alternative and promising material for new antibiotics development (MARTA et al., 2015; JAWORSKI et al., 2018; CHEN et al., 2020). Other biomedical applications rise due to its antimicrobial properties (DE MORAES, 2015; COBOS et al., 2020), including direct use in wound epidermis (ZHOU et al., 2016; RAN et al., 2017) or incorporated at implants in mice (XIE et al., 2017; BAKHSHESHI-RAD et al., 2020). Taken together, GO-AgNPs nanohybrid present advantages to a wide variety of technological applications due to its unique optical, thermal, electrical, catalytical and biological properties (YIN et al., 2015; SHARMA et al., 2017; MOHAMMED et al., 2020).

Given the altered physico-chemical characteristics and emergent proprieties, nanohybrids can display distinct toxicological and biological behaviour compared with their parent components (DA SILVA et al., 2018; DE LUNA et al., 2019; WIERZBICKI et al., 2019; ALIAN et al., 2021). Such changes (e.g. size, shape, crystalline structure, surface chemistry, dissolution rate, sorption characteristics, etc.) have shown to be responsible for specific cell-nanomaterials interactions. Environmental health and safety aspects are a recent concern associated with nanohybrids. Therefore, it is critical to advance on toxicological assessment and risk evaluation to nanohybrid materials linked with their technological applications and development working towards

safe-by-design graphene-silver based materials (PLAZAS-TUTTLE et al., 2015; PARK et al., 2017; MENG et al., 2018).

Zebrafish (*Danio rerio*) is an excellent model organism to assess the toxicity of chemicals and nanomaterials (CLEMENTE et al., 2017; PEREIRA et al., 2019; FRAGAL et al., 2020; CANEDO; ROCHA, 2021). The cell lines derived from zebrafish shows excellent potential for *in vitro* approaches to toxicity testing of nanomaterials (EIDE et al., 2014). Moreover, the cell lines support the 3 Rs principle (reduction, refinement, and replacement) of animal use and could be an alternative method for *in vivo* testing in nanotoxicology research (JOHNSTON et al., 2018). Zebrafish liver cells (ZFL) is an established cell line that shows general hepatocyte morphology (EIDE et al., 2014). As the liver is a critical organ target to many environmental contaminants (GUO et al., 2020), the ZFL cell line has been used as an *in vitro* model for toxicological screening as well as to understanding the toxicity mechanisms of nanomaterials in the zebrafish model (CHRISTEN et al., 2013; THIT et al., 2017; MOROZESK et al., 2018; MOROZESK et al., 2020; AL-AMMARI et al., 2021).

Fetal bovine serum (FBS) is commonly added to culture media as a source of essential biomolecules for cell proliferation and maintenance under *in vitro* conditions. FBS proteins, therefore, interact with the surface of graphene oxide (FRANQUI et al., 2019) and silver nanoparticles (DURÁN et al., 2015; ARGENTIERE et al., 2016), forming the protein corona, which affects their nano-biointeractions and cellular toxicological outcomes. The composition of the protein corona can be mainly influenced by the nanomaterial intrinsic physicochemical properties (e.g. size, topography, surface functional groups and electric charge) and the biological medium components (e.g. composition, pH and ionic strength). Therefore, it is very important to characterise the protein coronas associated with nanomaterials during toxicity assessment (PAULA et al., 2014; DE SOUSA et al., 2018; CHETWYND et al., 2019; PARK, 2020).

Despite the increasing interest of the nanotoxicology community in the Zebrafish model, there are no studies reported in the literature assessing the toxicity of nanohybrids on ZFL cells. Recently, our group developed an integrated approach to evaluate the toxicity of GO-AgNPs on Zebrafish embryos (DE MEDEIROS et al., 2021). Therefore, we continue this previous work focusing on ZFL cells to understand the cellular toxicity, mechanisms and nanobiointeractions associated with this promising nanohybrid. This initiative will be very important to advance on *in vitro*-*in vivo* toxicity

correlations in the Zebrafish model (STADNICKA-MICHALAK et al., 2014; REHBERGER et al., 2018; LUNGU-MITEA et al., 2021).

In this work, we assessed the toxicity of GO-AgNPs nanohybrid on ZFL cells for the first time. The following aspects were studied: i) protein corona formation and characterisation in ZFL culture medium containing 10% of FBS; ii) toxicity evaluation of nanohybrid and its counterparts using classical cell viability assays (AB, MTT and NR); and iii) cellular interaction and internalisation of nanohybrid in ZFL cells exploring two complementary optical-spectroscopy techniques (EDHM and Raman).

4.2. Material and methods

4.2.1. Preparation and characterisation of nanomaterials

GO was synthesised by modified Hummers' method. In this procedure, the GO was obtained through oxidative exfoliation of graphite using H_2SO_4/$KMnO_4$. The GO-AgNPs nanohybrid was synthesised through the chemical reduction of silver ions in GO aqueous dispersion using $NaBH_4$ as a reduction agent. The following characterization methods was realized: (i) Uv-Vis spectroscopy; (ii) X-ray Diffraction (XRD); (iii) Atomic Force Microscopy (AFM); (iv) Transmission Electron Microscopy (TEM); (v) Raman spectroscopy; (vi) X-ray photoelectron spectroscopic (XPS); (vii) Thermogravimetric analysis (TGA). The detailed synthesis methods and characterisation analyses were described in our previous study (DE MEDEIROS et al., 2021).

Silver nanoparticles were prepared according to Martin et al. (2010). In this procedure, 0.100 mL of an aqueous solution of the metal precursor of 50 nM of $AgNO_3$ with 50 nM of HCl (to guarantee the metal stability) is added at 9.900 mL of ultrapure water at a test tube. The chemical reducing agent was quickly added (0.300 mL of 50 nM of NaH_4 with the same molar amount of NaOH) while stirring at a mechanical shaker to ensure a uniform mixture. The final colour of the reaction was yellow. The AgNPs were characterised by UV-Vis spectroscopy, DLS and TEM analysis.

The $AgNO_3$ (silver nitrate salt; Sigma-Aldrich) was prepared by dissolving the appropriated amount of silver nitrate in ultrapure water to obtain a final concentration of 1.0 μg mL^{-1}.

The GO stock-dispersion (1 mg mL^{-1}) was prepared by sonication in an ultrasonic bath (CPXH; Cole-Parmer) at 40 Hz for 80 min. The GO-AgNPs and AgNPs final synthesis dispersion were utilised at biological assay after estimation of its final concentration. Prior assay, all dispersions were sonicated in an ultrasonic bath for 10 min. All nanomaterials stock-dispersions were stored in a sealed vessel protected from light at 4°C until utilisation.

4.2.2. Protein corona characterisation

The nanomaterials from stock-dispersion were diluted at 100 µg mL^{-1} concentration in zebrafish liver cells medium (50% L15 / 40% RPMI) supplemented with 10% of fetal bovine serum (Cultilab Ltda, Brazil), sterile, heat-inactivated and free from mycoplasma. The cell medium was kept refrigerated until utilisation. This dispersion was incubated for 1 h at 28 °C in thermoblock system (Thermomixer C, Eppendorf). To obtain the FBS-hard corona complexes, the samples were washed by three cycles of centrifugation (14,000 rpm; 1 h at 4 °C) and resuspended at cold phosphate-buffered saline pH 7.4 (PBS; ThermoFisher) to separate from unbound or weakly bound proteins (soft corona). Afterwards, the hard corona proteins were eluted from pellets by incubating with 3× loading buffer (New England BioLabs, USA) and 1:10 volume of 1.25 M DTT for 3 min at 99 °C. Subsequently, 10 µL of eluted hard corona proteins and the positive control (FBS diluted at 1:100 in ultrapure water) and the protein standard were loaded on SDS-PAGE (4% stacking gel and 15% resolving gel). The separated proteins on the resulting gel were stained with Coomassie Brilliant Blue G-250 solution. All experiments were performed in triplicate.

The surface roughness and thickness features of bare and FBS hard corona-coated nanomaterials were evaluated through topography images using atomic force microscopy (AFM; Bruker). The samples were analysed employing a Multimode 8 microscope with a Nano Scope 5 controller, with Peakforce tapping (Bruker, USA). AFM topographic images were processed on Gwyddion software (gwyddion.net).

4.2.3. Colloidal stability monitoring

The colloidal stability of nanomaterials at 50 µg mL^{-1} in ZFL medium, with and without the addition of 10% FBS, was monitored by spectrophotometric analysis (Multiskan GO; Thermo Scientific, USA). The samples were kept static for 24 h, and

the supernatant aliquot (100 µL) was removed from the surface of dispersion, and the absorbance at 400 nm was measured. All the samples were performed by independent triplicate. The hydrodynamic diameter (HD) and surface charge (zeta potential) of AgNPs were measured by dynamic light scattering (DLS) and electrophoretic light scattering (ELS) using the Zetasizer Ultra instrument (Malvern, UK).

4.2.4. Toxicity assessment

4.2.5. Zebrafish Liver cell culture conditions

The liver cell line from Zebrafish (ZFL) was obtained from Rio de Janeiro Cell Bank, Brazil. The cell culture media consists of 50% Leibovitz's (L15) and 40% Roswell Park Memorial Institute (RPMI), supplemented with 15 mM Hepes (Sigma–Aldrich), 1.0% penicillin-streptomycin–amphotericin (10,000 U/mL potassium penicillin, 10,000 µg/mL streptomycin) and 10% fetal bovine serum (FBS). ZFL cell was cultivated from passage number 7.0 to 40 in 75 cm^2 flasks in an incubator at 28 °C. The media were replaced with after every 2-3 days.

4.2.6. Viability assays

The cells were transferred to 96-wells plates one day before exposure at 2.5 x 10^5 cell/well concentrations. After stabilisation, the cells were exposed for 24 h to the following treatments: (I) negative control: culture medium without any nanomaterial; (II) positive control: culture medium with 10% of Dimethyl Sulfoxide - DMSO; (III) exposition to serial dilution of following treatments: GO-AgNPs; GO, AgNPs, $AgNO_3$ and filtrate-only control.

The purpose of dissolved ion control ($AgNO_3$) is to assess the impact of Ag^+ in the toxicity of the AgNPs to cells, while the filtrate-only control was performed to evaluate either impairment caused by dissolved ions throughout the assay. It was prepared after incubation of GO-AgNPs (100 µg mL^{-1}) in the culture media at the same conditions of exposition (24 h, 28 °C). Then, the dispersion was centrifuged (1 h @ 14,000 rpm), and the supernatant toxicity was evaluated.

Percentual viable cells were calculated as (%) viable cells = (well absorbance – positive control absorbance average)/(negative control absorbance average – positive control absorbance average) × 100. All the experiments were carried out in triplicates.

Afterwards, the half-maximal inhibitory concentration (IC_{50}) and 95% confidence intervals of each treatment were calculated using GraphPad software.

Alamar blue (AB) assay

This assay is based on the reduction of resazurin dye, blue and non-fluorescent, in resorufin, red and highly fluorescent. Following a 24-hour exposition to nanomaterials, cells were washed with PBS, and resazurin dye (20 µg mL^{-1} prepared in fresh medium without FBS or supplements) was added and incubated for 3 h. The optical density of the resorufin product was read at 540 nm with a UV-spectrophotometer (Multiskan GO; Thermo Scientific, USA)

Neutral red uptake (NRU) assay

The neutral red uptake assay for the estimation of cell viability was based on the ability of intact lysosomes in a living cell to retain the red dye. To this end, after the treatment, the cells were washed with PBS and incubated with neutral red solution (40 mg mL^{-1} prepared in fresh medium without FBS or supplements) for 3 h. To release the neutral red incorporated into viable cells, 150 µL of distain solution (50% absolute ethanol, 49% ultrapure water and 1.0% glacial acetic acid).was added into each well. After agitation, the absorbance was read at 540 nm in a microplate spectrophotometer (Multiskan GO; Thermo Scientific, USA).

Tetrazolium salt (MTT) Assay

The MTT Assay (3-(4,5- dimethylthiazol-2-yl)-2,5-diphenyltetrazolium bromide) was performed to assess cell metabolic activity. At the end of the exposition period, the old medium was removed, and the cells were washed with PBS. Then, it was replaced with MTT salt (50 mg mL^{-1}) prepared in a fresh medium (without FBS or supplements). After 3 h incubation, the cells were then lyzed with DMSO (150 µL / well) to dissolve the purple formazan crystals. The solution was mixed, and the absorbance was measure in a microplate spectrophotometer (Multiskan GO; Thermo Scientific, USA) at 570 nm.

4.2.7. Enhanced darkfield hyperspectral microscopy

ZFL cells were plated into a 24-wells plate containing gelatin-coated coverslips (12 mm diameter) at 5×10^4 cell/well. After stabilisation, the cells were exposed to the following treatment for 24 h at 28 °C in medium L-15/RPMI supplemented with 10% FBS: (I) control; (II) 3.0 µg mL^{-1} of GO-AgNPs; (III) 3.0 µg mL^{-1} of GO; (IV) 13 µg mL^{-1} of AgNPs. After the exposition period, the cells were washed with ultrapure water. Then, the coverslip was placed in a glass slide for examination using enhanced dark-field hyperspectral microscopy (EDHM) technique. The analyses were performed at Olympus microscope (BX-53) using 100× objective (Olympus UPlanFLN 40×, 0.6 NA) coupled with a VNIR hyperspectral camera (CytoViva®) and a high-resolution darkfield condenser (numerical aperture; 1.2–1.4 NA). The hyperspectra obtained from cell samples exposed to nanomaterials were filtered against control samples. The mapping of nanomaterials was realised by colouring the pixels whose spectra deviated from the control spectra library.

4.2.8. Confocal Raman spectroscopy

ZFL cells were plated into a 24-wells plate containing gelatin-coated coverslips (12 mm diameter) at 2.5×10^5 cell/well. After stabilisation, the cells were exposed to the following treatment for 24 h at 28 °C in medium L-15/RPMI supplemented with 10% FBS: (I) control; (II) 3.0 µg mL^{-1} of GO-AgNPs; (III) 3.0 µg mL^{-1} of GO; (IV) 13 µg mL^{-1} of AgNPs. After the exposition period, the cells were gently washed with PBS and fixed overnight with 4.0% paraformaldehyde in PBS. Next, the samples were washed with PBS, dehydrated in graded alcohol solution (30%, 50%, 70%, 80%, 90%, and 100%) and dried at room temperature. Then, the samples were analysed using XploRA™ PLUS Confocal Raman Microscope (Horiba Jobin Yvon, Japan). The cells were analysed with the laser operating at λ = 532 nm at random points under a magnification of 100X the objective. At the same point, 9 spectra were obtained at z axes with 1 nm of the distance between each.

4.3. Results and discussion

The physico-chemical proprieties of nanomaterials (e.g. purity, size, shape, crystallinity, etc.) and their behaviour at biological media (e.g. colloidal stability, surface charge, dissolution, adsorption of biomolecules, etc.) could critically influence the biological response (NEL et al., 2009; AZHDARZADEH; MASHAGHI, 2015). Thus, the complete characterization of nanomaterials and their state in the biological media is essential for toxicological assessment (MÜLHOPT et al., 2018). It provides key information about nanomaterials properties that allows the correlation of its characteristics and biological responses as well as be used as a reference point for comparing hazardous studies (SAYES; WARHEIT, 2009).

GO and GO-AgNPs samples used in this work were well-characterised in our previous work (DE MEDEIROS et al., 2021). GO was produced by the commonly used Hummer's method, which consists of chemical exfoliation and oxidation of graphite with a water-free mixture of concentrated sulfuric acid, sodium nitrate and potassium permanganate. Briefly, the UV-Vis absorption spectrum exhibits a peak at 230 nm, corresponding to π-π electronic transitions of C-C aromatic bonds. The XRD analysis shows diffraction peaks at 2θ values of 10.9 and 42.3, characteristic of the hexagonal structure of graphene oxide. AFM topography image confirmed the single layer aspect (< 1.5 nm thickness) and size distribution from 50 to 650 nm, and the mean size is 180 nm. The surface chemical composition of the GO surface was investigated by X-ray photoelectron spectroscopy (XPS). The deconvoluted C1s spectrum shows the presence of oxygen functional groups as epoxy/hydroxyl (C−O) (45.52%), carboxyl/esters (C=O) (9.11%) and π-π* transitions (8.07%), besides the graphitic/aromatic carbon (Csp2) (5.34%) and aliphatic carbon (Csp3) (31.97%).

The GO-AgNPs nanohybrid was synthesised by *in situ* chemical reduction of $AgNO_3$ on the surface of GO sheet, using the $NaBH_4$ as a reduction agent. The characteristic surface plasmon band at 415 nm on UV-Vis spectrum confirmed the growth of AgNPs on GO sheets surface. The XRD pattern suggests GO sheets reduction and the presence of diffraction planes of the Ag cubic phase (ICDD/PDF 01–1167). The ratio of the intensities of the D and G bands (ID/IG) increased from 1.15 (GO) to 1.35 (GO-AgNPs). The XPS survey spectrum revealed that the surface chemistry of GO-AgNPs is composed of 67.45% carbon, 29.67% oxygen,

and 2.88% silver with the presence of the following groups: epoxy/hydroxyl (C−O) (35.97%), carboxyl/esters (C=O) (11.88%) and π-π* transitions (8.73%), graphitic/aromatic carbon (Csp2) (9.78%) and aliphatic carbon (Csp3) (33.65%). TEM images of nanohybrids showed spherical shaped AgNPs on GO sheets with a mean size of 5.8 nm. These results confirm that both single layer and GO-AgNPs was successfully synthesised. Moreover, the GO also was partly reduced during the GO-AgNps synthesis. Similarly, Mahmoudi et al. (2015) used the same synthesis method and produced a similar nanohybrid. In this case, they observed spherical geometry silver nanoparticles uniform distributed onto GO sheets with diameters between 2– 5 nm. However, the synthesis conditions, as a reducing agent (ÇIPLAK et al., 2015), the ratio of GO and silver salt (KORDI et al., 2019) or surface microchemical (quantity of oxygen functional groups or debris) of bare GO (FARIA et al., 2012), critically influence on nanohybrids characteristics. Thus, it reinforces the importance of characterisation of the nanomaterial to understand the heterogeneity between samples and how it impacts the biological response.

AgNPs synthesised had a mean size of 6.2 ± 3.1 nm, as observed by TEM images. The plasmon resonance peak is ~400 nm, which is expected for this NPs size (Figure S1 – Appendix B). The hydrodynamic diameter (HD) and zeta (ζ) potential of Ag NPs were analysed by dynamic light scattering (DLS) and electrophoretic light scattering (ELS), respectively. In ultrapure water, the AgNPs displays an HD of 30.64 ± 0.25 nm, polydispersity index (PDI) of 0.58 ± 0.1 and ζ potential of -36.40 ± 0.84 mV. These results indicate the presence of micro-sized aggregates in polydispersity size distribution. Moreover, the small changes of these values after 24 hours (HD = 32.59 ± 0.25 nm and PDI = 0.58 ± 0.01) of dispersion preparation and the negative surface charge (ζ < - 30 mV) indicates good stability under these conditions.

This AgNPs synthesis has been chosen due to its similar size and the absence of any capping. Various methods and reagents could be applied to acquire AgNPs with different characteristics. Moreover, the final proprieties (such as size, shape, coating, surface charges) influence the toxicological profile of AgNPs (SHENG; LIU, 2017). The immobilisation of AgNPs onto GO sheets modify its proprieties, as dissolution rate, stability or even contact with biological membranes. Thus, bare AgNPs synthesized do not show all the proprieties (behaviour at biological media, size distribution, dissolution) that metallic counterpart of NHs.

Understanding the protein corona formation on nanohybrids is essential because it is well-known that this biomolecular coating on the surface of nanomaterials has critical influences on the toxicity and internalisation of nanomaterials (DURÁN et al., 2015*;* LIU et al., 2020; XU et al., 2020). A comparative characterisation between nanomaterials before and after interaction with ZFL medium supplemented with fetal bovine serum was performed. First, AFM technique was used to measure the surface roughness and thickness of graphene-based materials. Bare GO-AgNPs nanohybrid exhibit higher surface roughness (197.5 nm) and thickness (~ 4.0 nm) when compared to bare GO (56.9 nm and ~1.0 nm) due to the presence of silver nanoparticles. After 60 min of interaction with cell media, the thickness and roughness substantially increase, indicating FBS proteins adsorbed in the surface of GO and GO-AgNPs (Figure 1). Similar results have been reported for the interaction of FBS proteins and GO (DUAN et al., 2015; LUO et al., 2015; FRANQUI et al., 2019). SDS-PAGE analysis that composes the hard coronas adsorbed onto nanomaterials shows similar patterns between GO and GO-AgNPs (Figure 2). GO possess exceptionally adsorption capability due to the two-dimensional nanostructure that provides a high aspect ratio (lateral size to the atomic thickness ratio). The main interaction forces in forming the protein corona include *van der Waals forces* and hydrogen bonding (XU et al., 2018). Thus, the oxygen functional groups and surface defects of GO could serve as binding sites to proteins. During nanohybrid material synthesis, the reduction agent ($NaBH_4$) partially reduced the graphene oxide. The reduction of binding sites could explain the lower adsorption capacity of nanohybrid, which results in lighter protein bands intensity in the gel electrophoresis (stanning with coomassie blue dye).The FBS proteins can also bind to AgNPs according to SDS-PAGE analysis (Figure 2). In this case, the proteins and AgNPs complexes could be formed by van der Waals and electrostatic forces (DURÁN et al., 2015). It was possible to observe lower protein adsorption capability due to the light band on the electrophoresis gel. Moreover, the adsorption affinity is different from GO and only one band near 55 kDa could be observed. However, we speculate that this huge difference in adsorption capability between GO and AgNPs can be attributed to many factors during the protein corona formation, such as particle concentration, chemical composition and available surface area (LI; LEE, 2020; KOPAC, 2021).

Figure 1: Characterisation of GO and GO-AgNPs nanohybrid and after interaction with ZFL culture medium (FBS-protein corona formation). Atomic force microscopy (AFM) topography images (A, B) and the profile (E,F) of bare GO and GO coated with FBS proteins; Atomic force microscopy (AFM) topography images (C, D) and the profile (G,H) of bare GO-AgNPs and GO-AgNPs coated with FBS proteins

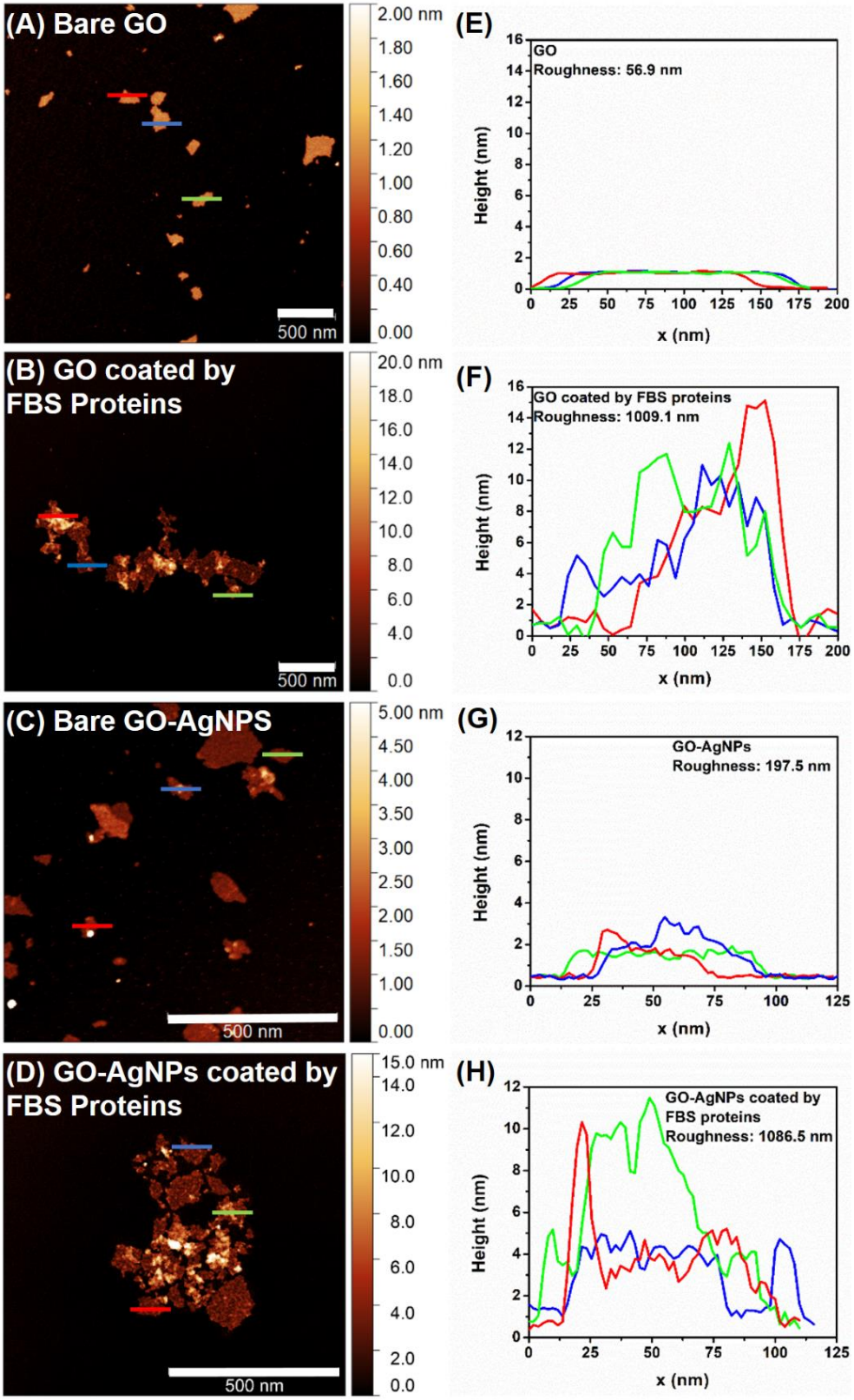

Figure 2: SDS-PAGE gel of fetal bovine serum (FBS) hard corona proteins extracted from GO, GO-AgNPs and AgNPs. FBS (control) represents 1 µg of total protein loaded in the gel (by Bradford assay). The separated proteins on the resulting gel were stained with Coomassie Brilliant Blue G-250 solution. All experiments were performed in triplicate

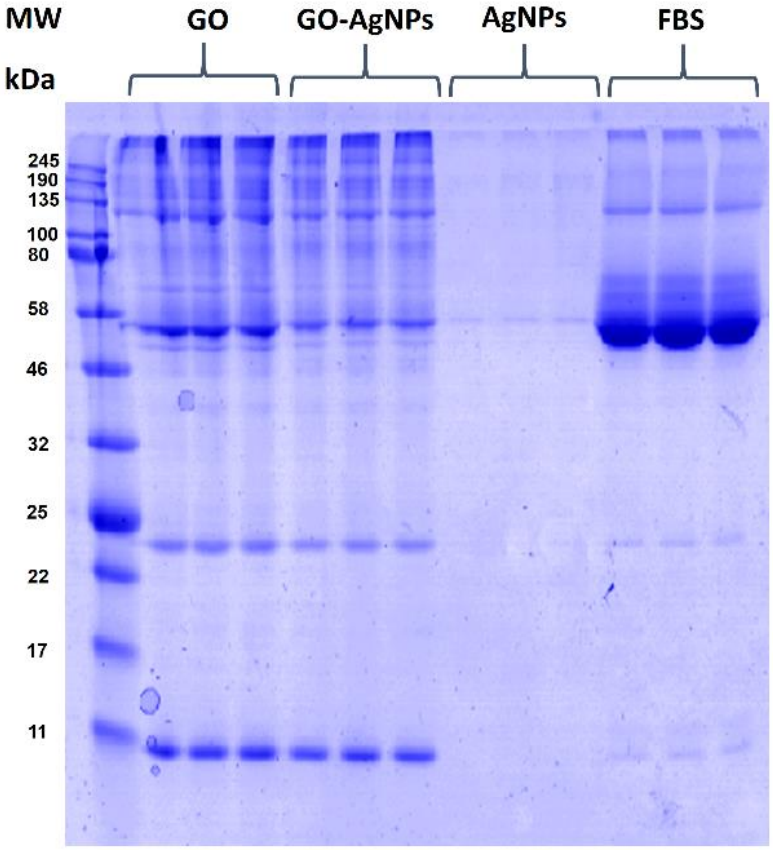

The protein corona formation also modifies the surface charge (ζ potential) of nanomaterial. The bare GO and GO-AgNPs show similar ζ potential (-42.01 ± 5.06 and -42.74 ± 5.75 mV). The negative charges observed could be attributed to oxygenated functional groups (negatively charged) on the NMs surface. After interaction with FBS, the ζ potential values refer to the charge of proteins adsorbed. Thus, the ζ potential of GO and GO-AgNPs with protein adsorbed (hard corona) was -32.73 ± 3.56 and -35.88 ± 2.59 mV. The surface charge modifications confirm the role of oxygenated functional groups protein corona formation. Similarly, the AgNPs also presents significant changes in ζ potential (-36.40 ± 0.84 and -26.97 ± 6.27 mV to bare and hard corona, respectively), showing the potential of protein adsorption at its surface.

Besides protein corona formation, upon contact with cell medium, the nanoparticle behaviour (i.e. NPs diffusion and aggregation/sedimentation) will be influenced by its chemical components and properties (e.g. protein supplemented, pH, electrolytes ionic strength) (PULIDO-REYES et al., 2017). Intrinsic properties of nanomaterials also affect the dispersion stability (i.e. composition, size, shape, surface chemistry, charge) (MOORE et al., 2015; FRANQUI et al., 2019; SUN et al., 2020).

Typically, *in vitro* toxicity assays use adherent cells in multiwell culture plates that contain nanomaterials dispersed in cell culture media, and the biological response is measured following incubation. Thus, the colloidal stability of NPs will influence *in vitro* behaviour (dosimetry, NP uptake, cytotoxicity). If nanomaterials are unstable in the cell culture media, that is, forming aggregates or particle clusters, these nanomaterials will be more susceptible to sedimentation and quickly concentrate around cells, increasing the dose delivered to the cells (DELOID et al., 2017).

Therefore, the colloidal stability of nanomaterials has an important influence on nanotoxicity. For example, Holt et al. (2021) showed lower cell viability of adipose-derived human mesenchymal stem cells (hMSCs) exposure to GO using the conventional upright *in vitro* cell culture configuration than obtained when an inverted setup was used. These authors suggested that even a tiny sedimentation rate could produce a “blanket effect” that directly decreases cellular viability. Similarly, Ha et al. (2018) reported the cytotoxicity of AgNPs under upright and inverted exposure. They observed a critical influence of agglomeration behaviour in determining the dose and cellular response.

By monitoring the colloidal dispersion stability of GO-AgNPs nanohybrid and the GO precursor in L15/RPMI medium with FBS supplementation, both nanomaterials feature desirable stability demonstrated by a small decrease of initial absorbance (~20%) over time. However, in absence of FBS, the absorbance at upper layer decreased to less than 20% of the initial over 6 hours. Nevertheless, the AgNPs display low colloidal stability in the cell medium. The initial absorbance at the upper layer was reduced to 31 and 8% after 24h for cell media with and without FBS, indicating the settling of nanoparticles over time (Figure 3). Moreover, the aggregation behaviour of AgNPs was also observed by DLS measurements. In the cell culture medium supplemented with 10% FBS, the initial hydrodynamic

diameter (HD) changed from 62.25 ± 1.35 nm to 81.51 ± 8.25 nm. As expected, an increase in the HD was more pronounced in the AgNPs dispersion in cell media without FBS. Under these conditions, the HD modified from 397.03 ± 49.21 nm to 7,775.67 ± 1,135.27 nm, and PDI showed noticeable changes and display high value after 24 hours (from 0.24 to 1.72), indicating a heterogeneous size distribution. The low stability of AgNPs could be provided by the lack of the use of stabilisers (such as chitosan; poly(ethylene glycol), PEG; poly(vinyl alcohol), PVA; poly(vinyl pyrrolidone), PVP) to capping the nanoparticles. A summary of the DLS results (HD and PDI) of AgNPs in ZFL cell culture medium over time can be found in Table S2 in the Appendix B.

Figure 3: Monitoring the dispersing stability of GO-AgNPs, GO and AgNPs (50 µg mL^{-1}) in ZFL cell culture medium (L15/RPMI) with and without 10% FBS at 28 °C (from 0 to 24 h). Percentage of initial absorbance monitored at 400 nm

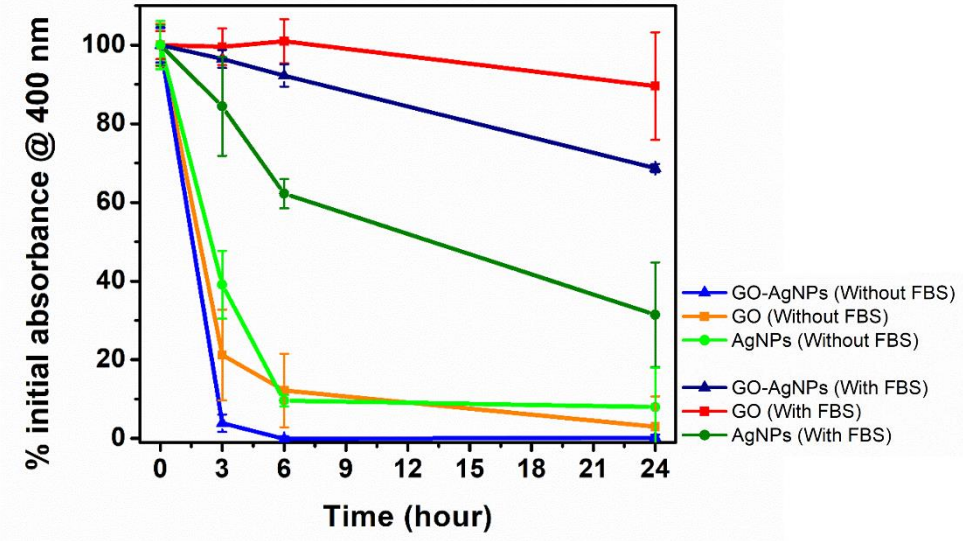

Indeed, the FBS protein corona formation could act as stabilising agent of nanomaterials. The decrease of aggregation and sedimentation rate of oxidised multiwalled carbon nanotubes and graphene oxide in cell culture media supplemented with 10% FBS were already reported by Morozesk et al. (2018) and Franqui et al. (2019), respectively. The higher stability of nanomaterials in the presence of proteins induce higher steric repulsion caused by the protein corona formation (MOORE et al., 2015, SUN et al., 2018). In addition, GO-AgNPs show higher sedimentation trends than GO (Figure 3). Reduced GO was more

hydrophobic and had lower adsorption capability due to surface functionality, as Qi et al. (2019) observed. In agreement with this result, De Medeiros et al. (2021) reported that the surface properties modified during GO-AgNPs synthesis lead to aggregation behaviour of nanohybrids in mineral reconstituted water.

Moreover, the presence of salts also could impact on NMs colloidal stability. Higher ion strength increases the attractive forces that lead to NMs agglomeration and, consequently, its sedimentation. As various cell culture media has been developed to attend to specific growth requirements of different cell lines, it was necessary to evaluate the colloidal stability case-by-case considering the assay conditions (DRASLER et al., 2017).

The liver is the main detoxification organ in vertebrates. The accumulation and histopathological alterations in this organ upon GO or AgNPs exposure on fishes have previously been reported (SOUZA et al., 2017; RAMACHANDRAN et al., 2018; KAKAKHEL et al., 2021; MANJUNATHA et al., 2021). Therefore, understanding the interaction of nanomaterials with liver cells *in vitro* is very complementary to *in vivo* studies reported in the literature. ZFL cell line was used by Christen et al. (2013) to access the toxic pathway of AgNPs. They observed that AgNPs exposition induced endoplasmatic reticulum stress that trigger apoptosis and inflammation response, and similar results were observed in zebrafish larvae. Therefore, ZFL cells can be considered a promising in vitro system and suitable for predicting the *in vivo* hazard effects towards *in vitro-in vivo* toxicity correlations.

Cellular viability was evaluated at 24 h post-exposure to different concentrations of GO-AgNPs, GO, AgNPs and $AgNO_3$ using three classical toxicity assays: Alamar Blue (AB), Tetrazolium Salt (MTT) and Neutral Red Uptake (NRU) (Figure 4). The results of the filtrate-only control was showed in Figure S2 in the Appendix B. The IC_{50} (half maximal inhibitory concentration, i.e. concentration that decreases the viability to 50% of initial response during the observation period) calculated for each treatment was present in Table 1.

Figure 4: Cytotoxicity results of ZFL cells exposed to different concentrations of GO-AgNPs (A), GO (B), AgNPs (C) and $AgNO_3$ (D) for 24 h at 28 °C. Three classical toxicity assays were used: Alamar Blue (AB), Tetrazolium Salt (MTT) and Neutral Red Uptake (NRU)

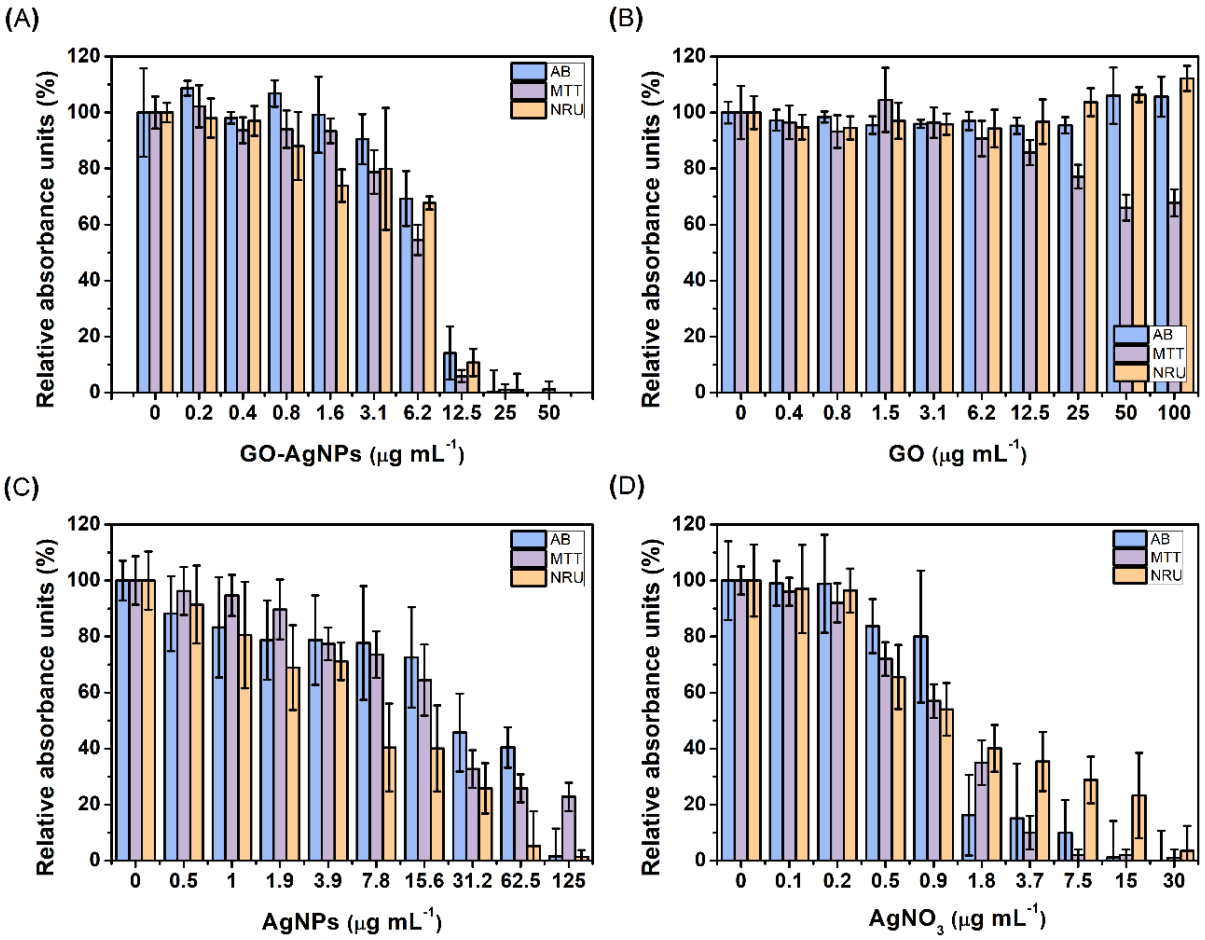

Table 1: calculated IC_{50} values (µg mL^{-1}) and their 95% confidence interval calculated from each cytotoxicity assay after exposure of ZFL cells to GO-AgNPs, GO, AgNPs and $AgNO_3$

IC_{50} values (µg mL^{-1})

	AB		MTT		NRU	
GO-AgNPs	7.0	(6.5 - 7.6)	5.7	(5.4-6.2)	6.5	(5.7 - 7.6)
GO	> 100 µg mL^{-1}					
AgNPs	25.8	(19.2-34.7)	15.9	(12.7 - 19.8)	6.5	(5.3 - 8.2)
$AgNO_3$	1.3	(1.1 - 1.5)	1.0	(0.46 - 5.1)	1.4	(1.1 -1.8)

A concentration-dependent reduction in cell viability following 24 hours of exposition to GO-AgNPs (concentration range from 0.2 to 50 mg L^{-1}) was observed

(Figure 4-A). The IC_{50} values ranged from 5.7 to 7.0 µg mL^{-1} across all toxicity endpoints.

Graphene oxide-silver nanoparticles *in vitro* toxicity has been reported by Kordi et al. (2019). They investigate the cell viability of 4 syntheses with different $AgNO_3$ concentrations of nanohybrids on the Neuro2A cell line (mouse albino neuroblastoma) using MTT assay. The nanohybrid synthesised with higher $AgNO_3$ concentration resulted in smaller AgNPs attached to GO sheets than with lower silver nitrate concentration. The IC_{50} obtained ranged between 1.5 to 35 µg L^{-1}. Interestingly, the higher cytotoxic was observed for nanohybrid synthesised with lower Ag concentration. A comparative cytotoxicity study of nanohybrids on hepatic normal (CHANG) and cancerous (HepG2) human cell was performed by Ali et al. (2018). The GO-AgNPs exposition induced oxidative stress (with increased oxidative enzymes such as lipid peroxide, superoxide dismutase and catalase), DNA damage and apoptosis. Moreover, HepG2 was slightly more susceptible. Together, these results suggest that the type of cell line used is a critical parameter to be considered during the cytotoxicity evaluation of nanohybrid materials.

After 24 hours of exposure, GO did not affect the ZFL cell viability until 100 µg $mL^{-1,}$ according to AB and NRU assays. However, the MTT assay showed a dose-dependent effect, and the cytotoxicity of GO was about 70% at 100 µg mL^{-1} (Figure 3-B). Additionally, the IC_{50} can not be calculated as is not observed the maximal response (100% of inhibition) at the highest concentration (100 µg L^{-1}) (SEBAUGH, 2011). In this assay, the enzymatic reduction of MTT to MTT-formazan is catalysed by mitochondrial succinate dehydrogenase. Hence, the lower cell viability could indicate a mitochondrial respiration impairment induced by GO exposure. However, it very important the care in interpreting MTT results during graphene toxicity evaluation. The GO could cause the adsorption, optical interferences, as well as electron transfer leading to the generation of artefacts for the *in vitro* evaluation of graphene based NMs toxicity (CHNG; PUMERA, 2013; JIAO et al., 2015). Thus, the observed effect of GO on ZFL cells could be less significant as the results indicated.

AgNPs exposure leads to a decrease of ZFL cell viability in a dose-response manner. The IC_{50} for each assay was calculated and ranged from 6.5 to 25.8 µg mL^{-1} across all toxicity endpoints. (Figure 4-C). The lowest IC_{50} value was observed with NRU assay, indicating lysosomal damage as a possible toxicity mechanism. Similarly, Connolly et al. (2015) reported the more susceptible effects on RTL-W1 (rainbow trout liver cell lines) towards NM-300k (commercial AgNPs, with an average hydrodynamic diameter of 209 nm in L15 media) with NRU assay (IC_{50} = 10.7 µg mL^{-1}) in comparative with others assays (AlamarBlue; IC_{50} = 75.9 µg mL^{-1} and CFDA-AM; IC_{50} = 15.9 µg mL^{-1}). Furthermore, in rainbow trout (*Oncorhynchus mykiss*) hepatocytes, Massarsky et al. (2014) reported the increase of lipid peroxidation after AgNPs (10 nm) exposure, which could compromise lysosomal integrity. Recently, the molecular mechanisms in ZF4 cells (an embryonic zebrafish cell line) underlying the cytotoxicity induced by AgNPs was studied by Quevedo et al. (2021). These authors reported that AgNPs could affect cellular membranes inducing lipid peroxidation. Moreover, they also observe AgNPs internalisation induced lysosomal dysfunction and permeabilisation of mitochondrial membrane and consequent reduction in the autophagy activity.

In the environment, the AgNPs could release silver ions (Ag^{+}) upon particle dissolution. Thus, a dissolved ion control ($AgNO_3$) was performed to investigate the toxicity of Ag^{+}. IC_{50} values corresponding to $AgNO_3$ ranged from 1.0 to 1.4 µg mL^{-1} across all toxicity endpoints (Figure 4-D and Table 1). Our results agree with Farkas et al. (2010) and Connolly et al. (2015), who reported an IC_{50} of 1.1 µg mL^{-1} following $AgNO_3$ exposure using primary and cell line (RTH-149) of rainbow trout hepatocytes with AB assay. Similar to AgNPs, Ag ions could induce lysosomal dysfunction, mitochondrial impairment, lipid peroxidation and, as a consequence, lower rates of autophagy activity (QUEVEDO et al., 2021).

A filtrate-only control was performed to assess the potential effects of dissolution of NPs under test conditions or the impact of toxic impurities of NHs synthesis (PETERSEN, 2015). The test conditions (without cells) were simulated, and the nanoparticles were removed from the media. After that, the assay was performed using the medium that was kept in contact with nanomaterials. The viability with filtrate-only control was near 60% without dilution with fresh media (Figure S2 – Appendix B). Thus, the impairments observed during GO-AgNPs exposition were promoted by the nanoparticles themselves and the silver ion release. Indeed, the dissolution behaviour

is an essential mechanism in potentiating AgNPs toxicity (ABRAMENKO et al., 2018; KLAESSIG, 2018). The cell media is a complex matrix that can alter the ion release. For example, the protein adsorption on AgNPs enhances the dissolution through sequestration of chemisorbed Ag^{+} by protein thiol groups (LIU et al., 2018; BOEHMLER et al., 2020).

Aggregation is another aspect that significantly influences biological response, as it alters *in vitro* behaviour (dosimetry, nanomaterials uptake) and fate (biodistribution) (MOORE et al., 2015). Thus, enhanced dark-field hyperspectral microscopy (EDHM) was applied to localise extracellular clusters of NMs in biological samples (Figure 5). This technique combines hyperspectral imaging (HSI) with dark-field reflectance systems to mapping nanomaterials. In the optical cell images, the coloured spots are correlated with the presence of NMs clusters. EDHM has been used to monitor the interaction of silver nanoparticles and graphene oxide with cells during *in vitro* toxicity studies (ROZHINA et al., 2019; MULENOS et al., 2020).

Moreover, the internalisation activity of carbon based NMs (GO and GO-AgNPs) was confirmed by Raman spectroscopy. The characteristic D and G bands (assigned at ~1330 and 1590 cm^{-1}) of the graphene family were monitored over z-depth to ensure the cell uptake (Figure 6). The phenylalanine band (typically assigned at 1002-1005 cm^{-1}) was used to determine that the laser location was inside the cell (Figure 6-A). As expected, no graphene fingerprint was found in the cell without treatment (control group) at EDHM or Raman analyses (Figure 5-A and Figure 6-B).

After treatment with 3 mg L-1 of GO-AgNPs over 24h, it is possible to visualise the interaction of GO aggregates with the cell membrane by images obtained by enhanced darkfield hyperspectral microscopy (EDHM) (Figure 5-B). However, few GO clusters were mapped in the cell exposure at the same concentration (Figure 5-C). Thus, the lack of cytotoxicity after GO exposure might be due to the low dose delivered. This observation was supported by the low sedimentation rate observed at monitoring the dispersing stability. The cells exposure to AgNPs shows interaction with a significant number of NMs clusters, probably due to low colloidal stability at cell media.

The Raman spectra collected inside the cells indicate the presence of nanohybrids inside the cells (Figure 6-C and D). Thus, the carbon signal could be mainly distributed in the cytoplasm undergo cellular internalisation.

Figure 5: Identification of nanomaterials in ZFL cell culture after exposure for 24h. Visualisation of extracellular clusters of nanomaterials (coloured spots) examined with EDHM after 24 h of exposition in dark-field images with 100x magnification: non-exposed (control) (A), GO-AgNps (B), GO (C) and AgNPs (D). Acquired hyperspectrum and its standard deviation of each treatment that was used to mapping the nanomaterials on the ZFL cells (E)

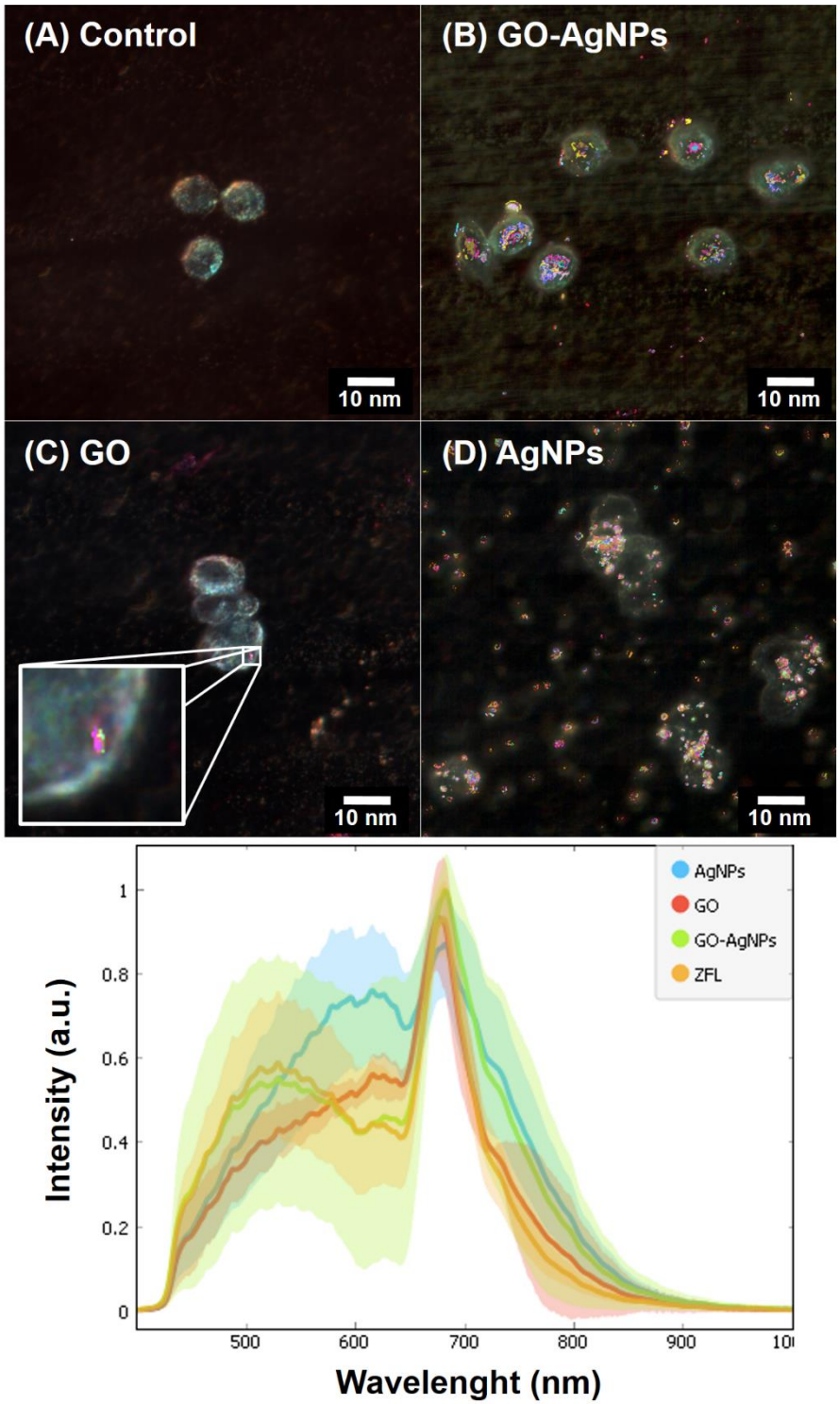

Figure 6: Raman spectra of the cell after incubation of carbon nanomaterial: Schematic illustration of Raman spectroscopy analyses to observed the carbon-nanomaterial uptake (A); control (B), GO-AgNPs (C) and GO (D) spectrum. The location of typical D and G bands of graphene based NMS are indicated as blue lines

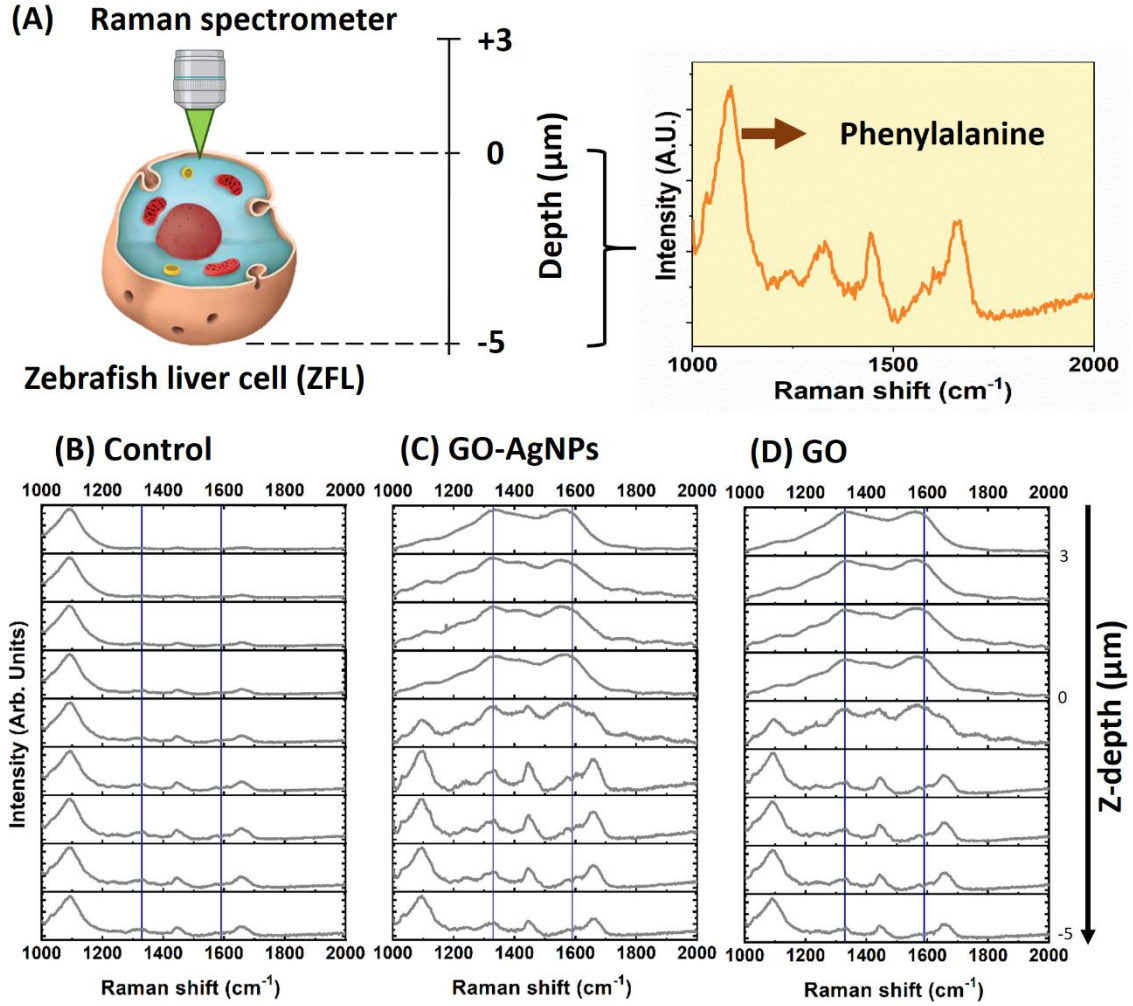

Numerous studies reported that GO exposition with different cell types sticks to the cell surface and internalisation. The cell uptake of graphene-family nanomaterials into cells is strongly influenced by the physic-chemical properties of graphene and the cellular context. The surface chemistry of nanomaterials critically affects the interaction of plasma membrane. For example, pristine graphene can trigger intracellular ROS stress, which leads to apoptosis without being internalised by Vero cells (monkey kidney cells). In contrast, GO was internalised by the cells without ensuing damage (SASIDHARAN et al., 2011).

Other intrinsic properties that influence GO uptake are the material size and shape. Smaller GO is easily uptake by the cells (ZHANG et al., 2013). Besides, the cellular uptake mechanisms could be size-depend. Small size GO entered the cells predominantly through clathrin-mediated endocytosis, while phagocytotic uptake was observed for large GO (MU et al., 2012). Thus, the cellular uptake pathways highly depend on GO physicochemical properties, as size and surface charge (TU et al., 2017).

The tendency of cellular uptake is higher with enhance of GO hydrophobicity (XIAOLI et al., 2020). This chemical transformation occurs at GO-AgNPs nanohybrids synthesis. The reduction agent ($NaBH_4$) led to a decrease in the number of hydrophilic groups. Therefore, the GO-AgNPs uptake could be higher than bare GO. For example, a comparative study of cellular uptake of GO-AgNPs nanohybrid and AgNPs on human lung cancer cells (A549 cells) and hepatocellular liver carcinoma cells (HepG2 cells) by ion beam microscopy (IBM) and by inductively coupled plasma mass spectrometry (ICP-MS) was conducted by Zhou et al. (2014). They reported higher cytotoxicity of AgNPs when they were conjugated onto GO sheets than free metal nanoparticles. Therefore, the nanohybrid's toxicity could be attributed to intracellular delivery properties of GO which leads to high metal concentration inside the cells.

In our previous study (DE MEDEIROS et al., 2021), we demonstrated the biocompatibility of GO and the low influence of dissolution on GO-AgNPs nanohybrids toxicity on Zebrafish embryos. Therefore, the GO may act as a good platform for assembling new nanohybrids in future technological applications of these materials

4.4. Conclusions

This study provides novel insights concerning the protein corona formation and *in vitro* toxicity of GO-AgNPs nanohybrids on ZFL cells. The main conclusions of this study were: i) The GO-AgNPs protein profile of hard corona was very similar to pristine GO, according AFM and SDS-PAGE analysis. Moreover, fetal bovine serum-hard corona plays a crucial role in the nanomaterial dispersion stability in ZFL culture medium; ii) GO-AgNPs nanohybrid shows higher cytotoxicity than AgNPs towards ZFL cells. GO shows good in vitro biocompatibility, even at a high

concentration (100 µg mL^{-1}), indicating that silver drove the toxicity in the nanohybrid. Moreover, the dissolution behaviour shows a minor influence on cell impairments; and iii) GO-AgNPs can be internalised by ZFL cells as confirmed by Raman spectroscopy. Finally, this work reinforces the potential use of zebrafish liver cells as *in vitro* model for toxicity assessment of nanohybrids, supporting the 3Rs principle (Replacement, Reduction and Refinement) in environmental nanosafety research.

References

ABRAMENKO, N. B.; DEMIDOVA, T. B.; ABKHALIMOV, E. V.; ERSHOV, B. G.; KRYSANOV, E. Y.; KUSTOV, L. M. Ecotoxicity of different-shaped silver nanoparticles: Case of zebrafish embryos. J **Journal of Hazardous Materials**, v. 347, p. 89-94, 2018.

AICH, N.; PLAZAS-TUTTLE, J.; LEAD, J. R.; SALEH, N. B. A critical review of nanohybrids: Synthesis, applications and environmental implications. **Environmental Chemistry**, v. 11, n. 6, p. 609–623, 2014.

AL-AMMARI, A.; ZHANG, L.; YANG, J.; WEI, F.; CHEN, C.; SUN, D. Toxicity assessment of synthesized titanium dioxide nanoparticles in fresh water algae Chlorella pyrenoidosa and a zebrafish liver cell line. **Ecotoxicology and Environmental Safety**, v. 211, art. 111948, 2021.

ALI, D.; ALARIFI, S.; ALKAHTANI, S.; ALMEER, R. S. Silver-doped graphene oxide nanocomposite triggers cytotoxicity and apoptosis in human hepatic normal and carcinoma cells. **International Journal of Nanomedicine**, v. 13, p. 5685–5699, 2018.

ALIAN, R. S.; DZIEWIĘCKA, M.; KĘDZIORSKI, A.; MAJCHRZYCKI, Ł.; AUGUSTYNIAK, M. Do nanoparticles cause hormesis? Early physiological compensatory response in house crickets to a dietary admixture of GO, Ag, and GOAg composite. **Science of The Total Environment**, v. 788, p. 147801, 2021.

AMIR, M. N. I.; HALILU, A.; JULKAPLI, N. M.; MA'AMOR, A. Gold-graphene oxide nanohybrids: A review on their chemical catalysis. **Journal of Industrial and Engineering Chemistry**, v. 83, p. 1–13, 2020.

ARGENTIERE, S.; CELLA, C.; CESARIA, M.; MILANI, P.; LENARDI, C. Silver nanoparticles in complex biological media: assessment of colloidal stability and protein corona formation. **Journal of Nanoparticle Research**, v. 18, art. 253, 2016.

AZHDARZADEH, M.; SAEI, A. A.; SHARIFI, S.; HAJIPOUR, M. J.; ALKILANY, A. M.; SHARIFZADEH, M.; RAMAZANI, F.; LAURENT, S.; MASHAGHI, A.; MAHMOUDI, M. Nanotoxicology : advances and pitfalls in research methodology. **Nanomedicine**, v. 10, n. 18, p. 2931–2952, 2015.

BAI, H.; LIU, L.; SUN, D. D. Stability investigation of graphene oxide–silver nanoparticles composites in natural reservoir water. **RSC Advances**, v. 3, p. 25331–25339, 2013.

BAKHSHESHI-RAD, H. R.; ISMAIL, A. F.; AZIZ, M.; AKBARI, M.; HADISI, Z.; KHOSHNAVA, S. M.; PAGAN, E.; CHEN, X. Co-incorporation of graphene oxide/silver nanoparticle into poly-L-lactic acid fibrous: A route toward the development of cytocompatible and antibacterial coating layer on magnesium implants. **Materials Science and Engineering C**, v. 111, art. 110812, 2020.

BOEHMLER, D. J.; O'DELL, Z. J.; CHUNG, C.; RILEY, K. R. Bovine Serum Albumin Enhances Silver Nanoparticle Dissolution Kinetics in a Size- And Concentration-Dependent Manner. **Langmuir**, v. 36, n. 4, p. 1053-1061, 2020.

CANEDO, A.; ROCHA, T. L. Zebrafish (Danio rerio) using as model for genotoxicity and DNA repair assessments: Historical review, current status and trends. **Science of the Total Environment**, v. 762, art. 144084, 2021.

CHEN, Y.; WU, W.; XU, Z.; JIANG, C.; HAN, S.; RUAN, J.; WANG, Y. Photothermal-assisted antibacterial application of graphene oxide-Ag nanocomposites against clinically isolated multi-drug resistant Escherichia coli. **Royal Society Open Science**, v. 7, n. 7, 2020. https://doi.org/10.1098/rsos.192019.

CHNG, E. L. K.; PUMERA, M. The Toxicity of Graphene Oxides: Dependence on the Oxidative Methods Used. **Chemistry - A European Journal**, v. 19, n. 25, p. 8227–8235, 2013.

CHRISTEN, V.; CAPELLE, M.; FENT, K. Silver nanoparticles induce endoplasmatic reticulum stress response in zebrafish. **Toxicology and Applied Pharmacology**, v. 272, n. 2, p. 519–528, 2013.

ÇIPLAK, Z.; YILDIZ, N.; CĄLIMLI, A. Investigation of graphene/Ag nanocomposites synthesis parameters for two different synthesis methods. **Fullerenes Nanotubes and Carbon Nanostructures**, v. 23, n. 4, p. 361–370, 2015.

CLEMENTE, Z.; CASTRO, V. L. S. S.; FRANQUI, L. S.; SILVA, C. A.; MARTINEZ, D. S. T. Nanotoxicity of graphene oxide: Assessing the influence of oxidation debris in the presence of humic acid. **Environmental Pollution**, v. 225, p. 118–128, 2017.

COBOS, M.; DE-LA-PINTA, I.; QUINDÓS, G.; FERNÁNDEZ, M. D.; FERNÁNDEZ, M. J. Graphene oxide–silver nanoparticle nanohybrids: Synthesis, characterization, and antimicrobial properties. **Nanomaterials**, v. 10, n. 2, 2020.

CONNOLLY, M.; FERNANDEZ-CRUZ, M. L.; QUESADA-GARCIA, A.; ALTE, L.; SEGNER, H.; NAVAS, J. M. Comparative cytotoxicity study of silver nanoparticles (Agnps) in a variety of rainbow trout cell lines (RTL-W1, RTH-149, RTG-2) and primary hepatocytes. **International Journal of Environmental Research and Public Health**, v. 12, n. 5, p. 5386–5405, 2015.

DE MEDEIROS, A. M. Z.; KHAN, L. U.; SILVA, G. H. DA; OSPINA, C. A.; ALVES, O. L.; CASTRO, V. L. DE; MARTINEZ, D. E. T. Graphene oxide-silver nanoparticle hybrid material: an integrated nanosafety study in zebrafish embryos. **Ecotoxicology and Environmental Safety**, v. 209, art. 111776, 2021.

DELOID, G. M.; COHEN, J. M.; PYRGIOTAKIS, G.; DEMOKRITOU, P. Preparation, characterization, and in vitro dosimetry of dispersed, engineered nanomaterials. **Nature Protocols**, v. 12, n. 2, p. 355–371, 2017.

DRASLER, B.; SAYRE, P.; STEINHÄUSER, K. G.; PETRI-FINK, A.; ROTHEN-RUTISHAUSER, B. In vitro approaches to assess the hazard of nanomaterials. **NanoImpact**, v. 8, p. 99–116, 2017.

DUAN, G.; KANG, S. G.; TIAN, X.; GARATE, J.A.; ZHAO, L.; GE, C.; ZHOU, R. Protein corona mitigates the cytotoxicity of graphene oxide by reducing its physical interaction with cell membrane. **Nanoscale**, v. 7, n. 37, p. 15214–15224, 2015.

DURÁN, N.; SILVEIRA, C. P.; DURÁN, M.; MARTINEZ, D. S. T. Silver nanoparticle protein corona and toxicity: a mini-review. **Journal of Nanobiotechnology**, v. 13, art. 55, 2015.

EIDE, M.; RUSTEN, M.; MALE, R.; JENSEN, K. H. M.; GOKSØYR, A. A characterization of the ZFL cell line and primary hepatocytes as in vitro liver cell models for the zebrafish (Danio rerio). **Aquatic Toxicology**, v. 147, p. 7–17, 2014.

FARIA, A. F.; MARTINEZ, D. S. T.; MORAES, A. C. M.; COSTA, M. E. H. M. DA; BARROS, E. B.; SOUZA FILHO, A. G.; PAULA, A. J.; ALVES, O. L. Unveiling the role of oxidation debris on the surface chemistry of graphene through the anchoring of ag nanoparticles. **Chemistry of Materials**, v. 24, n. 21, p. 4080–4087, 2012.

FARKAS, J.; CHRISTIAN, P.; URREA, J. A. G.; ROOS, N.; HASSELLÖV, M.; TOLLEFSEN, K. E.; THOMAS, K. V. Effects of silver and gold nanoparticles on rainbow trout (Oncorhynchus mykiss) hepatocytes. **Aquatic Toxicology**, v. 96, n. 1, p. 44–52, 2010.

FRAGAL, E. H.; FRAGAL, V. H.; SILVA, G. H. DA; GONÇALVES, S. P. C.; MARTINEZ, D. S. T.; RUBIRA, A. F.; SILVA, R. Enhancing Near-Infrared Photothermal Efficiency of Biocompatible Flame-Synthesized Carbon Nano-Onions with Metal Dopants and Silica Coating. **ACS Applied Bio Materials**, v. 3, n. 9, p. 5984–5994, 2020.

FRANQUI, L. S.; FARIAS, M. A. DE; PORTUGAL, R. V.; COSTA, C. A. R.; DOMINGUES, R. R.; SOUZA FILHO, A. G.; COLUCI, V. T.; LEME, A. F. P.; MARTINEZ, D.S. T. Interaction of graphene oxide with cell culture medium: Evaluating the fetal bovine serum protein corona formation towards in vitro nanotoxicity assessment and nanobiointeractions. **Materials Science and Engineering C**, v. 100, p. 363–377, 2019.

FU, Y.; ZENG, G.; LAI, C.; HUANG, D.; QIN, L.; YI, H.; LIU, X.; ZHANG, M.; LI, B.; LIU, S.; LI, L.; LI, M.; WANG, W.; ZHANG, Y.; PI, Z. Hybrid architectures based on noble metals and carbon-based dots nanomaterials: A review of recent progress in synthesis and applications. **Chemical Engineering Journal**, v. 399, art. 125743, 2020.

GUO, X.; SEO, J. E.; LI, X.; MEI, N. Genetic toxicity assessment using liver cell models: past, present, and future. **Journal of Toxicology and Environmental Health - Part B: Critical Reviews**, v. 23, n. 1, p. 27–50, 2020.

HA, M. K.; SHIM, Y. J.; YOON, T. H. Effects of agglomeration on in vitro dosimetry and cellular association of silver nanoparticles. **Environmental Science: Nano**, v. 5, p. 446–455, 2018.

HABIBA, K.; ENCARNACION-ROSADO, J.; GARCIA-PABON, K.; VILLALOBOS-SANTOS, J. C.; MAKAROV, V.; AVALOS, J. A.; WEINER, B. R.; MORELL, G. Improving cytotoxicity against cancer cells by chemo-photodynamic combined modalities using silver-graphene quantum dots nanocomposites. **International Journal of Nanomedicine**, v. 11, p. 107-119, 2015.

HOLT, B. D.; ARNOLD, A. M.; SYDLIK, S. A. The Blanket Effect: How Turning the World Upside Down Reveals the Nature of Graphene Oxide Cytocompatibility. **Advanced Healthcare Materials**, v. 10, n. 7, art. 2001761, 2021.

HUANG, X.; YIN, Z.; WU, S.; QI, X.; HE, Q.; ZHANG, Q.; YAN, Q.; BOEY, F.; ZHANG, H. Graphene-based materials: Synthesis, characterization, properties, and applications. **Small**, v. 7, n. 14, p. 1876–1902, 2011. Special Issue.

JAWORSKI, S.; WIERZBICKI, M.; SAWOSZ, E.; JUNG, A.; GIELERAK, G.; BIERNAT, J.; JAREMEK, H.; ŁOJKOWSKI, W.; WOŹNIAK, B.; WOJNAROWICZ, J.; STOBIŃSKI, L.; MAŁOLEPSZY, A.; MAZURKIEWICZ-PAWLICKA, M.; ŁOJKOWSKI, M.; KURANTOWICZ, N.; CHWALIBOG, A. Graphene oxide-based nanocomposites decorated with silver nanoparticles as an antibacterial agent. **Nanoscale Research Letters**, v. 13, n. 1, p. 116, 2018.

JIAO, G.; HE, X.; LI, X.; QIU, J.; XU, H.; ZHANG, N.; LIU, S. Limitations of MTT and CCK-8 assay for evaluation of graphene cytotoxicity. **RSC Advances**, v. 5, p. 53240–53244, 2015.

JOHNSTON, H. J.; VERDON, R.; GILLIES, S.; BROWN, D. M.; FERNANDES, T. F.; HENRY, T. B.; ROSSI, A. G.; TRAN, L.; TUCKER, C.; TYLER, C. R.; STONE, V. Adoption of in vitro systems and zebrafish embryos as alternative models for reducing rodent use in assessments of immunological and oxidative stress responses to nanomaterials. **Critical Reviews in Toxicology**, v. 48, n. 3, p. 252–271, 2018.

KAKAKHEL, M. A.; WU, F.; SAJJAD, W.; ZHANG, Q.; KHAN, I.; ULLAH, K.; WANG, W. Long-term exposure to high-concentration silver nanoparticles induced toxicity, fatality, bioaccumulation, and histological alteration in fish (Cyprinus carpio). **Environmental Sciences Europe**, v. 33, art. 14, 2021.

KLAESSIG, F. C. Dissolution as a paradigm in regulating nanomaterials. **Environmental Science: Nano**, v. 5, n. 5, p. 1070–1077, 2018.

KOPAC, T. Protein corona, understanding the nanoparticle–protein interactions and future perspectives: A critical review. **International Journal of Biological Macromolecules**, v. 169, p. 290–301, 2021.

KORDI, F.; KHORSAND ZAK, A.; DARROUDI, M.; HAZRATI SAEDABADI, M. Synthesis and characterizations of Ag-decorated graphene oxide nanosheets and their cytotoxicity studies. **Chemical Papers**, v. 73, n. 8, p. 1945–1952, 2019.

KOUSHIK, D.; SEN, S.; MALIYEKKAL, S. M.; PRADEEP, T. Rapid dehalogenation of pesticides and organics at the interface of reduced graphene oxide – silver nanocomposite. **Journal of Hazardous Materials**, v. 308, p. 192–198, 2016.

KUNDU, N.; MUKHERJEE, D.; MAITI, T. K.; SARKAR, N. Protein-Guided Formation of Silver Nanoclusters and Their Assembly with Graphene Oxide as an Improved Bioimaging Agent with Reduced Toxicity. **Journal of Physical Chemistry Letters**, v. 8, p. 2291–2297, 2017.

LI, Y.; LEE, J. S. Insights into characterization methods and biomedical applications of nanoparticle-protein corona. **Materials**, v. 13, n. 14, art. 3093, 2020.

LIANG, C.; ZHANG, X.; WANG, Z.; WANG, W.; YANG, M.; DONG, X. Organic/inorganic nanohybrids rejuvenate photodynamic cancer therapy. **Journal of Materials Chemistry B**, v. 8, n. 22, p. 4748–4763, 2020.

LIU, C.; LENG, W.; VIKESLAND, P. J. Controlled Evaluation of the Impacts of Surface Coatings on Silver Nanoparticle Dissolution Rates. **Environmental Science and Technology**, v. 52, n. 5, p. 2726–2734, 2018.

LIU, N.; TANG, M.; DING, J. The interaction between nanoparticles-protein corona complex and cells and its toxic effect on cells. **Chemosphere**, v. 245, art. 125624, 2020.

LUNA, L. A. V. DE; ZORGI, N. E.; MORAES, A. C. M. DE; SILVA, D. S. DA; CONSONNI, S. R.; GIORGIO, S.; ALVES, O. L. In vitro immunotoxicological assessment of a potent microbicidal nanocomposite based on graphene oxide and silver nanoparticles. **Nanotoxicology**, v. 13, n. 2, p. 189–203, 2019.

LUNGU-MITEA, S.; VOGS, C.; CARLSSON, G.; MONTAG, M.; FRIEBERG, K.; OSKARSSON, A.; LUNDQVIST, J. Modeling Bioavailable Concentrations in Zebrafish Cell Lines and Embryos Increases the Correlation of Toxicity Potencies across Test Systems. **Environmental Science and Technology**, v. 55, n. 1, p. 447–457, 2021.

LUO, N.; NI, D.; YUE, H.; WEI, W.; MA, G. Surface-engineered graphene navigate divergent biological outcomes toward macrophages. **ACS Applied Materials and Interfaces**, v. 7, n. 9, p. 5239–5247, 2015.

MAHMOUDI, E.; NG, L. Y.; BA-ABBAD, M. M.; MOHAMMAD, A. W. Novel nanohybrid polysulfone membrane embedded with silver nanoparticles on graphene oxide nanoplates. **Chemical Engineering Journal**, v. 277, p. 1–10, 2015.

MANJUNATHA, B.; SEO, E.; PARK, S. H.; KUNDAPUR, R. R.; LEE, S. J. Pristine graphene and graphene oxide induce multi-organ defects in zebrafish (Danio rerio) larvae / juvenile : an in vivo study. **Environmental Science and Pollution Research International**, 2021 doi: 10.1007/s11356-021-13058-7.

MARTA, B.; POTARA, M.; ILIUT, M.; JAKAB, E.; RADU, T.; IMRE-LUCACI, F.; KATONA, G.; POPESCU, O.; ASTILEAN, S. Designing chitosan-silver nanoparticles-graphene oxide nanohybrids with enhanced antibacterial activity against Staphylococcus aureus. **Colloids and Surfaces A: Physicochemical and Engineering Aspects**, v. 487, p. 113–120, 2015.

MARTIN, M. N.; BASHAM, J. I.; CHANDO, P.; EAH, S. K. Charged gold nanoparticles in non-polar solvents: 10-min synthesis and 2D self-assembly. **Langmuir**, v. 26, p. 7410–7417, 2010.

MASSARSKY, A.; ABRAHAM, R.; NGUYEN, K. C.; RIPPSTEIN, P.; TAYABALI, A. F.; TRUDEAU, V. L.; MOON, T. W. Nanosilver cytotoxicity in rainbow trout (Oncorhynchus mykiss) erythrocytes and hepatocytes. **Comparative Biochemistry and Physiology - C Toxicology and Pharmacology**, v. 159, n. 1, p. 10–21, 2014.

MENG, H.; LEONG, W.; LEONG, K. W.; CHEN, C.; ZHAO, Y. Walking the line : The fate of nanomaterials at biological barriers. **Biomaterials**, v. 174, p. 41–53, 2018.

MOHAMMED, H.; KUMAR, A.; BEKYAROVA, E.; AL-HADEETHI, Y.; ZHANG, X.; CHEN, M.; ANSARI, M. S.; COCHIS, A.; RIMONDINI, L. Antimicrobial Mechanisms and Effectiveness of Graphene and Graphene-Functionalized Biomaterials. A Scope Review. **Frontiers in Bioengineering and Biotechnology**, v. 8, 2020. https://doi.org/10.3389/fbioe.2020.00465.

MOORE, T. L.; RODRIGUEZ-LORENZO, L.; HIRSCH, V.; BALOG, S.; URBAN, D.; JUD, C.; ROTHEN-RUTISHAUSER, B.; LATTUADA, M.; PETRI-FINK, A. Nanoparticle colloidal stability in cell culture media and impact on cellular interactions. **Chemical Society Reviews**, v. 44, n. 17, p. 6287–6305, 2015.

MORAES, A. C. M. DE. Graphene oxide-silver nanocomposite as a promising biocidal agent against methicillin- resistant Staphylococcus aureus. **International Journal of Nanomedicine**, v. 10, p. 6847–6861, 2015.

MOROZESK, M.; FRANQUI, L. S.; MANSANO, A. S.; MARTINEZ, D. S. T.; FERNANDES, M. N. Interactions of oxidized multiwalled carbon nanotube with cadmium on zebrafish cell line: The influence of two co-exposure protocols on in vitro toxicity tests. **Aquatic Toxicology**, v. 200, p. 136–147, 2018.

MOROZESK, M.; FRANQUI, L. S.; PINHEIRO, F. C.; NÓBREGA, J. A.; MARTINEZ, D. S. T.; FERNANDES, M. N. Effects of multiwalled carbon nanotubes co-exposure with cadmium on zebrafish cell line: Metal uptake and accumulation, oxidative stress, genotoxicity and cell cycle. **Ecotoxicology and Environmental Safety**, v. 202, art. 110892, 2020.

MU, Q.; SU, G.; LI, L.; GILBERTSON, B. O.; YU, L. H.; ZHANG, Q.; SUN, Y.-P.; YAN, B. Size-dependent cell uptake of protein-coated graphene oxide nanosheets. **ACS Applied Materials and Interfaces**, v. 4, n. 4, p. 2259–2266, 2012.

MULENOS, M. R.; LUJAN, H.; PITTS, L. R.; SAYES, C. M. Silver nanoparticles agglomerate intracellularly depending on the stabilizing agent: Implications for nanomedicine efficacy. **Nanomaterials**, v. 10, n. 10, art. 1953, 2020.

MÜLHOPT, S.; DIABATÉ, S.; DILGER, M. et al. Characterization of Nanoparticle Batch-To-Batch Variability. **Nanomaterials**, v. 8, n. 5, art. 311, 2018.

NAEEM, H.; AJMAL, M.; QURESHI, R. B.; MUNTHA, S. T.; FAROOQ, M.; SIDDIQ, M. Facile synthesis of graphene oxide–silver nanocomposite for decontamination of water from multiple pollutants by adsorption, catalysis and antibacterial activity. **Journal of Environmental Management**, v. 230, p. 199–211, 2019.

NEL, A. E.; MÄDLER, L.; VELEGOL, D.; XIA, T.; HOEK, E. M. V.; SOMASUNDARAN, P.; KLAESSIG, F.; CASTRANOVA, V.; THOMPSON, M. Understanding biophysicochemical interactions at the nano-bio interface. **Nature materials**, v. 8, n. 7, p. 543–557, 2009.

PARK, M. V. D. Z.; BLEEKER, E. A. J.; BRAND, W.; CASSEE, F. R.; VAN ELK M.; GOSENS, I.; DE JONG, W. H.; MEESTERS, J. A. J.; PEIJNENBURG, W. J. G. M.; QUIK, J. T. K.; VANDEBRIEL, R. J.; SIPS, A. J. A. M. Considerations for Safe Innovation: The Case of Graphene. **ACS Nano**, v. 11, n. 10, p. 9574–9593, 2017.

PAULA, A. J.; SILVEIRA, C. P.; MARTINEZ, D. S. T.; SOUZA FILHO, A. G.; ROMERO, F. V.; FONSECA, L. C.; TASIC, L.; ALVES, O. L.; DURÁN, N. Topography-driven bionano-interactions on colloidal silica nanoparticles. **ACS Applied Materials and Interfaces**, v. 6, n. 5, p. 3437–3447, 2014.

PEREIRA, A. C.; GOMES, T.; FERREIRA MACHADO, M. R.; ROCHA, T. L. The zebrafish embryotoxicity test (ZET) for nanotoxicity assessment: from morphological to molecular approach. **Environmental Pollution**, v. 252, p. 1841–1853, 2019.

PETERSEN, E. J. **Control experiments to avoid artifacts and misinterpretations in nanoecotoxicology testing**. Gaithersburg, MD: National Institute of Standards and Technology, 2015. (NIST Special Publication). https://doi.org/10.6028/NIST.sp.1200-11.

PLAZAS-TUTTLE, J.; ROWLES, L.; CHEN, H.; BISESI JUNIOR, J. H.; SABO-ATTWOOD, T.; SALEH, N. B. Dynamism of Stimuli-Responsive Nanohybrids: Environmental Implications. **Nanomaterials**, v. 5, n. 2, p. 1102–1123, 2015.

PULIDO-REYES, G.; LEGANES, F.; FERNÁNDEZ-PIÑAS, F.; ROSAL, R. Bio-nano interface and environment: A critical review. **Environmental Toxicology and Chemistry**, v. 36, n. 12, p. 3181–3193, 2017.

QUEVEDO, A. C.; LYNCH, I.; VALSAMI-JONES, E. Silver nanoparticle induced toxicity and cell death mechanisms in embryonic zebrafish cells. **Nanoscale**, v. 13, p. 6142-6161, 2021.

RAMACHANDRAN, R.; KRISHNARAJ, C.; KUMAR, V. K. A.; HARPER, S. L.; KALAICHELVAN, T. P.; YUN, S.-I. In vivo toxicity evaluation of biologically synthesized silver nanoparticles and gold nanoparticles on adult zebrafish: a comparative study. **3 Biotech**, v. 8, n. 10, p. 441, 2018.

RAN, X.; DU, Y.; WANG, Z.; WANG, H.; PU, F.; REN, J.; QU, X. Hyaluronic acid-templated Ag nanoparticles/graphene oxide composites for synergistic therapy of bacteria infection. **ACS Applied Materials and Interfaces**, v. 9, n. 23, p. 19717–19724, 2017.

REHBERGER, K.; KROPF, C.; SEGNER, H. In vitro or not in vitro: a short journey through a long history. **Environmental Sciences Europe**, v. 30, n. 1, p. 23, 2018.

ROZHINA, E.; BATASHEVA, S.; DANILUSHKINA, A.; KRYUCHKOVA, M.; GOMZIKOVA, M.; CHEREDNICHENKO, Y.; NIGAMATZYANOVA, L.; AKHATOVA, F.; FAKHRULLIN, R. Kaolin alleviates the toxicity of graphene oxide for mammalian cells. **MedChemComm**, v. 10, n. 8, p. 1457–1464, 2019.

SALEH, N. B.; AICH, N.; PLAZAS-TUTTLE, J.; LEAD, J. R.; LOWRY, G. V. Research strategy to determine when novel nanohybrids pose unique environmental risks. **Environmental Science: Nano**, v. 2, n. 1, p. 11–18, 2015.

SASIDHARAN, A.; PANCHAKARLA, L. S.; CHANDRAN, P.; MENON, D.; NAIR, S.; RAOB, C. N. R.; KOYAKUTTY, M. Differential nano-bio interactions and toxicity effects of pristine versus functionalized graphene. **Nanoscale**, v. 3, n. 6, p. 2461–2464, 2011.

SAYES, C. M.; WARHEIT, D. B. Characterization of nanomaterials for toxicity assessment. **Wiley Interdisciplinary Reviews: Nanomedicine and Nanobiotechnology**, v. 1, n. 6, p. 660–670, 2009.

SEBAUGH, J. L. Guidelines for accurate EC50/IC50 estimation. **Pharmaceutical Statistics**, v. 10, n. 2, p. 128–134, 2011.

SHARMA, S.; PRAKASH, V.; MEHTA, S. K. Graphene/silver nanocomposites-potential electron mediators for proliferation in electrochemical sensing and SERS activity. **TrAC - Trends in Analytical Chemistry**, v. 86, p. 155–171, 2017.

SHENG, Z.; LIU, Y. Potential impacts of silver nanoparticles on bacteria in the aquatic environment. **Journal of Environmental Management**, v. 191, p. 290–296, 2017.

SILVA, G. H. DA; CLEMENTE, Z.; KHAN, L. U.; COA, F.; NETO, L. L.R.; CARVALHO, H. W. P.; CASTRO, V. L.; MARTINEZ, D. S. T.; MONTEIRO, R. T. R. Toxicity assessment of TiO2-MWCNT nanohybrid material with enhanced photocatalytic activity on Danio rerio (Zebrafish) embryos. **Ecotoxicology and Environmental Safety**, v. 165, p. 136–143, 2018.

SOROUSH, A.; MA, W.; SILVINO, Y.; RAHAMAN, M. S. Surface modification of thin film composite forward osmosis membrane by silver-decorated graphene-oxide nanosheets. **Environmental Science: Nano**, v. 2, n. 4, p. 395–405, 2015.

SOUSA, M. DE; MARTINS, C. H. Z.; FRANQUI, L. S.; FONSECA, L. C.; DELITE, F. S.; LANZONI, E. M.; MARTINEZ, D. S. T.; ALVES, O. L. Covalent functionalization of graphene oxide with d-mannose: Evaluating the hemolytic effect and protein corona formation. **Journal of Materials Chemistry B**, v. 6, n. 18, p. 2803–2812, 2018.

SOUZA, J. P.; BARETTA, J. F.; SANTOS, F.; PAINO, I. M. M.; ZUCOLOTTO, V. Toxicological effects of graphene oxide on adult zebrafish (Danio rerio). **Aquatic Toxicology**, v. 186, p. 11–18, 2017.

STADNICKA-MICHALAK, J.; TANNEBERGER, K.; SCHIRMER, K.; ASHAUER, R. Measured and modeled toxicokinetics in cultured fish cells and application to in vitro - in vivo toxicity extrapolation. **PLoSONE**, v. 9, e92303, 2014. https://doi.org/10.1371/journal.pone.0092303

SUN, B.; ZHANG, Y.; CHEN, W.; WANG, K.; ZHU, L. Concentration Dependent Effects of Bovine Serum Albumin on Graphene Oxide Colloidal Stability in Aquatic Environment. **Environmental Science and Technology**, v. 52, n. 13, p. 7212–7219, 2018.

SUN, B.; ZHANG, Y.; LIU, Q.; YAN, C.; XIAO, B.; YANG, J.; LIUA, M.; ZHU, L. Lateral size dependent colloidal stability of graphene oxide in water: impacts of protein properties and water chemistry. **Environmental Science: Nano**, v. 7, n. 2, p. 634–644, 2020.

THIT, A.; SKJOLDING, L. M.; SELCK, H.; STURVE, J. Effects of copper oxide nanoparticles and copper ions to zebrafish (Danio rerio) cells, embryos and fry. **Toxicology in Vitro**, v. 45, p. 89–100, 2017.

TU, Z.; ACHAZI, K.; SCHULZ, A.; MÜLHAUPT, R.; THIERBACH, S.; RÜHL, E.; ADELI, M.; HAAG, R. Combination of Surface Charge and Size Controls the Cellular Uptake of Functionalized Graphene Sheets. **Advanced Functional Materials**, v. 27, art. 1701837, 2017.

ULLAH, S.; AHMAD, A.; SUBHAN, F.; JAN, A.; RAZA, M.; KHAN, A. U.; RAHMAN, A.-U.; KHAN, U. A.; TARIQ, M.; YUAN, Q. Tobramycin mediated silver nanospheres/graphene oxide composite for synergistic therapy of bacterial infection. **Journal of Photochemistry and Photobiology B: Biology**, v. 183, p. 342–348, 2018.

VICENTE-MARTÍNEZ, Y.; CARAVACA, M.; SOTO-MECA, A.; FRANCISCO-ORTIZ, O. DE; GIMENO, F. Graphene oxide and graphene oxide functionalized with silver nanoparticles as adsorbents of phosphates in waters. A comparative study. **Science of the Total Environment**, v. 709, art. 136111, 2020.

WANG, D.; SALEH, N. B.; SUN, W.; PARK, C. M.; SHEN, C.; AICH, N.; PEIJNENBURG, W. J. G. M.; ZHANG, W.; JIN, Y.; SU, C. Next-Generation Multifunctional Carbon − Metal Nanohybrids for Energy and Environmental Applications. **Enviromental Science & Technology**, v. 53, n. 13, p. 7265–7287, 2019.

WIERZBICKI, M.; JAWORSKI, S.; SAWOSZ, E.; JUNG, A.; GIELERAK, G.; JAREMEK, H.; ŁOJKOWSKI, W.; WOŹNIAK, B.; STOBIŃSKI, L.; MAŁOLEPSZY, A.; CHWALIBOG, A. Graphene Oxide in a Composite with Silver Nanoparticles Reduces the Fibroblast and Endothelial Cell Cytotoxicity of an Antibacterial Nanoplatform. **Nanoscale Research Letters**, v. 14, n. 1, art. 320, 2019.

XIAOLI, F.; QIYUE, C.; WEIHONG, G.; YAQING, Z.; CHEN, H.; JUNRONG, W.; LONGQUAN, S. Toxicology data of graphene-family nanomaterials: an update. **Archives of Toxicology**, v. 94, n. 6, p. 1915–1939, 2020.

XIE, X.; MAO, C.; LIU, X.; ZHANG, Y.; CUI, Z.; YANG, X.; YEUNG, K. W. K.; PAN, H.; CHU, P. K.; WU, S. Synergistic Bacteria Killing through Photodynamic and Physical Actions of Graphene Oxide/Ag/Collagen Coating. **ACS Applied Materials and Interfaces**, v. 9, n. 31, p. 26417–26428, 2017.

XU, L.; XU, M.; WANG, R.; YIN, Y.; LYNCH, I.; LIU, S. The crucial role of environmental coronas in determining the biological effects of engineered nanomaterials. **Small**, art. 2003691, 2020. https://doi.org/10.1002/smll.202003691.

XU, X.; MAO, X.; WANG, Y.; LI, D.; DU, Z.; WU, W.; JIANG, L.; YANG, J.; LI, J. Study on the interaction of graphene oxide-silver nanocomposites with bovine serum albumin and the formation of nanoparticle-protein corona. **International Journal of Biological Macromolecules**, v. 116, p. 492–501, 2018.

YIN, P. T.; SHAH, S.; CHHOWALLA, M.; LEE, K. Design, Synthesis, and Characterization of Graphene − Nanoparticle Hybrid Materials for Bioapplications. **Chemical Reviews**, v. 115, p. 2483–2531, 2015.

ZHANG, H.; PENG, C.; YANG, J.; LV, M.; LIU, R.; HE, D.; FAN, C.; HUANG, Q. Uniform ultrasmall graphene oxide nanosheets with low cytotoxicity and high cellular uptake. **ACS Applied Materials and Interfaces**, v.5, n.5, p.1761–1767, 2013.

ZHAO, N.; YAN, L.; ZHAO, X.; Chen, X.; Li, A.; Zheng, D.; Zhou, X.; Dai, X.; Xu, F.-J. Versatile Types of Organic / Inorganic Nanohybrids : From Strategic Design to Biomedical Applications. **Chemical Reviews**, v. 119, p. 1666–1762, 2018.

ZHOU, X.; DORN, M.; VOGT, J.; SPEMANN, D.; YU, W.; MAO, Z.; ESTRELA-LOPIS, I.; DONATH, E.; GAO, C. A quantitative study of the intracellular concentration of graphene/noble metal nanoparticle composites and their cytotoxicity. **Nanoscale**, v. 6, p. 8535–8542, 2014.

ZHOU, Y.; CHEN, R.; HE, T.; XU, K.; DU, D.; ZHAO, N.; CHENG, X.; YANG, J.; SHI, H.; LIN, Y. Biomedical Potential of Ultrafine Ag / AgCl Nanoparticles Coated on Graphene with Special Reference to Antimicrobial Performances and Burn Wound Healing. **Acs Applied Materials & Interfaces**, v. 8, n. 24, p. 15067–15075, 2016.

APPENDIX

Appendix A: Supplementary Information of chapter 2

Graphene oxide-silver nanoparticle hybrid material: an integrated nanosafety study in zebrafish embryos

Figure S.1: TGA curves of GO and GO-AgNPs at a heating rate of 10 °C min^{-1} from 25°C to 750°C in a synthetic air flow of 50 mL mi^{n-1}

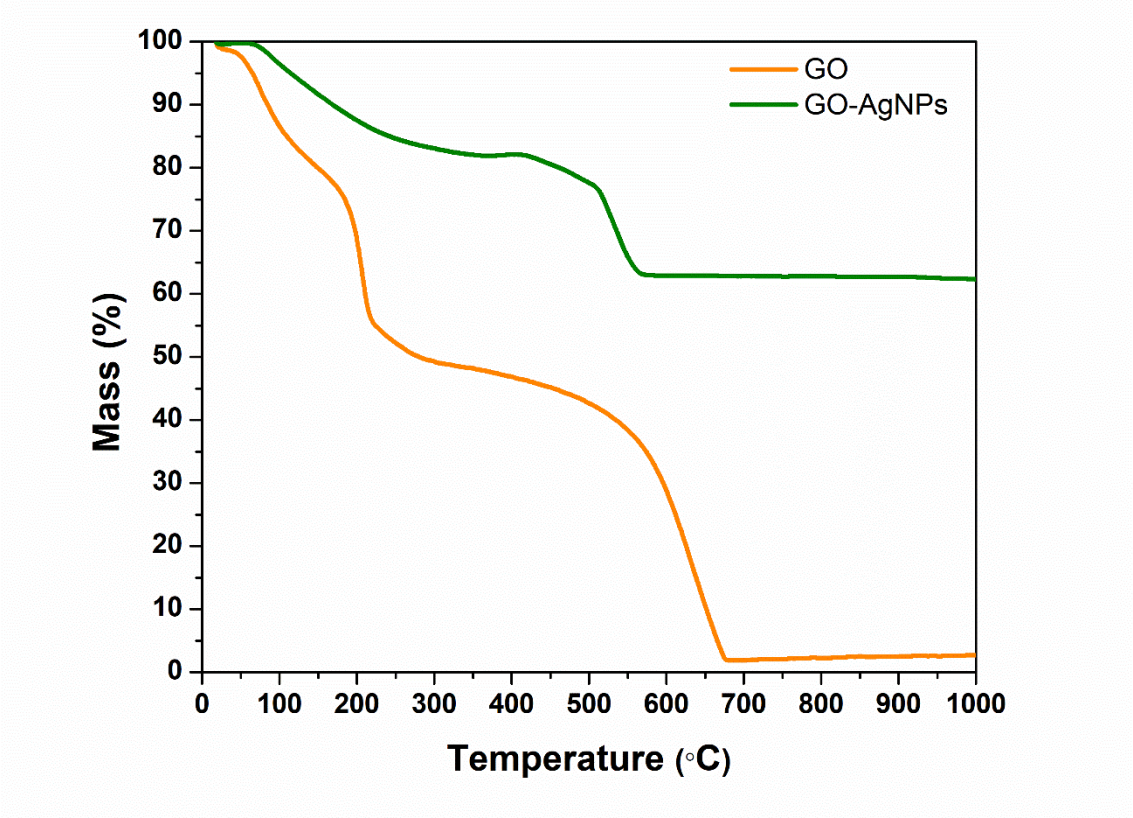

Figure S.2: Fish Embryo Toxicology (FET) assay. Fishes exposure to GO in the absence or presence of NOM (20 mg L^{-1}). Visual inspection of larvaes with 96 hpf. Deleterious effects were not observed. The arrow indicates the digestive tract with GO (A). Raman spectroscopy to confirm the presence of nanomaterial in gill and stomach (B) Visual inspection of gill. The arrow shows the presence of graphene oxide (C)

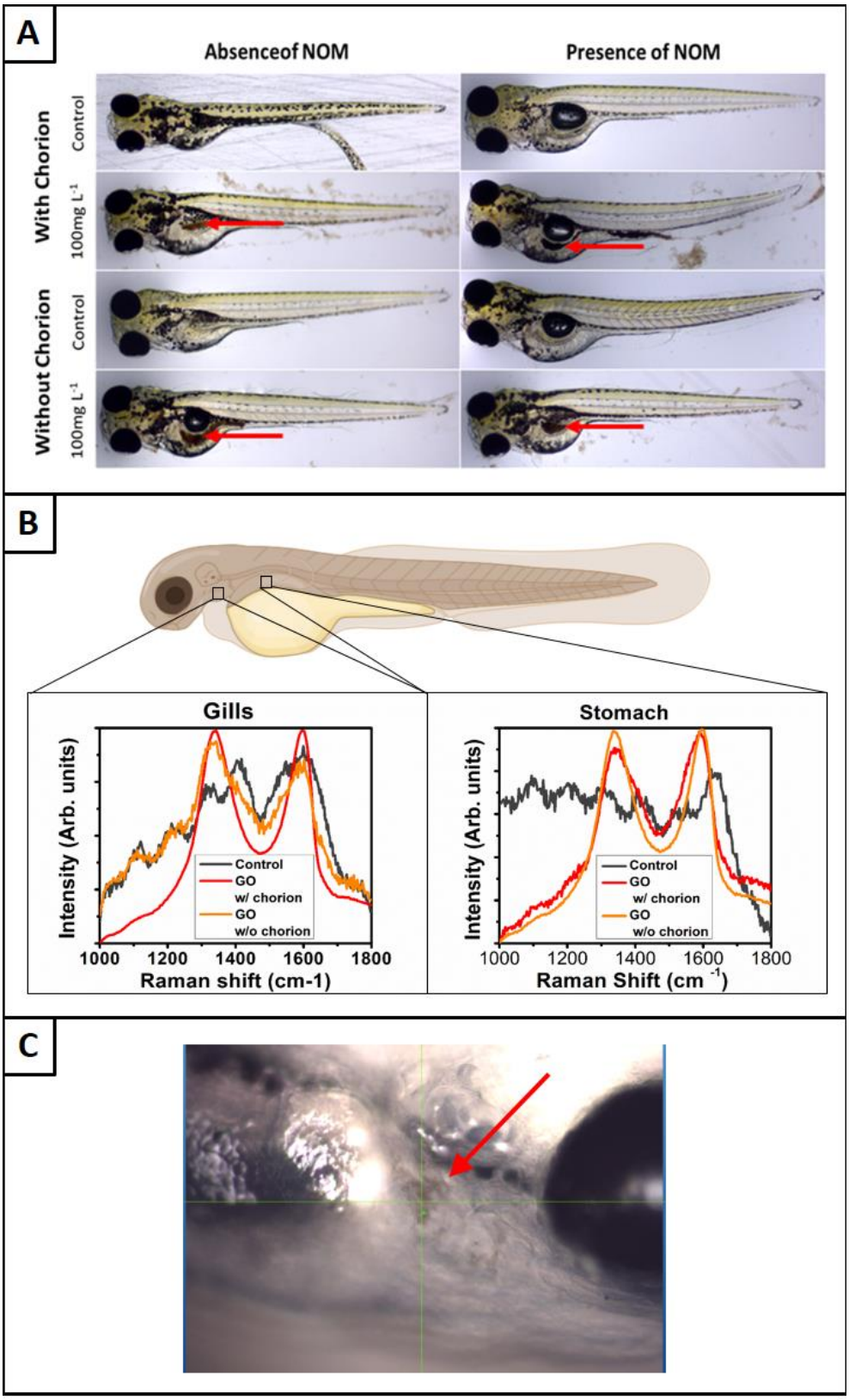

Figure S.3: Fish Embryo Toxicology (FET) assay. Fishes exposure to filtrate of GO-AgNPs (filtrate only control) in the absence of NOM. Visual inspection of larvaes with 96 hpf (A). Deleterious effects (%) observed at final of exposure (B). Total length and yolk sac size for larvae exposure to filtrate (C)

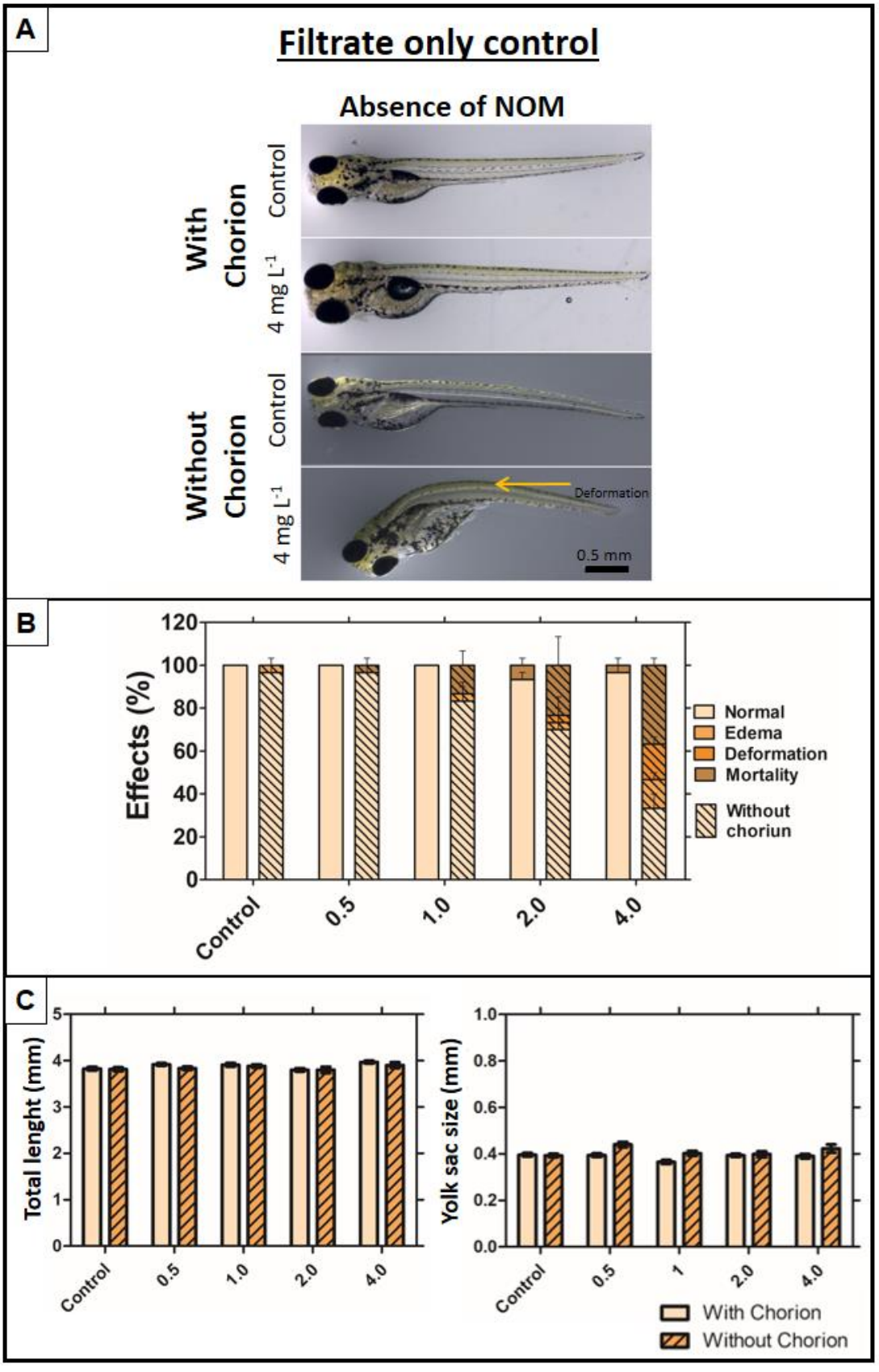

Table S.1: Silver speciation at the surface (wt.%) calculated by devolution of high-resolution XPS spectra. The average value of 3 different sample regions (spatial resolution 400 nm), in the absence and presence of NOM (20 mg L^{-1})

		Ag^0, metallic (wt.%)	**Ag^{2+}, ionic (wt.%)**
Absence of NOM	Control (0h)	85.26 ± 3.15	14.74 ± 3.15
	After 72h	85.46 ± 3.94	14.57 ± 3.90
Presence of NOM	Control (0h)	88.40 ± 3.94	11.60 ± 7.39
	After 72h	88.63 ± 2.53	11.40 ± 2.58

Figure S.4: High-resolution XPS spectra at the silver binding energy region of GO- AgNPs after exposure of FET conditions (fish embryo media, 28 C, photoperiod). Control (0h) (A) and after 72 hours (B) in the absence of NOM. Control (0h) (C) and after 72 hours (D) in the presence of NOM (20 mg L^{-1})

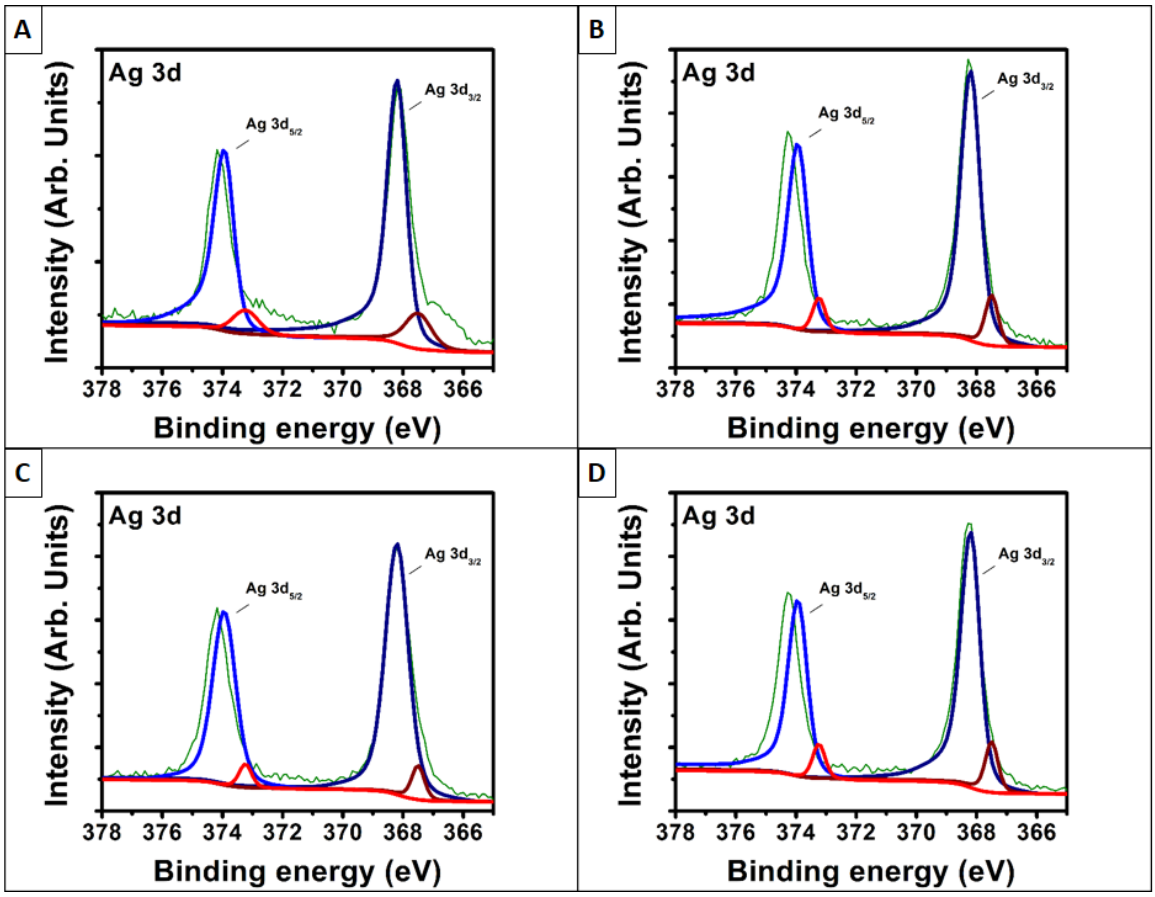

Appendix B: Supplementary Information of chapter 3

Toxicity assessment of graphene oxide-silver nanoparticles hybrid material on Zebrafish liver cells

Figure S.1: AgNPs characterisation: Typical TEM images (A); TEM image, high resolution (B); Histogram AgNPs size distribution based on TEM images (C); UV-Vis absorption spectrum with plasmon resonance @ 400 nm (D); Particle size distribution (E) and its cumulative distribution curve (F) in ultrapure water measured by centrifugal sedimentation (CPS)

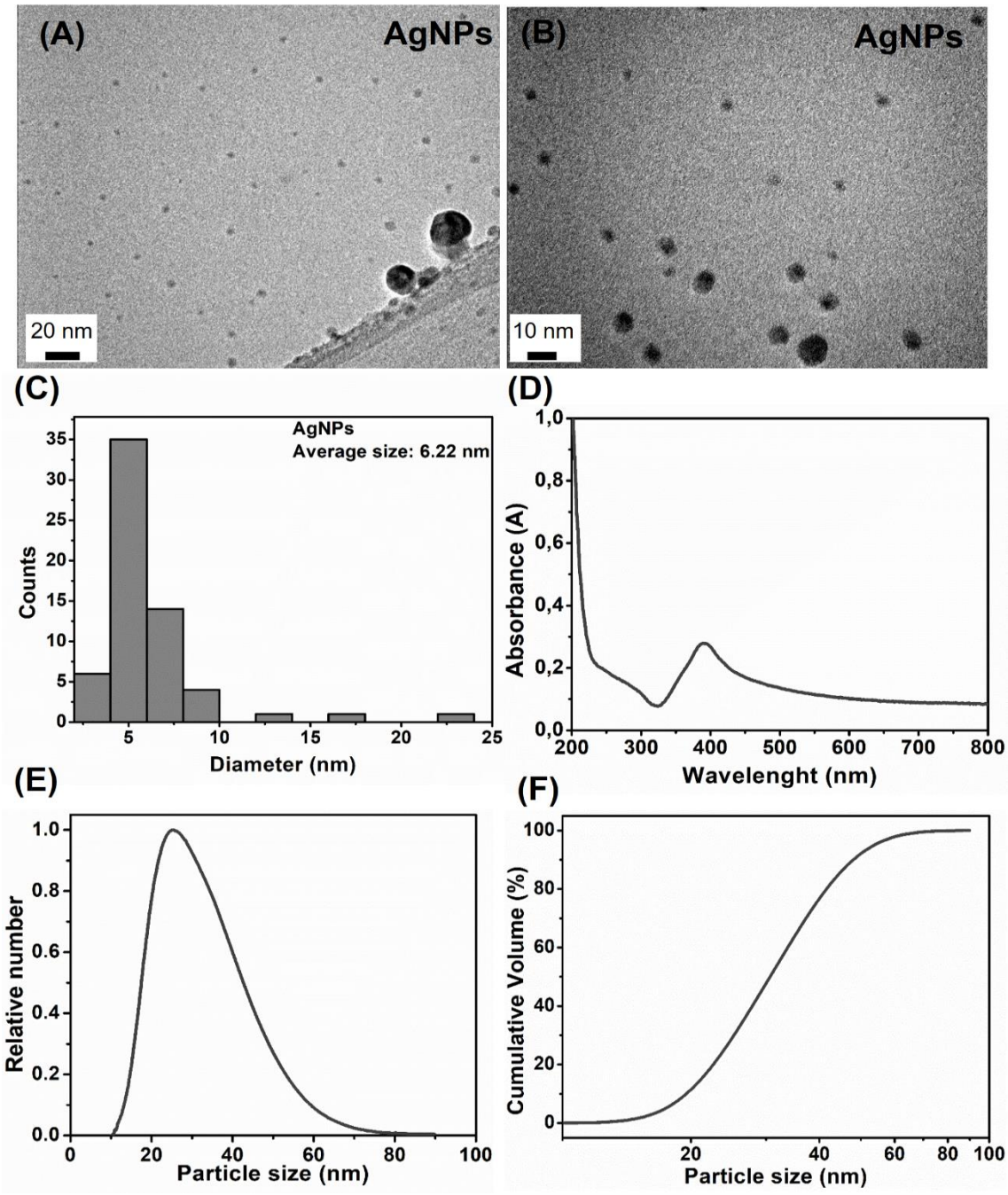

Table S.1: Hydrodynamic diameter (HD) and polydispersity index (PdI) measurements of AgNPs dispersions (50 mg L^{-1}) in ultrapure water and cell medium (RPMI / L15) with and without FBS supplementation

AgNPs			
Hydrodynamic diameter (nm)			
Time (h)	**Utrapure water**	**Cell medium without FBS**	**Cell medium without FBS**
0	30.64 ± 0.25	397.03 ± 49.21	62.25 ± 1.35
3	32.59 ± 2.29	3068.89 ± 407.47	120.22 ± 40.00
6	28.74 ± 0.68	4459.89 ± 412.39	110.35 ± 23.43
24	31.21 ± 9.31	7775.67 ± 1135.27	81.51 ± 8.25
Polydispersity index (PDI)			
Time (h)	**Utrapure water**	**Cell medium without FBS**	**Cell medium without FBS**
0	0.58 ± 0.01	0.24 ± 0.03	0.43 ± 0.02
3	0.58 ± 0.02	1.16 ± 0.15	0.48 ± 0.09
6	0.55 ± 0.01	1.70 ± 0.13	0.38 ± 0.11
24	0.58 ± 0.03	1.72 ± 0.73	0.42 ± 0.03

Figure S.2: Cell viability results of ZFL cells exposed for 24 h to GO-AgNPs filtrate-only control and RPMI/L15 medium supplemented 10% of FBS with Alamar blue (AB), Tetrazolium salt (MTT) and neutral red uptake (NRU)